The Chemical Structure of Coal Tar and Char During Devolatilization

A Thesis
Presented to the
Department of Chemical Engineering
Brigham Young University

In Partial Fulfillment
of the Requirement for the Degree
Master of Science

Eric M. Hambly
April 1998

This thesis by Eric M. Hambly is accepted in its present form by the Department of Chemical Engineering of Brigham Young University as satisfying the thesis requirement for the degree of Master of Science.

_____

Thomas H. Fletcher, Advisor

_____

Ronald J. Pugmire, Advisory Committee

_____

Paul O. Hedman, Advisory Committee

_____

Merrill W. Beckstead, Acting Department Chair

_____

Date

Table of Contents

List of Figures

List of Tables

Acknowledgments

I would like to thank Dr. Thomas H. Fletcher for all his support and advice during my undergraduate and graduate studies at Brigham Young University. I greatly appreciate the opportunity to work with and learn from him. I would like to thank Dr. Ronald Pugmire and Dr. Mark Solum of the University of Utah for their major contributions of NMR data and technical advice. I am also grateful for the funding that was received from the Advanced Combustion Engineering Research Center and from the Department of Energy, grant number DE-FG22-95PC95215.

I would like to thank Catherine Poulos, Jim Anderson, Travis Faddis, Michael Busse, Dominic Genetti and Steve Perry for their help in performing experiments and analyses. I would especially like to thank Hugh Palmer for his hard work and dedication. I greatly appreciate all his help during the reconstruction of the Drop Tube Reactor and the countless experiments and analyses.

Finally, I would like to thank my parents and my parents by marriage for their support and encouragement. I would particularly like to thank my wife Mary for her love, support and encouragement during this project.

Nomenclature

an	anthracite coal
B.L.	bridges and loops per cluster
C_{Cl}	aromatic carbons per cluster
CD_2Cl_2	deuterated methylene chloride
CP	cross-polarization
daf	dry, ash free
DECS	Department of Energy Coal Sample
DNP	dynamic nuclear polarization
f_a	total percent of sp^2-hybridized carbon
f_a'	percent of aromatic carbon
f_a^B	percent of bridgehead aromatic carbon
f_a^C	percent of carbonyl carbon
f_a^H	percent of aromatic carbon with proton attachment
f_a^N	percent of nonprotonated aromatic carbon
f_a^P	percent of phenolic or phenolic ether aromatic carbon
f_a^S	percent of alkylated aromatic carbon
f_{al}	total percent aliphatic carbon
f_{al}^*	percent aliphatic carbon that is nonprotonated or CH_3
f_{al}^H	percent aliphatic carbon that is CH or CH_2
f_{al}^O	percent aliphatic carbon that is bound to oxygen
FFB	methane air flat-flame burner
FTIR	fourier transform infrared spectroscopy
f_{Ti}^{ash}	mass fraction of titanium in the ash
f_{Ti}^{coal}	mass fraction of titanium in the dry coal

f_{Ti}^{char}	mass fraction of titanium in the dry char
HCN	hydrogen cyanide
HPCP	High Pressure Controlled-Profile reactor
hvAb	high volatile A bituminous coal
hvBb	high volatile B bituminous coal
hvCb	high volatile C bituminous coal
i	coal, char or tar
ICP	inductively coupled plasma
ligA	lignite A
lvb	low volatile bituminous coal
MAS	magic angle spinning
m_i	mass of coal, char or tar
m_{ash}	mass of the ash
m_{coal}	mass of the coal
m_{char}	mass of the char
$\dot{m}_{coal}$	mass flow rate of coal
$\dot{m}_{coal\ N}$	mass flow rate of coal nitrogen
M_{Cl}^{N}	mass of nitrogen per cluster
mvb	medium volatile bituminous coal
MW_{Cl}	side chains per cluster
MW_{δ}	average molecular weight of the cluster attachments
MW_N	molecular weight of nitrogen
$\dot{n}_{coal\ N}$	molar flow rate of coal nitrogen
$\dot{n}_{HCN}$	molar flow rate of hydrogen cyanide
$\dot{n}_{N_2}$	total molar flow rate of nitrogen gas
$\dot{n}_T$	total molar flow rate
N_{Char}	percentage of coal nitrogen that remains in char

n_{Cl}	moles of clusters per kilogram of daf coal
N_{Cl}	moles of nitrogen per cluster
N_{HCN}	percentage of coal nitrogen that is released as HCN
NMR	nuclear magnetic resonance spectroscopy
NO_X	nitrogen oxides (NO, NO_2 and N_2O)
N_{Tar}	percentage of coal nitrogen that is released in the tar
ppb	parts per billion
P_0	fraction of attachments that are bridges
PSOC	Penn State Office of Coal Research
sa	semi-anthracite coal
subA	subbituminous A coal
subB	subbituminous B coal
subC	subbituminous C coal
TG-FTIR	thermogravimetric fourier transform infrared spectroscopy
Ti	titanium
x_N	mass fraction of nitrogen
x_N^{coal}	mass fraction of nitrogen in coal
X_N^{HCN}	fraction of dry, ash free coal nitrogen that is converted to hydrogen cyanide
XPS	X-ray photoelectron spectroscopy
y_{HCN}	mole fraction of hydrogen cyanide
Y_{vol}	total volatile yield
Δ	percentage of nitrogen not measured in mass balance
$\sigma+1$	total attachments per cluster
χ_b	fraction of bridgehead carbons

1. Introduction

The power generation industry in the United States is being driven by environmental legislation to reduce levels of pollutant emissions. Recently, particular attention has been given to nitrogen oxide (NO_X) pollution. In coal combustion processes, the majority of the nitrogen oxide pollution that is generated is formed from the nitrogen found in the coal. When coal burns, nitrogen is released in two stages. In the first stage, nitrogen is released as volatiles in the tar and light gases. Tar is generally defined as those volatiles that condense to a solid or liquid at room temperature. This initial stage of combustion, in which the tar and light gases are driven out of the coal, is know as devolatilization or pyrolysis. During this stage, the coal particle is heated, but no oxidation reactions occur (only thermal decomposition). Later, when the tar and light gases mix with gaseous oxygen and combust, the species containing nitrogen may be oxidized to form NO_X. The second stage of nitrogen release occurs as the char is combusted. Char is the solid material that remains after light gases and tar have been released from the coal particle. As the char is oxidized, the nitrogen in the char reacts with oxygen to form nitrogen oxides.

Control of nitrogen oxides has traditionally been achieved with staged combustion and with catalytic conversion processes using ammonia or urea. Catalytic processes using ammonia or urea have proven to be quite effective, but they are very expensive to implement and operate. Staged combustion has provided a fair amount of control of NO_X formed from the volatiles, but it has had little effect on the formation of NO_X from the char. Recently, advanced staging processes, known as low-NO_X burners, have been developed. These low-NO_X burners are designed on the basis that volatile nitrogen may be converted to N_2 rather than NO_X under locally fuel-rich conditions with sufficient residence time at appropriate temperatures. The amount and chemical form of nitrogen

released during devolatilization greatly influences the amount of NO_X reduction achieved using this strategy. Since the nitrogen in the char is released by heterogeneous oxidation, these burner design modifications have no effect on NO_X formed from the char nitrogen. Low-NO_X burners alter the near-burner aerodynamics of the combustor. This alteration influences the devolatilization process and therefore influences the amount and chemical form of nitrogen released during devolatilization.[1-3] Low-NO_X burners provide the least expensive emission control strategy currently available and are therefore the preferred method to limit the amount of NO_X formed during combustion. Current low-NO_X burners are designed using empirical relationships of nitrogen evolution during devolatilization. In order to effectively design more advanced low-NO_X burners, the fundamental chemistry and detailed reaction kinetics of coal nitrogen evolution are necessary.

Coal is thought to consist of a large polymeric matrix of aromatic structures, commonly called the coal macromolecule.[4] This macromolecule network consists of clusters of aromatic carbon that are linked to other aromatic structures by bridges. Bridges between the aromatic clusters are formed from a wide variety of structures. Most bridges are thought to be aliphatic in nature, but may also include other atoms such as oxygen and sulfur.[5, 6] There are other attachments to the aromatic clusters that do not form bridges. These attachments are referred to as side chains and are thought to consist mainly of aliphatic and oxygen functional groups.

During coal pyrolysis, covalent bonds throughout the coal macromolecule are broken. Bonds in the bridges that connect aromatic clusters are broken along with bonds in the side chains. When these bonds are broken, fragments of the coal molecule are formed. If these fragments are small enough, they will form a vapor and be released to the gas phase as light gases and tars. The larger fragments remain in the solid phase and can recombine with the coal macromolecule.

In order to more fully understand the devolatilization process, more must be learned about the structure of coal and the products of devolatilization, char, tar and light gases. Many analysis techniques are being employed to gather more information about the chemical structure of coal and its pyrolysis products. Solid-state ^{13}C NMR spectroscopy has become one of the most useful techniques for obtaining average chemical structural features of coal and char. ^{1}H NMR has been used to analyze coal tars. Recently, solvents have been used in conjunction with liquid ^{13}C NMR to analyze coal tars. Other techniques such as fourier transform infrared spectroscopy (FTIR), gas chromatography, pyridine extraction and X-ray photoelectron spectroscopy (XPS) analysis have also been used to gather chemical structural information about coal and its pyrolysis products.

This study seeks to improve the understanding of the chemical structure of coal pyrolysis products and the role these structures play in the devolatilization process. Special attention has been given to the nitrogen structures in coal and its pyrolysis products. Pyrolysis experiments were performed in an electrically heated drop tube furnace and in a methane air flat-flame burner. Chemical analyses of the parent coals and the pyrolysis products were performed both at Brigham Young University and at outside laboratories (University of Utah). This work represents the first reported solid-state ^{13}C NMR analysis of matched coal-char-tar samples. In order to get a more complete picture of the fate of coal nitrogen during devolatilization, an on-line hydrogen cyanide (HCN) analyzer was used to analyze the gaseous products. This thesis contains a review of the current state of coal pyrolysis research, a description of the experiments and analysis techniques that were performed, and a discussion of the results and their contribution to the state of coal pyrolysis research.

2. Literature Review

A literature review containing the current state of coal pyrolysis research is given here, with emphasis on the chemical structure of coal and its pyrolysis products. Special attention is given to the fate of coal nitrogen during the devolatilization process and the structure of resulting nitrogen containing compounds. First, the structure of coal and the nitrogen forms in coal are discussed. This is followed by a discussion of the pyrolysis process in general. Next, the structure and nitrogen chemistry of the pyrolysis products are discussed. Finally, a summary of the current state of coal pyrolysis research is presented.

Coal

Coal is thought to consist of a large polymeric matrix of aromatic structures, commonly called the coal macromolecule.[4, 7] This macromolecule network consists of clusters of aromatic carbon that are linked to other aromatic structures by bridges. Bridges between the aromatic clusters are formed from a wide variety of structures. Most bridges are thought to be aliphatic in nature, but may also include other atoms such as oxygen and sulfur.[5, 6] Those bridges that contain oxygen as ethers are thought to have relatively weak bond strengths.[8] Other bridges are made up of aliphatic functional groups only. Some bridges consist of a single bond between aromatic clusters; this is known as a bi-aryl linkage. Due to the large variety of functional groups that make up the bridge structures of coal, bridges have a large distribution of bond strengths.[9] This distribution of bond strengths becomes important during the pyrolysis process as the weakest bonds are broken first. There are other attachments to the aromatic clusters that do not form bridges. These attachments are referred to as side chains and are thought to consist mainly of aliphatic and carbonyl functional groups. Figure 2.1 is a diagram of a

hypothetical coal macromolecule. The various features of bridges and side chains are indicated in the figure.

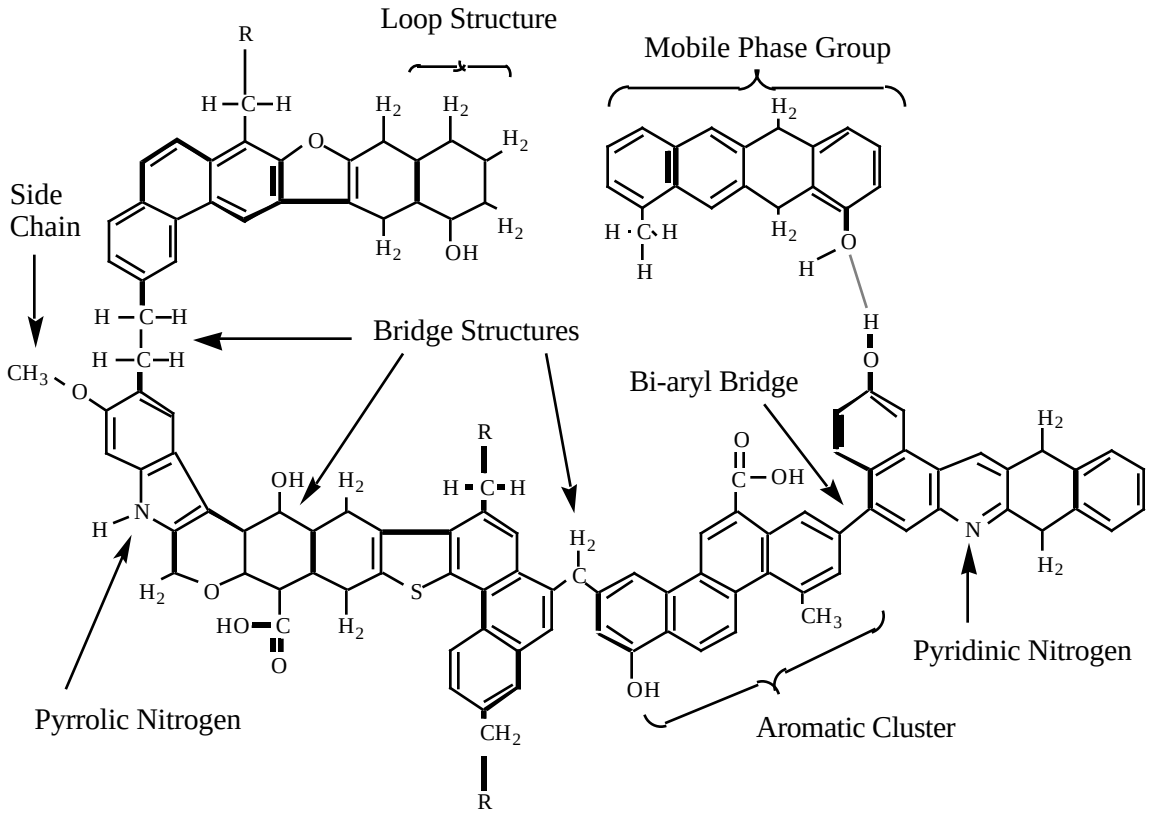

Figure 2.1. A Hypothetical Coal Macromolecule. Modified from Solomon et al.[10]

There is also evidence that a mobile phase exists in coal. This mobile phase is interspersed with the coal macromolecule. This mobile phase is thought to consist of smaller molecular structures that are not strongly bonded to the macromolecule.[11, 12] The mobile phase is considered to be either (a) trapped in the molecular structure of the coal or (b) weakly bonded to the coal macromolecule with hydrogen bonds or van der Waals type interactions. Figure 2.1 contains a mobile phase group as it is theorized to exist in the coal.

As previously mentioned, solid-state ^{13}C NMR spectroscopy has become one of the most useful techniques for obtaining average chemical structural features of coal. Solid-state ^{13}C NMR spectroscopy is one of the few methods available to study coal structure in a nondestructive manner. Other techniques such as pyrolysis mass spectroscopy, fourier transform infrared spectroscopy (FTIR) and pyridine extraction/chromatography have also been used to study coal structure by a number of researchers,[10, 13-18] but such techniques are destructive. The coal is pyrolyzed or treated with solvent and structural features of the resulting gases or liquid are used to extrapolate back to the structure of the coal. Such an extrapolation to the coal structure from extracts or pyrolysis products must be performed with care since the complete coal structure is not analyzed; in many cases the gas or liquid products analyzed represent only a small mass fraction of the coal.[7] Due to its success and reliability in obtaining average chemical structural features of whole, untreated coal, ^{13}C NMR spectroscopy as it relates to coal structure is discussed here.

^{13}C Solid-State NMR Spectroscopy

A number of researchers have used solid-state ^{13}C NMR spectroscopy to describe the average chemical structural features of the coal macromolecule.[19-22] As described elsewhere[19, 22], cross-polarization (CP), magic angle spinning (MAS) and dipolar dephasing techniques permit direct measurement of the number and diversity of aromatic and nonaromatic carbons present in a coal sample. Many coals of broadly varying rank have been analyzed with these techniques. The results of the solid-state ^{13}C NMR analyses of some of these coals are presented in Tables 2.1 and 2.2. Table 2.1 contains the structural parameters that are directly measured and Table 2.2 contains the derived structural parameters for these coals. The coals in Tables 2.1 and 2.2 are listed in order of increasing rank.

Table 2.1
Structural Parameters of the ACERC Coals Determined from ^{13}C NMR[a19, 22]

Coal	Rank	f_a	f_a^C	f_a'	f_a^H	f_a^N	f_a^P	f_a^S	f_a^B	f_{al}	f_{al}^H	f_{al}^*	f_{al}^O
Beulah Zap	ligA	65	10	55	22	33	9	15	9	35	26	9	11
Lower Wilcox	ligA	63	7	56	17	39	10	17	12	37	26	11	8
Wyodak	subC	63	8	55	17	38	8	14	16	37	27	10	10
Dietz	subB	64	8	56	19	37	9	15	13	36	25	11	5
Illinois #6	hvCb	72	0	72	26	46	6	18	22	28	19	9	5
Blind Canyon	hvBb	63	2	61	22	39	7	14	19	38	27	11	5
Pittsburgh #8	hvAb	71	1	70	27	43	6	15	22	29	21	8	4
Upper Freeport	mvb	81	0	81	28	53	4	20	29	19	11	8	2
L. Stockton	mvb	75	0	75	27	48	5	21	22	25	17	8	4
Pocahontas #3	lvb	86	0	86	33	53	2	17	34	14	9	5	1
Buck Mountain	an	95	1	94	24	70	1	8	61	5	4	1	3

[a]Percentage carbon (error): f_a = total sp^2-hybridized carbon (±3); f_a' = aromatic carbon (±4); f_a^C = carbonyl, d > 165 ppm (±2); f_a^H = aromatic with proton attachment (±3); f_a^N = nonprotonated aromatic (±3); f_a^P = phenolic or phenolic ether, d = 150-165 ppm (±2); f_a^S = alkylated aromatic d = 135-150 ppm (±3); f_a^B = aromatic bridgehead (±4); f_{al} = aliphatic carbon (±2); f_{al}^H = CH or CH_2 (±2); f_{al}^* = CH_3 or nonprotonated (±2); f_{al}^O = bonded to oxygen, d = 50-90 ppm (±2).

Table 2.2
Derived Structural Parameters from ^{13}C NMR for the ACERC Coals[b19]

Coal	Rank	χ_b	C_{Cl}	σ+1	P_0	B.L.	S.C.	MW_{Cl}	MW_δ
Beulah Zap	ligA	0.16	9	3.9	0.63	2.5	1.4	269	40
Lower Wilcox	ligA	0.21	10	4.8	0.59	2.8	2.0	297	36
Wyodak	subC	0.29	14	5.6	0.55	3.1	2.5	408	42
Dietz	subB	0.23	11	4.7	0.54	2.5	2.2	310	37
Illinois #6	hvCb	0.31	15	5.0	0.63	3.2	1.8	321	27
Blind Canyon	hvBb	0.31	15	5.1	0.49	2.5	2.6	368	36
Pittsburgh #8	hvAb	0.32	16	4.5	0.62	2.9	1.6	310	28
Upper Freeport	mvb	0.36	18	5.3	0.67	3.6	1.7	310	17
L. Stockton	mvb	0.29	14	4.8	0.69	3.3	1.5	270	20
Pocahontas #3	lvb	0.4	20	4.4	0.74	3.3	1.1	307	13
Buck Mountain	an	0.65	49	4.7	0.89	4.2	0.5	656	12

[b]χ_b = fraction of bridgehead carbons, C_{Cl} = aromatic carbons per cluster, σ+1 = total attachments per cluster, P_0 = fraction of attachments that are bridges, B.L. = bridges and loops per cluster, S.C. = side chains per cluster, MW_{Cl} = the average molecular weight of an aromatic cluster, MW_δ = the average molecular weight of the cluster attachments.

The parameters obtained directly from the ^{13}C NMR analysis detail the general carbon structure of the coal. The value of f_a is the total fraction of aromatic, carboxyl and carbonyl carbons. This value is subdivided into f_a^C, which is the fraction of carbonyl and carboxyl carbons, and f_a', which is the fraction of sp^2-hybridized carbons present in aromatic rings. The value of f_a' is subdivided into protonated (f_a^H) and non-protonated (f_a^N) aromatic carbons. The non-protonated aromatic carbons are further subdivided into the fractions of phenolic (f_a^P), alkylated (f_a^S) and bridgehead (f_a^B) carbons. The fraction of aliphatic carbons is labeled f_{al}. This value is divided into the fraction of CH and CH_2 groups (f_{al}^H) and the fraction of CH_3 groups (f_{al}^*). The aliphatic carbons that are bonded to oxygen are labeled as f_{al}^O.

The derived structural parameters provide the most meaningful description of the coal molecule. These parameters are derived from the measured ^{13}C NMR structural parameters, the elemental composition of the coal sample and a correlation.[19] As described elsewhere[22], a correlation between the fraction of bridgehead carbons (χ_b) and the number of aromatic carbons per cluster (C_{Cl}) was developed from an analysis of polycondensed aromatic hydrocarbons. This value of C_{Cl} is then used in the determination of the remaining derived parameters. The average number of attachments to the aromatic cluster is labeled σ+1. The fraction of intact bridges, P_0, is the fraction of these attachments that are bridges between neighboring aromatic clusters. The number of bridges and loops per aromatic cluster is labeled B.L. The ^{13}C NMR techniques commonly used to analyze coal structure are not able to differentiate between (a) bridges and (b) attachments that form a loop on the aromatic cluster. Attachments to the aromatic cluster that are not bridges or loops are known as side chains. The number of side chains per cluster is labeled S.C. These chemical structural features are illustrated in Figure 2.1. The average molecular weight per aromatic cluster is labeled MW_{Cl}. The average weight of attachments to the aromatic cluster is known as MW_δ.

As seen in Tables 2.1 and 2.2, several trends in the ^{13}C NMR data are readily apparent. The aromatic content of the coals increases with rank, as observed in the values of aromaticity (f_a') and the number of aromatic carbons per cluster. The aliphatic content of the coals decreases with increasing rank. This can be seen by observing the change in the values of f_{al} and MW_δ with rank. These trends are also observed and described in detail by other investigators.[20, 22]

Nitrogen in Coal

The average coal contains between one and two weight percent nitrogen. The amount of nitrogen in coal is not strongly rank dependent. The largest fraction of nitrogen is generally found in coals with approximately 85% carbon.[23, 24] Nitrogen is thought to be incorporated into the coal macromolecule in heterocyclic aromatic structures resembling pyridine and pyrrole. These nitrogen functional groups are indicated in Figure 2.1. It is thought that very little, if any, nitrogen is found in the side chains or bridges of the coal macromolecule.

Several investigators have used X-ray photoelectron spectroscopy (XPS) and X-ray absorption near edge spectroscopy (XANES) to confirm that coal nitrogen is found in pyridine and pyrrole type structures.[24-28] XPS and XANES have proven to be useful in identifying and distinguishing between the types of nitrogen found in the coal macromolecule. The relative amounts of the different nitrogen functionalities found in coal have been shown to vary slightly with coal rank (the amount of carbon in the coal is used as an indicator of coal rank). As can be seen in Figure 2.2, XPS and XANES studies have shown that the pyridinic nitrogen increases slightly with coal rank, while the pyrrolic nitrogen decreases slightly with rank.[26-28] However, these trends are not accepted by all investigators and there is some question as to the accuracy of both techniques.[24, 29] One limitation of XPS and XANES is that they are both surface techniques and may therefore not accurately represent the entire coal macromolecule.

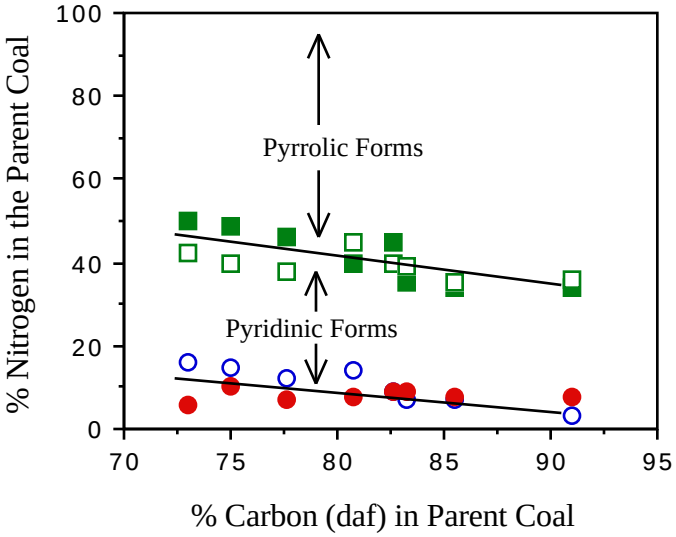

Figure 2.2. Nitrogen Functional Groups in Coals as Found by XANES(open) and XPS(closed) (taken from Solomon and Fletcher[1]).

Recent studies with more sensitive XPS equipment have confirmed the presence of quaternary nitrogen functional groups within the coal macromolecule.[26-28, 30] Some studies have indicated that these quaternary nitrogen structures are protonated nitrogen in 6-membered rings that may be chemically associated with oxygen functionalities.[27, 28] Quaternary nitrogen functionalities mostly occur in the low rank coals, with very little to no quaternary forms found in anthracites.[27, 28] One XANES study reported the presence of amine structures in the Argonne Premium coals at concentrations up to ten percent.[31] XPS has not yet been able to confirm the existence of amine structures in coal; however, at levels less than 5 percent amine, structures are indistinguishable with XPS.[27, 28, 30] The presence of amine structures in coal tar[27, 28, 30] may indicate that coal contains amine structures in low levels.

The major limitation of XPS and XANES techniques is that they do not provide detailed nitrogen chemical structure information. Only general structural forms can be

detected, such as pyridinic, pyrrolic and quaternary forms.[26-28, 31] Solid-state ^{15}N NMR techniques, similar to the ^{13}C NMR techniques described above, are currently being developed for the study of coal nitrogen structure. ^{15}N NMR has the potential to provide detailed nitrogen chemical structural features, but this technique suffers from low signal to noise problems. These problems are discussed elsewhere.[32-35] New experiments known as Dynamic Nuclear Polarization (DNP)[34, 35] are currently being developed to overcome these signal to noise problems. Current ^{15}N NMR results will be discussed later in this thesis.

Coal Pyrolysis

The first stage of coal combustion is known as pyrolysis or devolatilization. As the coal particle is heated in the absence of oxygen, tar and light gases (volatiles) are driven out of the particle and a solid residue known as char remains. Tar is generally defined as those volatiles that condense to a solid or liquid at room temperature. Pyrolysis may be defined as the thermal decomposition and reorganization of the coal macromolecule in the absence of oxygen. The pyrolysis behavior of a coal is known to be effected by the temperature, heating rate, particle size, pressure, coal type and many other factors.[1, 4, 36-39]

As the coal particle temperature rises during the pyrolysis process, the bonds between the aromatic clusters in the coal macromolecule break, creating fragments that are detached from the macromolecule. The larger fragments are referred to as metaplast. During pyrolysis, the metaplast will either vaporize and escape from the coal or be reincorporated into the coal macromolecule in a process known as cross-linking. The portion of the metaplast that is vaporized usually consists of the lower molecular weight fragments; these released fragments become what is known as tar. Side chains on the aromatic clusters are released from the coal as light gases. These light gases are generally

oxides (CO_2, CO, H_2O) and light hydrocarbons(C_1-C_4).[18, 40-44] Figure 2.3 shows a schematic of how this pyrolysis process may occur for the hypothetical coal macromolecule presented earlier in Figure 2.1.

The pyrolysis behavior of a coal is a strong function of coal type or rank. Low rank coals, such as lignites and subbituminous coals, produce relatively high levels of light gases and very little tar. Bituminous coals produce significantly more tar than the low rank coals and moderate amounts of light gases. The higher rank coals produce relatively low levels of both light gases and tar. These pyrolysis trends with rank can be seen in Figure 2.4, where the weight percent carbon in the coal is used as an indicator of rank.

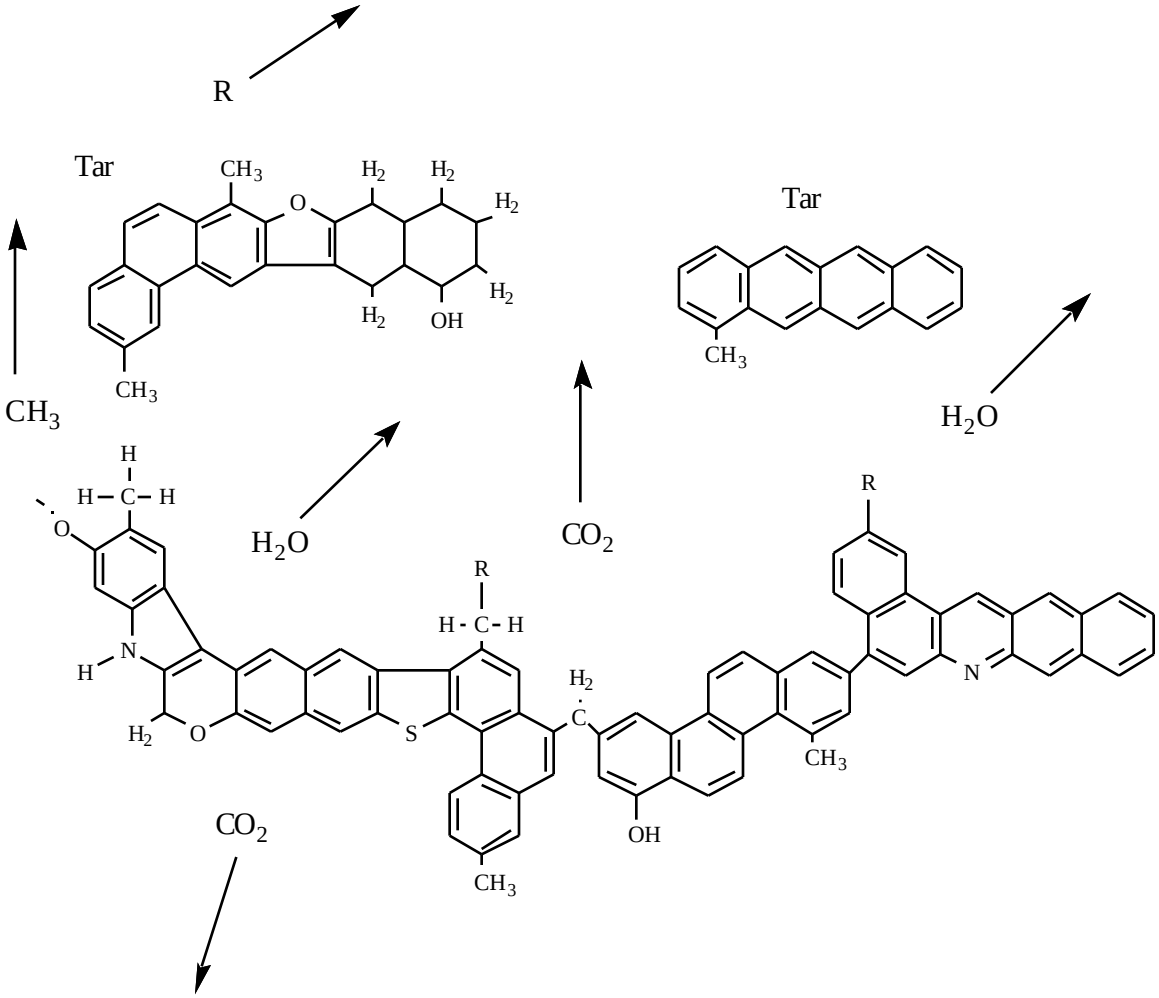

Figure 2.3. Hypothetical Coal Pyrolysis Reaction. Modified from Solomon, et al.[10]

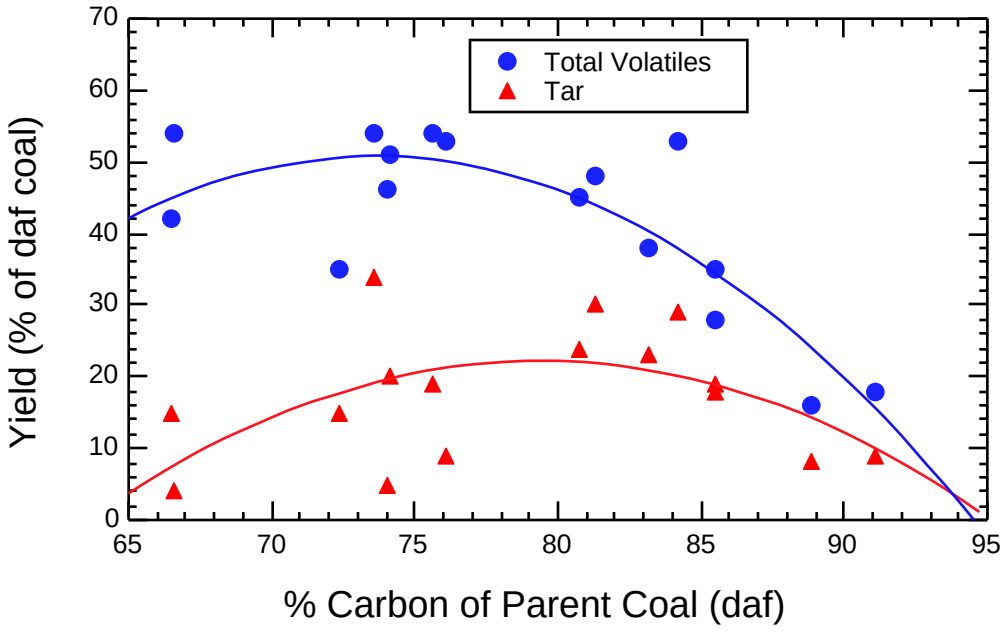

Figure 2.4. Tar and Total Volatile Yields from Devolatilization as a Function of the Carbon Content of the Parent Coal (adapted from Fletcher, et al.[45]). Solid lines are quadratic curve fits to the data, and are shown only for illustrative purposes.

Several investigators have attempted to isolate and determine the general characteristics of the individual steps that occur during pyrolysis.[37, 46] Suuberg et al. pyrolyzed a lignite at a heating rate of 1000 K/s and indicated that at temperatures of just over 370 K the coal residual moisture evolves.[37] The evolution of light gases begins at temperatures of 470 K to 770 K; these early gases consist mainly of oxides (CO and CO_2) and light hydrocarbons. Tar formation was seen in low heating rate experiments to begin at around 600 K and increases to temperatures above 800 K.[46] Cross-linking reactions are thought to occur at different temperatures, depending on the coal and heating rates. This is due to different kinetics of the competing processes of bond breaking, vaporization and bond formation. Pyrolysis experiments conducted with a number of coals at a heating rate of 30 K/min indicated that early cross-linking begins in the range of

670 to 770 K, later cross-linking continues as temperatures increase.[10, 42] The exact temperatures at which these pyrolysis steps occur are dependent on many factors. It is likely that heating rate and coal type have the largest effect on the temperatures at which these step occur. However, the basic pyrolysis steps are believed to occur in the sequence described above.

The chemical structure of the coal may also effect the pyrolysis process. Coal contains an average of at least one heteroatom (e.g., N, O, S) per aromatic cluster. Many of these heteroatoms are oxygen. Recent work has suggested that oxygen found as heteroatoms in the aromatic coal clusters may contribute to depolymerization reactions.[47, 48] A significant amount of the oxygen in coal is also found in the bridges between aromatic clusters. These bridges containing oxygen have relatively weak bonds, creating breakage points for the depolymerization of the coal macromolecule.[8] It is possible that sulfur and nitrogen atoms may also be active in effecting the pyrolysis process; however, the mechanisms for such processes are not currently known.

Pyrolysis of Coal Nitrogen

As previously mentioned, the effectiveness of a low-NO_x burner is determined by the amount and chemical form of volatile nitrogen that is released during devolatilization.[3, 49, 50] For this reason, many investigators have begun to study the distribution of coal nitrogen between the volatiles and char during devolatilization and the chemical structure of the resulting tar. Pohl, et al.,[49] devolatilized and combusted a lignite and a bituminous coal in a furnace at 1500 K and at a heating rate of approximately $2x10^4$ K/s. It was found that the volatile nitrogen contributed approximately 60 to 80 percent of the total NO_x levels. Other studies which used coal-fired burners found that as much as 50% of fuel nitrogen may be converted to NO_x, and that approximately 75% of exhaust NO_x comes from the fuel nitrogen in the coal.[3, 50]

The amount of nitrogen that is released during the pyrolysis process is known to be a function of temperature. Blair, et al.[2] placed pulverized coal particles on a preheated graphite ribbon in an argon atmosphere. It was shown that as the pyrolysis temperature increased, volatile nitrogen increased proportionately and at a much faster rate than overall volatile release. Solomon and Colket[51] devolatilized coal with the use of a heated grid at temperatures of 570 to 1270 K and a heating rate of 600 K/s. They concluded that initial nitrogen evolution was found to be proportional to the evolved tar. Recent experiments in which coal particles were heated to 1000 K further support the hypothesis that tar release is the primary mechanism for nitrogen evolution during pyrolysis, even though it is not the only mechanism.[40, 41] As previously mentioned, most coals exhibit light gas release either earlier or concurrent with tar release. Since the light gases generally do not contain nitrogen species, nitrogen evolution generally lags total mass release during devolatilization.

As a general trend, the total volatile nitrogen release is a function of coal rank. As indicated in Figure 2.5, the fraction of coal nitrogen that is released to the volatiles at high heating rates (~10^5 K/s) is relatively constant for low rank to high volatile bituminous coal (64 - 82% carbon), and then drops dramatically with increasing rank.[1, 52] It is also apparent that large differences in volatile nitrogen release occur with coals of the same rank. This fact is quite obvious when comparing Illinois #6 and Blue #1 coals.

Freihaut, et al.[44, 53, 54] pyrolyzed coal in heated grid experiments at moderate heating rates of 500 K/s. These experiments indicated that the distribution of nitrogen between the volatiles and the char is a function of coal rank. It was shown that low rank coals preferentially release nitrogen as hydrogen cyanide (HCN), while the bituminous coals release more nitrogen in the tar.[44, 53] Also, Freihaut showed that in high rank coals (low-volatile bituminous and higher) a larger portion of the nitrogen remains in the char. This finding is in agreement with the data of Mitchell et al.,[52] which was presented previously in Figure 2.5.

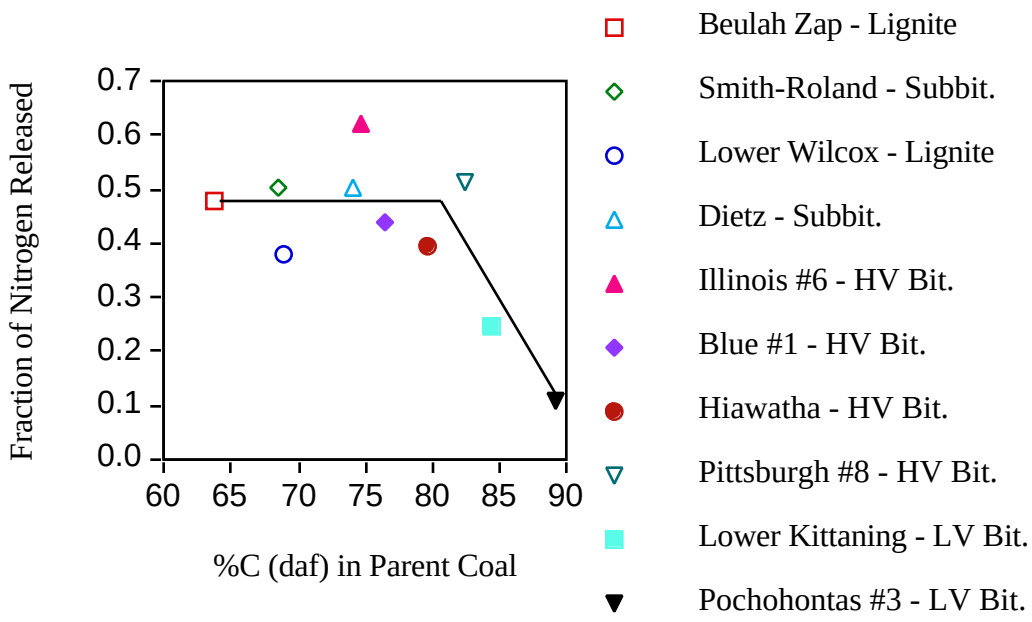

Figure 2.5. Nitrogen Volatiles Release versus Rank. Solid lines, provided as a guide for the reader, are not curve fits of data. Coal pyrolyzed in 6 mole % O_2 with flat flame methane burner, 47 ms, $5x10^4$ K/s (taken from Solomon and Fletcher[1]).

The release of HCN is reported to come from (a) ring opening reactions in the char and (b) ring opening reactions in the tar.[44, 55] It is thought that these two processes occur simultaneously at higher temperatures after the tar is released. The presence of HCN in the volatiles is generally taken as an indication that secondary pyrolysis has occurred. Secondary pyrolysis is the further break-down and reorganization of pyrolysis tars, at high temperatures in inert atmospheres, into (a) lighter molecular structures through cracking reactions or (b) polymerization reactions to form soot. Freihaut, et al.[44] used a heated grid apparatus and an entrained flow reactor to pyrolyze coal to show that HCN was produced after tar release occurred and at temperatures in excess of 1050 K. This finding is in agreement with that of many other researchers.[40, 41, 55-57] It is thought that the heterocyclic aromatic ring structures of the tar and char begin to thermally rupture at these temperatures.

Attempts have been made to correlate HCN production during pyrolysis with the relative amounts of the different functional forms of nitrogen in the coal (pyridinic, pyrrolic and quaternary).[29, 56] These attempts have not been very successful, indicating that the mechanisms for the release of nitrogen as HCN are complex. For example, it is not clear why two coals of similar rank and nitrogen content release different amounts of HCN during devolatilization. It is currently desired that the nitrogen release characteristics of a coal may be determined from the coal properties. It is clear that additional experiments are necessary to attain this goal.

There is also some evidence that ammonia (NH_3) may be formed during pyrolysis.[44, 53, 55] It has been suggested, however, that NH_3 is formed by the reaction of HCN with some other species, possibly the char itself.[29, 55-57]

Structure and Nitrogen Chemistry of Pyrolysis Products

Char Structure and Nitrogen Chemistry

The chemical structure of coal char has been studied by several researchers. The most successful analysis techniques have been solid-state ^{13}C NMR[58-60] and, to a lesser extent, thermogravimetric fourier transform infrared spectroscopy (TG-FTIR).[18, 43]

Several attempts have been made to study coal char structure with TG-FTIR techniques.[18, 42, 43] Solomon et al.[43] pyrolyzed five coals, ranging in rank from lignite to high volatile bituminous, at heating rates of 0.5 K/s, 3K/s and at constant temperature in a thermogravimetric analyzer. The temperatures used in this study ranged from 470 to over 1200 K. The results of this study indicated several trends during pyrolysis. It was shown that the char structure did not change significantly until temperatures exceeded approximately 600 K. Above this temperature, the most significant changes to the char structure were those of the side chains and bridges of the coal. Low rank coals, which typically contain relatively large amounts of oxygen-containing functional groups (mainly

carboxyl and hydroxyl groups), demonstrated cross-linking reactions at low temperatures. The decrease in tar formation during pyrolysis for low rank coals as compared to bituminous coal was attributed to this low temperature cross-linking behavior. Similar experiments by Ibarra et al.[42] confirmed these findings. The work of Solomon et al. also indicated that as pyrolysis proceeds, the char structure becomes increasingly aromatic. This finding are in agreement with ^{13}C NMR analyses described below.

The most successful technique for studying char structure has been solid-state ^{13}C NMR. Fletcher et al.[58] studied five coals of different rank with NMR. Five coals, ranging in rank from lignite to low volatile bituminous, were devolatilized and collected at various residence times. Pyrolysis conditions consisted of 100% nitrogen gas at temperatures of 1050 and 1250 K and particle heating rates of $2x10^4$ K/s. The resulting char samples were analyzed with the use of solid-state ^{13}C NMR. The changes in several key structural features were observed during pyrolysis.

Fletcher et al.[58] found that the total number of attachments per aromatic cluster (σ+1) did not change significantly during pyrolysis and that the number of bridges and loops per aromatic cluster (B.L.) increased with increasing mass release. This result indicates that cross-linking reactions probably occur at sites of existing side chains. Perhaps the most interesting finding of this study was that the carbon aromaticity, cluster molecular weight and number of aromatic carbons per cluster of fully devolatilized chars are very similar. This result was surprising since these parameters differ greatly in the parent coals. This similarity in the fully devolatilized char structure indicates that similar reactions are taking place for all coals. It was shown that the carbon aromaticity of these chars also increased with increasing mass release, confirming the findings of Solomon et al.[43] These findings were confirmed by Pugmire et al.[59] and Watt[61] in similar experiments.

Another useful technique for analyzing coal char nitrogen structures is X-ray photoelectron spectroscopy (XPS). Recently, chars produced in a drop tube reactor were

analyzed by XPS.[30] Five coals of differing rank were pyrolyzed in a drop tube reactor under 100% nitrogen gas at a gas temperature of 930 K and a particle heating rate of approximately 10^4 K/s. The resulting XPS nitrogen (1s) line shapes were fitted with peaks corresponding to pyridinic, pyrrolic and quaternary nitrogen functionalities. A quaternary nitrogen is one with four bonds to the nitrogen atom, creating a positively charged nitrogen structure. The levels of quaternary nitrogen in the chars were compared to that of the parent coals and a slight rank effect was observed. Chars from the low rank coals showed a slight increase or no change in quaternary nitrogen content as compared to the coals. The higher rank coals showed slight increases in quaternary nitrogen content. For all coals, the mole percent of pyridinic nitrogen in the chars remained relatively constant during pyrolysis (very slight increase for some). Also, for all coals, the levels of pyrrolic nitrogen decreased with pyrolysis. These data indicate that changes in the nitrogen functionalities of coal char occur during pyrolysis, although the mechanisms for such changes are not yet clear.

The pyrolysis of a Wyodak subbituminous coal was studied as a function of mass release in experiments similar to those described above.[30] Pyrolysis experiments were performed and the resulting char samples were analyzed with XPS. The nitrogen functional group distributions were found to be similar in all of the chars produced. Relative to the starting coal, there was a slight decrease in the levels of quaternary nitrogen and a slight increase in the levels of pyridinic nitrogen as pyrolysis proceeded. These data indicate that quaternary nitrogen species are preferentially lost at the very beginning of pyrolysis and are then released at the same rate as the total mass release.[30] This finding is in agreement with earlier work by Kelemen et al.[28] and Wojtowicz et al.[26]

Currently, very little is known about the nitrogen structure of coal char during pyrolysis. Further experiments and more sensitive analysis techniques are necessary in order to increase the understanding of these structures.

Tar Structure and Nitrogen Chemistry

The chemical structure of coal tar has been studied by many researchers and with many analysis techniques. Traditionally, coal tar has been studied with analysis techniques that require a liquid or a gas, such as mass spectroscopy, gas chromatography, field ionization mass spectrometry (FIMS), FTIR and ^{1}H NMR.[56, 59, 62, 63] Recently, high resolution liquid ^{13}C NMR has been used to study coal tar structure.[61, 64] The results of several experiments with these analysis techniques are discussed below.

Mass spectroscopy and gas chromatography experiments have shown that the molecular weight distributions of coal tar maximize in the range of 300 to 450 amu.[53, 65] Although the techniques employed in these experiments do have some weaknesses, it is generally accepted that this molecular weight range is correct. Based on chromatography and FTIR experiments, Freihaut et al.[53] reported that low rank coals produce tar with higher molecular weights than high rank coals. This work also indicated that tars from the lower rank coals are less like their parent coals than are tars from higher rank coals. Solomon, et al.[43] used FIMS to analyze the structural differences in the tars from the eight Argonne premium coals at slow heating rates (0.05 K/s). This FIMS analysis indicated that low rank coals produce tar with lower molecular weights than high rank coals. Meuzelaar, et al.[65] performed FIMS analysis on tars from the Argonne Premium coals at a heating rate of 100 K/s. This analysis was in general agreement with that of Solomon et al.[43] Other studies employing different techniques have also shown that tar structure is coal rank dependent.[53, 56, 62]

^{1}H NMR spectroscopy has been used to analyze coal tar structure.[59, 62] Five coals, ranging in rank from lignite to low volatile bituminous, were devolatilized and collected at various residence times. Pyrolysis conditions consisted of 100% nitrogen gas at temperatures of 1050 and 1250 K and particle heating rates of 2×10^{4} K/s. The resulting tar samples were analyzed with the use of ^{1}H NMR. These experiments indicated that pyrolysis temperature has a profound effect on the structure of the evolved tars. The

hydrogen aromaticity of the coal tars was seen to increase dramatically as the pyrolysis temperature increased. Decreases in α, β and γ hydrogens (in aliphatic structures) with increasing pyrolysis temperatures indicated that substantial bond rupture may be occurring in the bridge structures of the tar. These bond ruptures indicate that, at the elevated temperature (1250K), secondary tar reactions are occurring in the gas phase following tar evolution.[59]

Recently, a high resolution liquid ^{13}C NMR technique[21] was used to analyze the chemical structural features of coal tars. This technique used spin-lattice relaxation to differentiate protonated from nonprotonated carbons in liquid samples, based on relaxation differences arising from direct CH dipolar interactions. After the ratio of protonated to nonprotonated carbons was determined, many of the chemical structural features were calculated by comparing the data to numerous model compounds. Comparison studies were performed on model compounds between liquid NMR and solid-state NMR methods.[21] It was found that both methods gave comparable quantitative information regarding the carbon skeletal structure. In order to apply this technique to coal tars, the tar samples were dissolved in deuterated methylene chloride (CD_2Cl_2) and then filtered. The portion of the tar that was soluble in CD_2Cl_2 was analyzed with this liquid ^{13}C NMR technique. The nonsoluble portion was analyzed with standard solid-state ^{13}C NMR techniques.

Watt et al.[61, 64] pyrolyzed three coals of differing rank in a drop tube reactor under 100% nitrogen gas at a gas temperature of 930 K and a particle heating rate of approximately 10^4 K/s. The resulting tars were collected and analyzed with the ^{13}C NMR techniques described above. The data indicated that the chemical structure of the tar was significantly different from the original coal. Specifically, the number of aromatic carbons per cluster (C_{Cl}) in the tar was reported to be significantly lower than that of the parent coal. Additionally, the number of bridges and loops per cluster (B.L.) in the tar was reported to be much lower than that of either the coal or the matching char. These

results were surprising and were subject to question based on (a) the use of solvents prior to analysis of the tar and (b) collection of tar at relatively low temperatures where devolatilization was not complete.

Initial work on tar nitrogen chemistry indicated that the nitrogen structure of tar is similar to the nitrogen structures in the parent coal.[51] It was thought that nitrogen in coal exists in tightly bound compounds and hence the most thermally stable structures in the coal during devolatilization. It was thought that these nitrogen compounds are released without rupture as part of the tar. For this reason, it was thought that the nitrogen structure of tar is similar to the nitrogen structures in the parent coal.

Nelson et al.[56] applied nitrogen-specific gas chromatography to the study of coal tars. Three coals were pyrolyzed at temperatures ranging from 900 to 1300 K at a heating rate of approximately 10^4 K/s in a fluidized bed apparatus. The tars were collected and analyzed with nitrogen-specific gas chromatography. Pyridinic and pyrrolic nitrogen functionalities were identified in the tars. The data also indicated that the complexity (variety of nitrogen containing compounds) of the tars increases with increasing rank. Additionally, it was found that the pyrrole:pyridine ratio of the tars increased with coal rank. Nelson's data are helpful, but are limited in value since the parent coal and char can not be analyzed with this technique. This prevents the study of solid-phase nitrogen chemistry during devolatilization with this technique.

XPS has been applied to the study of tar nitrogen chemistry.[27, 28, 30] A study of coal tar, produced at a temperature of 673 K and a 0.5 K/s heating rate, confirmed that nitrogen in tar is located in pyridinic and pyrrolic forms.[27, 28] Recently, tars produced in a drop tube reactor were analyzed by XPS.[30] Five coals of differing rank were pyrolyzed in a drop tube reactor under 100% nitrogen gas at a gas temperature of 930 K and a particle heating rate of approximately 10^4 K/s. The resulting XPS nitrogen (1s) line shapes were fitted with peaks corresponding to pyridinic, pyrrolic, quaternary and amino nitrogen functionalities. It was found that the tars contained lower levels of quaternary

nitrogen than the parent coals. The tars also contained low levels of amino nitrogen functionalities (8-13 mole %), which were not seen in the parent coals.[30]

As can be seen from this discussion, little is currently known about the nitrogen structure of coal tar during pyrolysis. Additional experiments with more sensitive analysis techniques, such as Dynamic Nuclear Polarization (DNP) ^{15}N NMR, are necessary in order to increase the understanding of these structures.

Literature Summary

The previous sections contain a literature review of the current state of coal pyrolysis research. Solid-state ^{13}C NMR techniques have been used successfully to elucidate the chemical structural features of coal and char. The chemical structural features of tar are still not well known. A summary of the results of the coal tar structural analyses that are available in the literature is provided in Table 2.3. As seen in the table, the current knowledge of coal tar structure is quite limited. Recent advances in ^{13}C NMR have made possible a quantitative, in-depth study of the structure of coal tar. The weakest link in a more complete understanding of the coal devolatilization process is the lack of information available on the chemical structure of coal tar during this process. This thesis is designed to provide additional insight into the chemical structure of coal char and tar during the devolatilization process. Since the structure of tar is not known as well as the structure of the other pyrolysis products, particular attention is given to the structure of tar in this thesis. The results of this thesis are necessary to increase the understanding of the devolatilization process.

Table 2.3

Summary of Coal Tar Analyses Reported in the Literature

Analysis Technique	Reference	Results
Mass Spectroscopy	Freihaut et al.[53]	Tar molecular weight range is 300 to 450 amu
	Simmleit et al.[65]	Tar molecular weight range is 220 to 450 amu
	Solomon, et al.[43]	Low rank coals produce tar with lower molecular weights than high rank coals
FTIR	Freihaut et al.[53]	Low rank coals produce tar with higher molecular weights than high rank coals
^{1}H NMR	Pugmire et al.[59]	Hydrogen aromaticity increases with pyrolysis temperature; bond rupture may be occurring in bridge structures
	Fletcher et al.[62]	Only small changes occur to the tar structure below 1050 K
Liquid-state ^{13}C NMR	Watt et al.[61, 64]	C_{Cl} in tar significantly lower that C_{Cl} in coal
Gas Chromatography	Nelson et al.[56]	Pyridinic and Pyrrolic nitrogen functionalities identified in coal tar; pyrrolic:pyridinic ratio increased with coal rank
XPS	Kelemen et al.[27, 28]	Pyridinic, pyrrolic and quaternary nitrogen functionalities identified in coal tar
	Kelemen et al.[30]	Tars contain low levels of amino nitrogen functionalities (8-13 mole %) which were not seen in the parent coals

3. Objectives and Approach

The three main objectives of this study are (1) to improve the understanding of the chemical structure of coal tar and char during pyrolysis, (2) to increase the understanding of the chemical processes that occur during pyrolysis and (3) to improve the understanding of the fate of coal nitrogen during pyrolysis. In order to gain these additional insights, pyrolysis experiments were performed to collect char, tar and gaseous samples for analysis by various techniques.

Pyrolysis experiments were performed in two separate reactors: (1) an electrically heated drop tube furnace was used to perform experiments at low to moderate temperatures (850 to 1220 K) with heating rates on the order of ~10^4 K/s and (2) additional pyrolysis experiments were performed using a methane air flat-flame burner (FFB). The peak temperature used in the FFB was 1650 K while the heating rate was ~10^5 K/s. The heating rates of these FFB experiments approach those expected in pulverized coal furnaces (~10^5 to 10^6 K/s) and therefore the results of this study should be pertinent to processes occurring in such furnaces. All experiments in this study were performed at atmospheric pressure.

Five coals of different rank were pyrolyzed in the drop tube furnace. Eleven coals that span a range of rank, from lignite to anthracite, were pyrolyzed in the FFB. The experiments performed in the FFB provided char samples under conditions of complete pyrolysis. Three different temperature conditions were used in the drop tube furnace to provide matching sets of char, tar and gaseous samples that were pyrolyzed to different degrees.

4. Description of Experiments

Two different reactors were used to pyrolyze the coal particles; a drop tube entrained flow system and a methane air flat-flame burner. The drop tube furnace employed in this study was a modified form of the High Pressure Controlled-Profile (HPCP) drop tube reactor previously used by other researchers. These reactors were used to pyrolyze coal particles at different temperatures, particle heating rates and extents of devolatilization. A description of the modification of the HPCP, experimental apparatus, chemical analysis techniques and experimental procedure used in this study is found below.

Apparatus

Drop Tube Reactor Modifications

The drop tube furnace employed in this study is a modified form of the High Pressure Controlled-Profile (HPCP) drop tube reactor[66, 67] previously used by other researchers.[61, 64, 66-70] Although several modifications were made to the HPCP, its high pressure capability was maintained. Due to excessively high failure rates, the heating elements were replaced. Also, the performance of the original preheater was not acceptable and it was entirely redesigned. These modifications are described in more detail below.

The HPCP reactor and preheater sections were unreliable because of the frequent failure of the Super Kanthal heating elements (see Figure 4.1 for a schematic diagram of the HPCP in original form). These heating elements typically failed at a rate of approximately one every two weeks. These Super Kanthal heating elements were used to control the temperature inside the reactor and preheater sections of the HPCP. The instability of the Super Kanthal heating elements limited the time available to perform

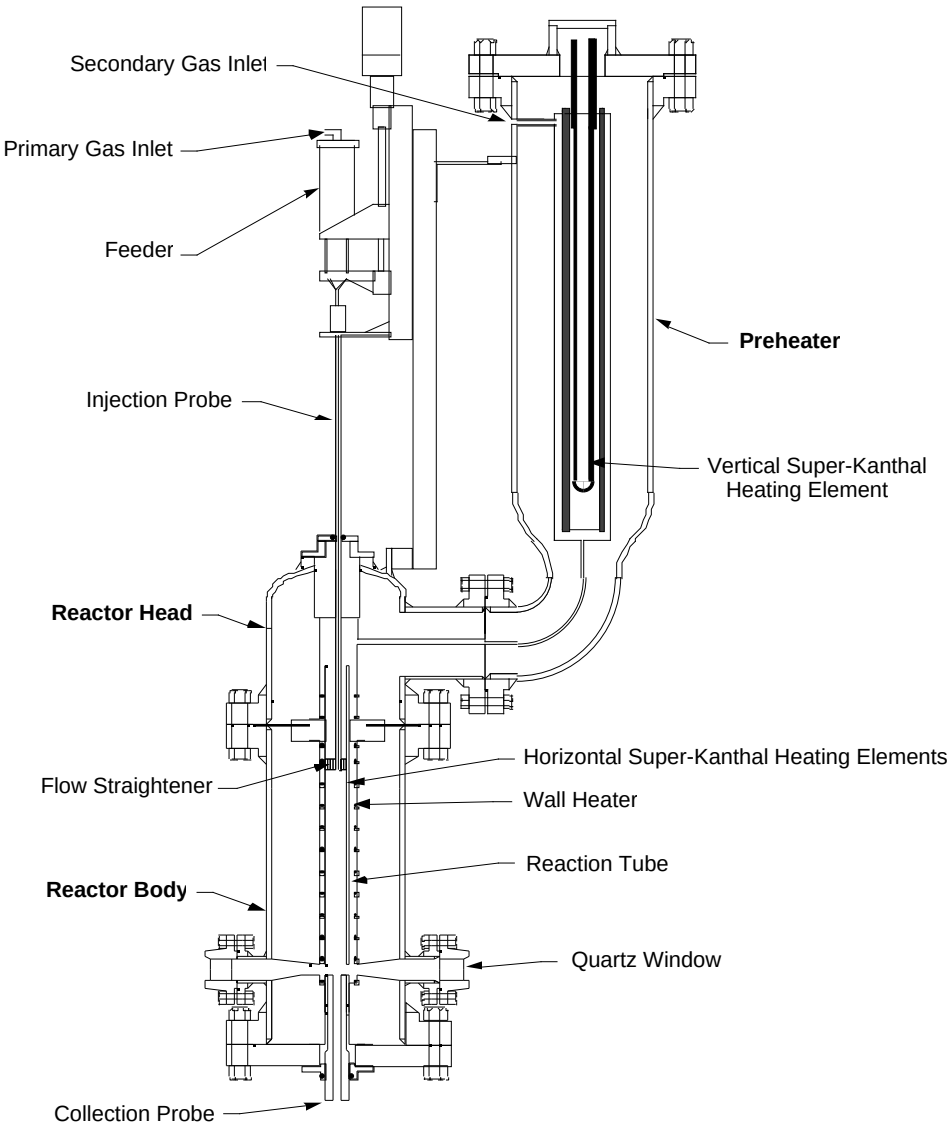

Figure 4.1. Schematic of the High Pressure Controlled Profile (HPCP) Drop Tube Reactor in Original Form.[66]

experiments. It was therefore decided that these heating elements should be replaced with more conventional and reliable heating elements. In the reactor section of the HPCP, the twelve horizontally oriented Super Kanthal heating elements were replaced with two semi-cylindrical nichrome wire heating elements. In the preheater section of the HPCP, the one Super Kanthal element was replaced with two semi-cylindrical nichrome wire heating elements (see Figure 4.2 for a schematic diagram of the Drop Tube Reactor in its modified form). These nichrome wire heating elements are manufactured by Thermcraft of Winston-Salem, SC and are rated to 1473 K. They consist of a twisted pair of nichrome wires embedded in a ceramic support.

Due to the extreme change in the type of heating elements used, the insulation system of the reactor also required replacement. The internals of the reactor body and the preheater were completely removed. The new insulation package consists of two semi-cylinders of high temperature compressed fiber ceramic insulation wrapped with a layer of blanket type ceramic fiber insulation. This type of insulation package was used in both the reactor body and the preheater (see Figures 4.2, 4.3 and 4.4).

Due to the nature of the heating element changes, the temperature control system of this apparatus also required modification. The previous IBM-computer-based control system was replaced with a microprocessor-based temperature/power controller unit. This unit was built to specifications by Thermcraft. This temperature controller uses a microprocessor-based proportional-integral-derivative (PID) controller to separately maintain the temperature of the reactor and preheater.

The design of the gas flow channel in the original HPCP preheater also came into question due to poor performance. At high temperature settings (~1300 K) and moderate gas flow rates, the preheater was generating exit gas temperatures of only 500 K. After visual inspection of the insulation system and an analysis of the gas flow path, it was suspected that only a fraction of the incoming gas was passing through the heated annulus as intended. An alternate flow path may have developed, which enabled the gas to be

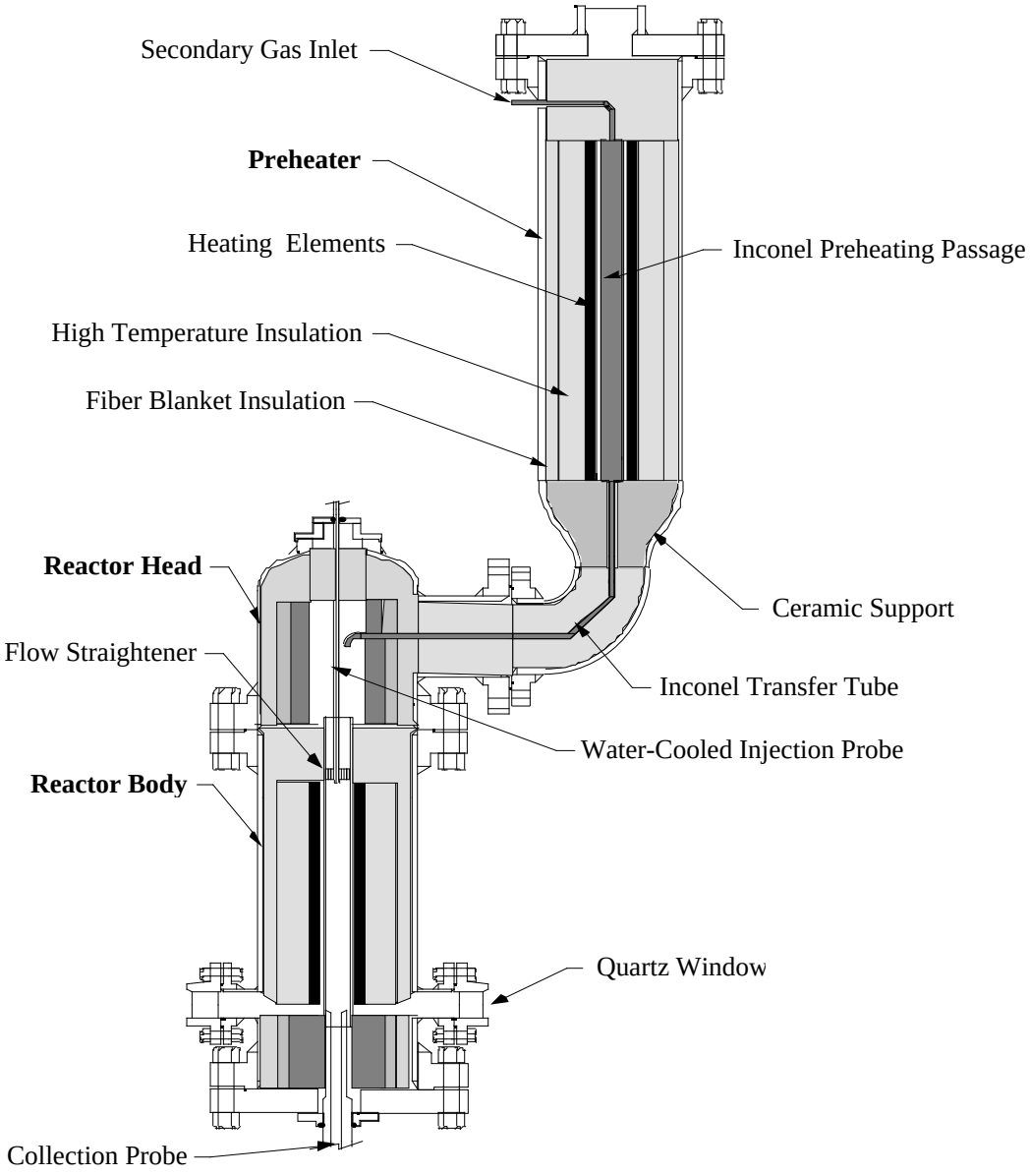

Figure 4.2. Schematic of the High Pressure Controlled Profile (HPCP) Drop Tube Reactor in Modified Form.

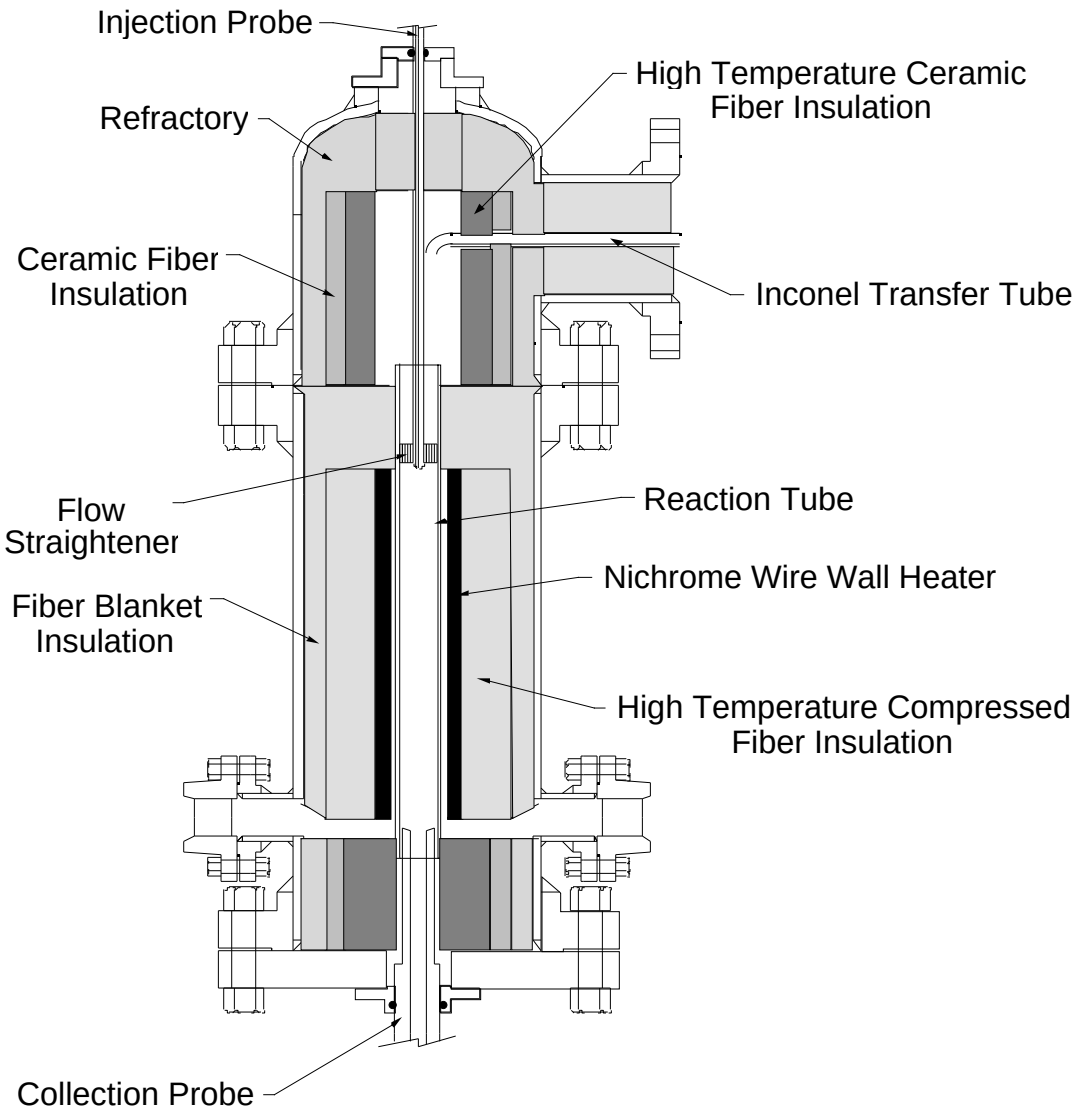

Figure 4.3. Cross-section of Reactor Body in Modified Form.

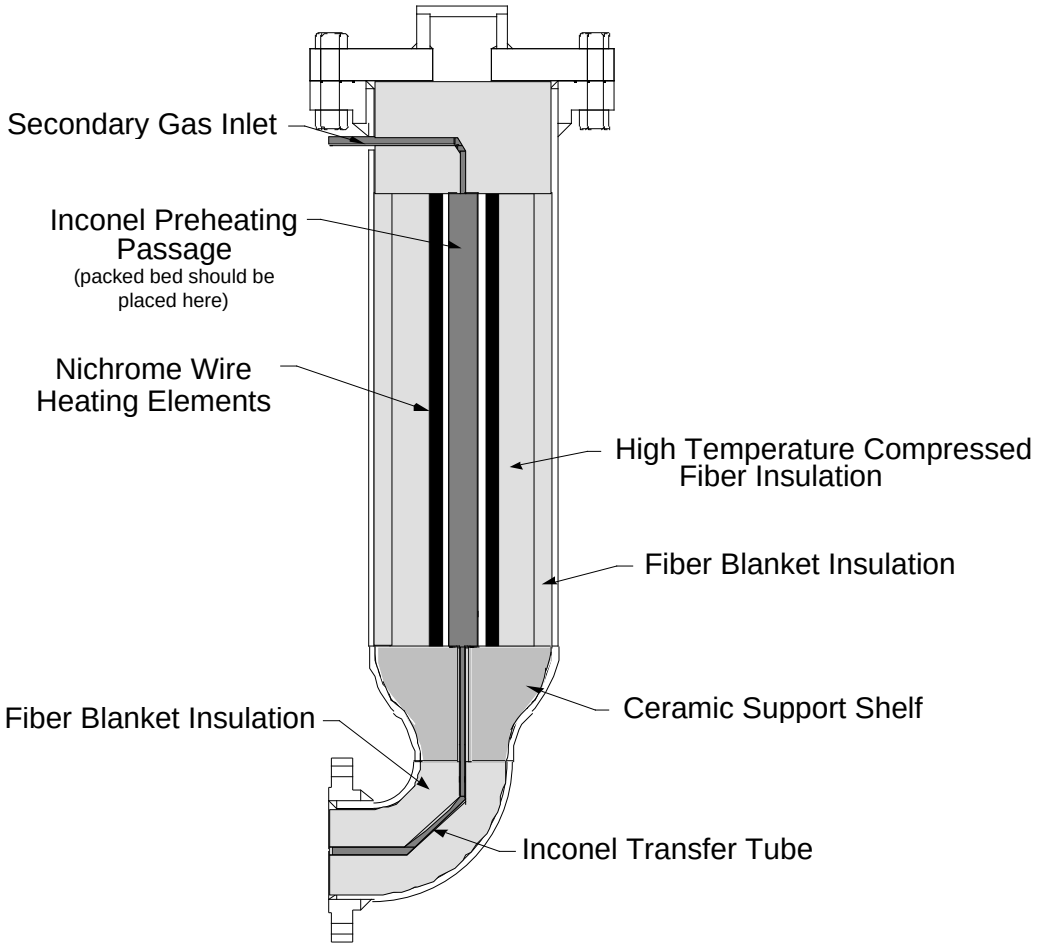

Figure 4.4. Cross-section of Preheater in Modified Form.

diverted around the intended heating zone. For this reason, the gas flow path of the preheater was redesigned. The gas now flows inside a tubing system for the entire length of the preheater (see Figure 4.2). Incoming gas travels to a cylindrical Inconel canister. This canister is surrounded by two semi-cylindrical nichrome wire heating elements as described above. At the exit of this heated canister, the gas flows through a tubing system into the reactor head. This heated canister is currently empty, but has the capability to be packed with ceramic beads or other materials larger than 1/8" diameter. Exit gas temperatures of the preheater are now approximately 800 K. It is expected that these temperatures would increase if the preheater were operated in packed bed mode.

Since completion of these modifications, no unexpected heater-related shutdowns have occurred. This was a major contribution of this research project, and permitted the completion of the pyrolysis experiments described in this study. It is anticipated that these modifications will also benefit many future pyrolysis and char oxidation experiments.

Drop Tube Reactor

The Drop Tube Reactor is a laminar flow furnace with a controlled wall temperature. Solid and gaseous products are aerodynamically separated and collected for analysis. A schematic diagram of the Drop Tube Reactor is shown in Figure 4.2. Pulverized coal particles are fed with the primary gas through a water-cooled injection probe. This probe may be moved in order to vary the injection point in the reactor and hence the particle residence time. A collection probe collects the entire gaseous and particle flow and quenches the particle reaction. The collection probe is water-cooled with gas quench jets in the probe tip. A permeable liner inside the main probe tube allows quench gas to be injected radially along the length of the probe to reduce particle and tar deposition inside the probe. A virtual impactor follows in-line with the collection probe to aerodynamically separate the gases from the heavier particles. A cyclone

follows the virtual impactor to further separate the aerosols from the heavier char particles. The char particles are captured in the cyclone and the tars are collected on polycarbonate filters that are located after the virtual impactor and the cyclone (see Fig 4.5 for a flow diagram of the collection system). The tar is scraped from the polycarbonate filters after completion of the experiment. The light gases pass through the filters and are analyzed for hydrogen cyanide (HCN) concentration before being vented. A description of the gas phase analysis for HCN is described below. Detailed design information of the collection system is found elsewhere.[71]

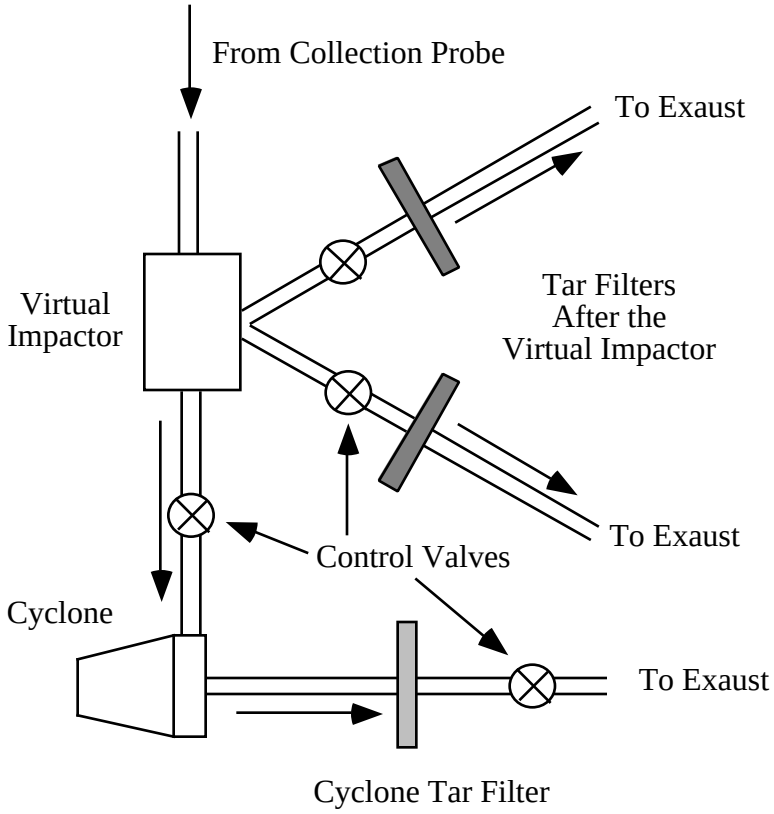

Figure 4.5. Flow Diagram of the Drop Tube Reactor Collection System.[71]

Watt[61] performed an analysis to determine the amount of tar deposition on the inner walls of this collection system (i.e., the virtual impactor, cyclone, and associated

tubing). For a set of pyrolysis experiments, the tar was scraped from the collection system and weighed. The deposition per unit surface area was obtained and applied to surfaces where it was impossible to scrape, such as in some of the tubing. The mass of tar lost to deposition on the walls of the collection system was compared to the mass of tar collected on the tar collection filters. Based on this analysis, the mass of tar collected is corrected by 20% to account for deposition on the walls of the collection system. This is similar to the correction factors of ~10% used by Chen[72] and 15% used by Ma[73, 74] in similar experiments.

Methane Air Flat-Flame Burner System (FFB)

A schematic diagram of the flat-flame burner reactor system is shown in Fig. 4.6. It consists of a Hencken flat flame burner, similar to that used at Sandia.[52, 75] A detailed description is found elsewhere.[74] The air, methane and hydrogen burn to provide a high-temperature flame environment for coal pyrolysis. The outlet of the burner is a 2" by 2" square. The flow rates of air, methane and hydrogen are adjusted to obtain a horizontally uniform flame. The velocity of the hot gas above the burner is approximately 3 m/s (i.e., laminar flow). The coal particles are fed into the burner by a syringe particle feeder, driven by a stepping motor. The pulse signal used for driving the stepping motor is generated by a computer. The feed rate of coal particles can be adjusted by changing the frequency of the pulse signal (i.e., the stepping rate of the motor). The coal particles are entrained by a stream of carrier nitrogen gas. The hot combustion products from the methane/hydrogen/air flame heat the coal particles which are injected along the centerline of the laminar flow reactor. The flat flame can be operated under either fuel-rich or fuel-lean conditions so that the post-flame gases provide a reducing or oxidizing atmosphere for coal devolatilization and/or oxidation. Fuel-rich conditions with no post-flame oxygen were used in these experiments. The flame temperature can be adjusted by changing the flow rates of inert gas, fuel and oxidizer. Flame temperatures along the height of the

tower are measured in the absence of particles using a fine-wire silica-coated type B thermocouple. Measured thermocouple readings are corrected for radiation heat loss as described below. The particle feed rate used is ~1 g/hr, which is small enough to achieve single particle behavior.

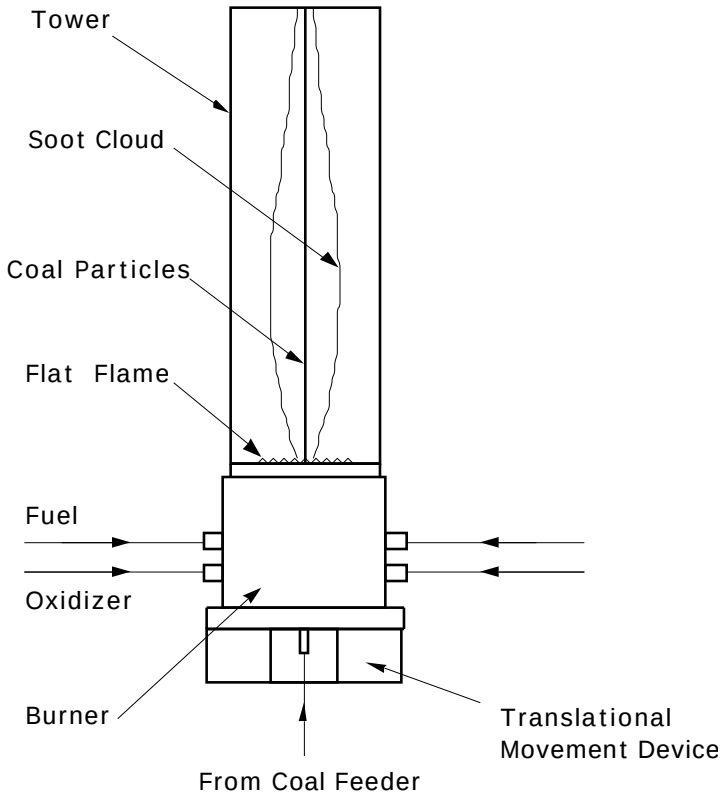

Figure 4.6. Schematic of the Methane Air Flat-Flame Burner (FFB).[61]

The FFB is equipped with a water-cooled, gas-quench probe with porous liner for reduced deposition, and the probe is followed by a virtual impactor, cyclone, and filter system patterned after the collection system described above in the Drop Tube Reactor. The FFB experiments performed in this research provide char and soot samples from a high temperature, high heating rate environment, with products of hydrocarbon combustion present. The FFB environment is closer to industrial combustor

environments than conventional drop tube furnaces, due to higher particle heating rates, temperatures and gas composition. The FFB experiments give data regarding complete devolatilization, while the Drop Tube Reactor experiments can be used to study the intermediate char, tar and gaseous products of devolatilization.

Chemical Analysis Techniques

A number of analysis techniques were used to study the char, tar and gaseous samples that were produced in this study. A full explanation of these different methods is found below.

Proximate and Ultimate Analysis

Proximate analysis was performed on the coal and char samples following ASTM standard procedures. Proximate analysis is the term used when the amount of moisture and non-combustible material (i.e. ash) in the samples is measured. An electrically heated oven is used to dry the sample. The sample is then weighed and returned to the oven, where the samples is heated further to combust the organic matter. The ash that remains is then weighed.

Ultimate analyses (i.e. elemental composition) were performed for the coal, char and tar samples of this study. Carbon, hydrogen, nitrogen and sulfur contents were determined at BYU with the use of a LECO CHNS-932 elemental analyzer. The analyzer was calibrated with several coal standards of known composition (obtained from Leco Corporation, origin unknown).

ICP Analysis

Inductively coupled plasma (ICP) atomic emission spectroscopy was used to determine the mass fraction of Titanium (Ti) in the parent coal and char samples. This analysis techniques is used to help confirm the mass release occurring during the pyrolysis experiments of this study (Ti is used as a tracer).[76] The ICP analysis was

performed at the BYU with the use of a Perkin Elmer Plasma 2 ICP machine. Assuming no Ti loss in the pyrolysis and ashing processes, the mass fractions of Ti in parent dry coal (f_{Ti}^{coal}), in dry char (f_{Ti}^{char}) and in ash (f_{Ti}^{ash}) are related to the masses of the coal (m_{coal}), char (m_{char}) and ash (m_{ash}) by:

$$m_{coal} f_{Ti}^{coal} = m_{char} f_{Ti}^{char} = m_{ash} f_{Ti}^{ash} \tag{4.1}$$

The percentage mass release or total volatile yield Y_{vol} (on dry ash free basis) during pyrolysis can then be calculated:

$$Y_{vol} = \frac{m_{coal} - m_{char}}{m_{coal} - m_{ash}} = \frac{m_{coal} - \frac{f_{Ti}^{coal}}{f_{Ti}^{char}} m_{coal}}{m_{coal} - \frac{f_{Ti}^{coal}}{f_{Ti}^{ash}} m_{coal}} = \left(\frac{f_{Ti}^{char} - f_{Ti}^{coal}}{f_{Ti}^{ash} - f_{Ti}^{coal}}\right)\left(\frac{f_{Ti}^{ash}}{f_{Ti}^{char}}\right) \tag{4.2}$$

The mass release determined from the Ti-tracer technique is compared to the ash tracer technique (from proximate analysis) and to the mass balance (mass of coal fed to the reactor compared with the mass of char collected). In most cases the mass balance and the Ti-tracer technique agree to within 5%. Since the Ti-tracer technique is based on a comparison of the relative amounts of Ti in the coal and char, absolute calibration of the ICP analyzer is not necessary. It has been shown that at high temperatures, ash and even Ti can volatilize, giving incorrect mass loss values.[77] In the case of the experiments performed for this study, the temperatures are not high enough to be affected by Ti volatilization to any significant degree.[61]

HCN Concentration

As mentioned above, the gaseous pyrolysis products generated in the Drop Tube Reactor are analyzed for hydrogen cyanide (HCN) concentration before being vented

(concentrations were much lower than the threshold limit value or TLV). Gas samples are taken continuously (800 cc/min) from sample ports located immediately after the primary tar filters (see Figure 4.5). These gases travel a short distance through Teflon tubing to a Zellweger Analytics Model 7100 Toxic Gas Monitor equipped with a Low Level Hydrogen Cyanide Chemcassette. This detector employs a chemiluminescent analysis technique in which the sampled gas reacts with chemicals on the chemcassette and forms a stain that is simultaneously read by an electro-optical sensing system. This electro-optical sensing system determines the concentration of the gas from the color of the stain and calibrated concentration/stain relationships. The claimed repeatability of this device is ~±5% at 10 ppm. It is expected that the repeatability of this analyzer is significantly worse at the concentrations encountered in this study (0 to 1500 ppb). The detection range of this analyzer is 90 to 4000 ppb HCN.

The HCN analyzer was calibrated prior to use in the pyrolysis experiments of this study. Gas ampoules of HCN were obtained from Mine Safety Appliances Company of Pittsburgh, PA. The HCN gas in these ampoules is known to dilute to 10 ppm in 5 liters. Three sizes of Tedlar gas sampling bags (20.3, 37.7 and 85.7 liters) were used to dilute the HCN in the ampoules to three known (standard) concentrations. For each sample, an ampoule was introduced into a tubing system that connected the gas sampling bag to a cylinder of nitrogen gas. The ampoule was broken as the gas sampling bag was filled with nitrogen gas, mixing and diluting the HCN into the nitrogen gas. The gas in the sampling bag was then analyzed with the HCN monitor until the bag was empty. The HCN monitor determined the time-weighted average HCN concentration of the gas. For each bag size, three analyses were performed and the results averaged. These measured concentrations were compared to the known concentration of the gas (see Table 4.1).

Table 4.1
Results of HCN Analyzer Calibration

Standard HCN Concentration (ppb)	Measured HCN Concentration (ppb)
583	266
1326	534
2463	1168

Figure 4.7 contains a plot of measured HCN concentrations versus standard HCN concentrations (the markers represent the average concentration of the three repeat analyses, the error bars represent ±2 times the standard deviation). As seen in the figure, the error in the HCN analyzer is linear. All HCN concentrations used in this study have been corrected by dividing the measured concentration by the slope of the line in Figure 4.7.

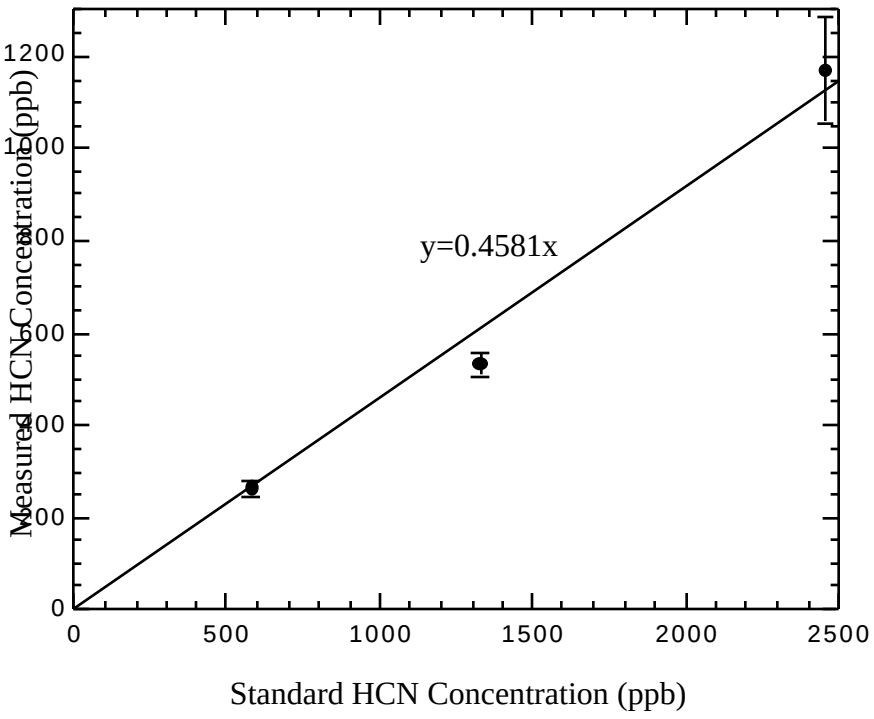

Figure 4.7. Measured and Standard HCN Concentrations during Calibration Procedure. Error bars represent ±2σ.

NMR Analyses

Standard solid-state ^{13}C NMR spectroscopic techniques were used to determine the chemical structural features of the coals, chars and tars in this study. Cross-polarization (CP), magic angle spinning (MAS) and dipolar dephasing techniques permit direct measurement of the number and diversity of aromatic and nonaromatic carbons present in the sample.[19, 22] It has been shown that carbon aromaticities obtained from this technique compare favorably with carbon aromaticities obtained from the Bloch decay experiments.[60] Two of the coal-tar-char sets produced in this study were also examined with solid-state ^{15}N NMR (CP/MAS) techniques.[32]

Experimental Procedure

Test Matrix

In order to improve the understanding of the chemical structure of coal tar and char during pyrolysis and to increase the understanding of the fate of coal nitrogen during pyrolysis, pyrolysis experiments were performed in the Drop Tube Reactor and in the Flat Flame Burner. The test variables used in this study are: maximum gas temperature, residence time and coal type. In the Drop Tube Reactor, five coals of different rank were pyrolyzed at three different experimental conditions (temperatures and residence times) and hence degrees of pyrolysis. These five coals were obtained from the suite of coals selected by the DOE Pittsburgh Energy Technology Center's Direct Utilization/AR&TD (PETC) program. These coals were crushed and aerodynamically classified to the 63 - 75 μm size range. The properties of these five coals are located in Table 4.2. In the FFB, eleven coals that span a range of rank, from lignite to anthracite, were pyrolyzed at one condition. These coals were crushed and classified to the 53 to 75 μm size range. The properties of these eleven coals are located in Table 4.3.

Table 4.2
Properties of Coals Used in Drop Tube Reactor Experiments

Coal	PSOC ID	Rank	%C (daf)	%H (daf)	%N (daf)	%S (daf)	%O (daf) (by diff.)	%Ash (dry)
Beulah Zap	1507D	ligA	64.16	4.78	0.94	1.81	28.32	13.92
Blue #1	1445D	subA	74.23	5.48	1.30	0.65	18.35	3.29
Illinois #6	1493D	hvCb	74.81	5.33	1.48	4.85	13.54	9.65
Pittsburgh #8	1451D	hvAb	82.77	5.61	1.74	0.98	8.90	4.29
Pocahontas #3	1508D	lvb	90.92	4.51	1.34	0.82	2.41	11.92

Table 4.3
Properties of Coals Used in Flat Flame Burner Experiments

Coal	ID #	Rank	%C (daf)	%H (daf)	%N (daf)	%S (daf)	%O (daf) (by diff.)	%Ash (dry)
Bottom	D-1[a]	lig	70.68	5.83	1.47	1.18	20.83	15.19
Adaville #1	D-7	subA	72.48	5.22	1.17	1.04	20.09	3.55
Beulah	D-11	lig	68.46	4.94	1.00	0.64	24.96	7.74
Sewell	D-13	mvb	85.54	4.91	1.72	0.72	7.12	4.25
Kentucky #8	D-18	hvBb	79.37	5.62	1.74	4.71	8.57	12.23
Elkhorn #3	D-20	hvAb	82.74	5.73	1.78	0.99	8.76	4.98
Lykens Valley #2	D-21	an	93.78	2.72	0.92	0.62	1.96	10.37
Deadman	D-27	subA	76.51	5.24	1.53	0.76	15.95	12.44
Penna. Semain C	P-1515	sa	88.40	4.02	1.24	0.86	5.47	25.93
Lower Kittanning	P-1516	lvb	86.24	4.86	1.81	2.45	4.64	17.73
Smith Roland	P-1520	subC	67.40	5.37	1.00	1.84	24.39	13.62

[a]D = DECS, P=PSOC

As previously mentioned, the pyrolysis experiments performed in the Drop Tube Reactor were carried out at three different gas temperatures and residence times. These conditions provided different degrees of devolatilization. The experimental conditions used in the Drop Tube Reactor experiments are shown in Table 4.4. These experiments were performed at atmospheric pressure in a nitrogen gas atmosphere. The reactor, preheater and flow settings that were used to obtain these three conditions are provided in

Appendix A. The pyrolysis experiments performed in the FFB were under conditions of excess methane fuel (0% post flame O_2, fuel equivalence ratio = 1.48, 10% by volume dilution N_2) with a maximum gas temperature of 1650 K, 15 ms residence time and a heating rate of approximately 10^5 K/s.

Table 4.4
Experimental Conditions Used in Drop Tube Reactor

Condition	Maximum Gas Temp. (K)	Residence Time(ms)
Low Temp	820	170
Medium Temp	1080	285
High Temp	1220	412

Temperature Profiles and Particle Residence Times

In order to properly interpret the results of the pyrolysis experiments performed in this study, it is important to know the temperature history of the coal particles. The centerline gas temperature profiles in the Drop Tube Reactor and the FFB were measured for each condition employed. This measurement process is described elsewhere, in detail, for each apparatus.[61, 74] The measured thermocouple temperatures are corrected for radiation effects to obtain the correct gas temperatures. This correction process is described by Watt.[61] Gas temperature histories are then used to determine particle temperature histories. The centerline gas temperature profiles in the Drop Tube Reactor are shown in Figure 4.8 for each experimental condition used. In the future, these conditions will be referred to by their approximate maximum gas temperatures. It is difficult to align the thermocouple probe along the precise centerline of the Drop Tube Reactor. For this reason, it is expected that centerline gas temperatures are accurate to within ~±30 K of the stated measurement.

Experimental conditions in the FFB are different than those in the Drop Tube Reactor. The flame conditions in the FFB were analyzed by Ma.[74] The maximum

centerline gas temperature for all the experiments in the FFB was 1640 K. The centerline gas temperature profile for the FFB experiments is shown in Fig. 4.9. It is noted that the temperature decreases slightly near the burner, due to a small amount of ambient temperature nitrogen gas used to carry the coal particles to be injected into the flame.

The particle residence times reported in this thesis were determined in a manner similar to that used by Watt.[61] The reader is referred to Watt's work for a detailed description of the residence time calculations.

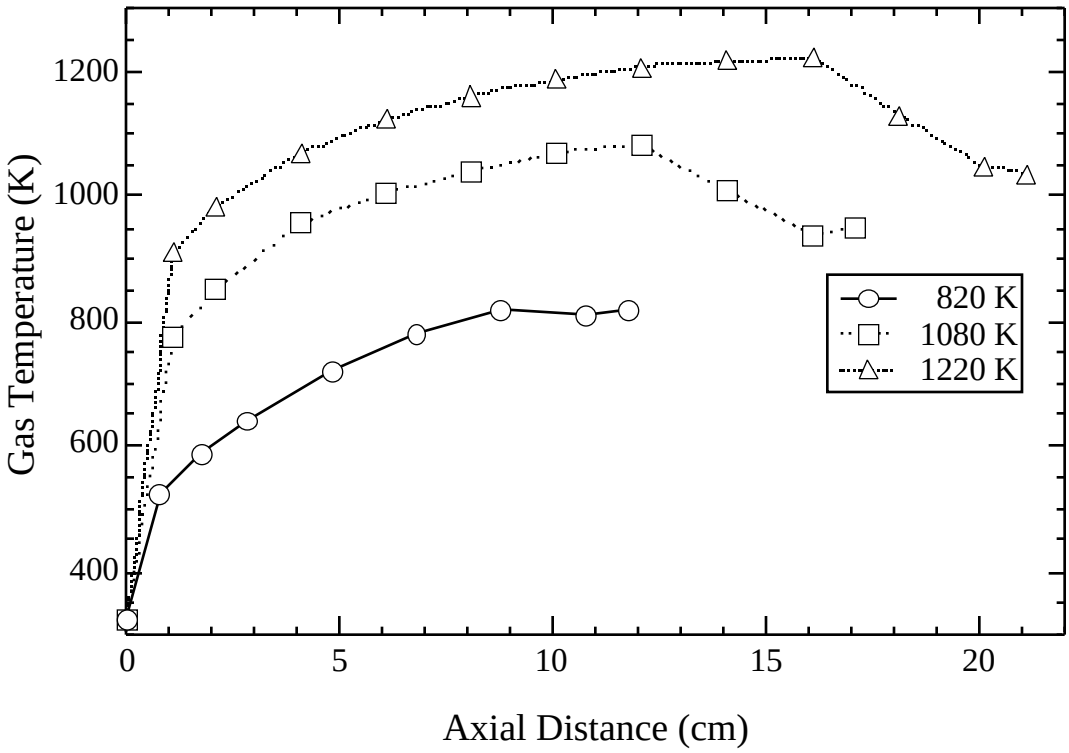

Figure 4.8. Centerline Gas Temperature Profiles for the Experiments Performed in the Drop Tube Reactor.

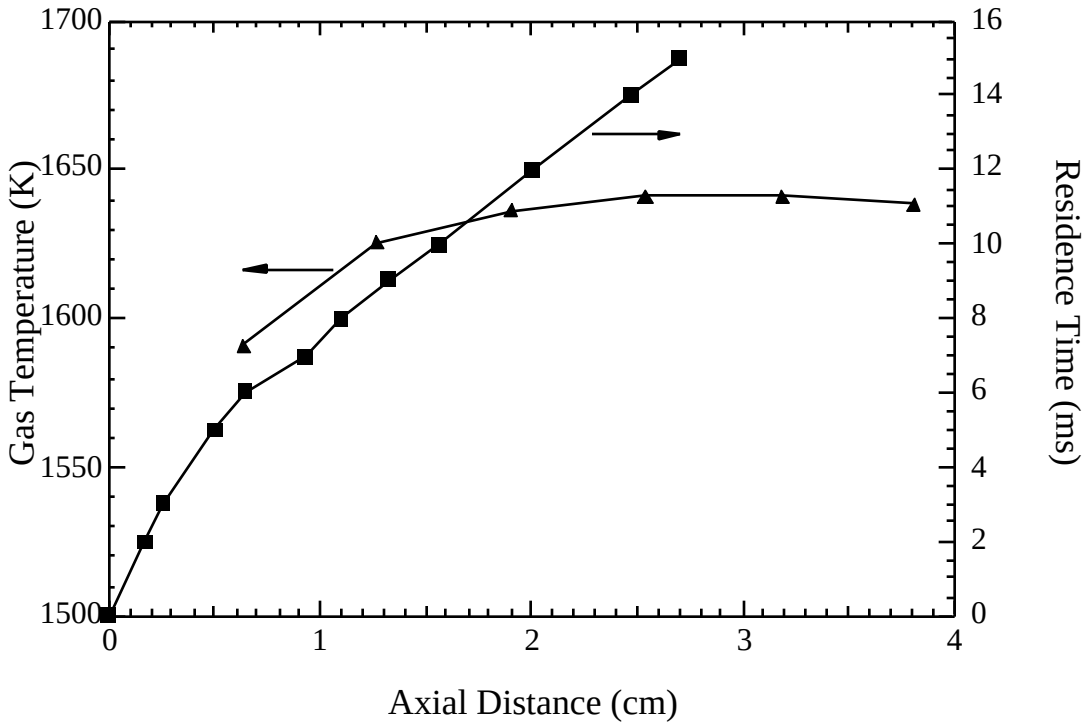

Figure 4.9. Centerline Gas Temperature Measurements for the Experiments Performed in the FFB.[74]

5. Experimental Results

Mass, Tar and Nitrogen Release

Drop Tube Reactor Pyrolysis Experiments

Fifteen different pyrolysis experiments were performed in the Drop Tube Reactor. Table 5.1 contains a summary of these experiments. Mass, tar and nitrogen release are reported as a fraction of dry, ash-free (daf) coal. The mass release is calculated by comparing the mass of daf coal fed to the mass of daf char collected.

Table 5.1
Summary of Drop Tube Reactor Pyrolysis Experiments

Coal	Condition	Mass Release (daf)	Tar Release (daf)	Nitrogen Release (daf)
Beulah Zap	820 K	0.294	0.008	0.217
	1080 K	0.519	0.033	0.352
	1220 K	0.495	0.016	0.306
Blue #1	820 K	0.107	0.010	0.085
	1080 K	0.512	0.145	0.372
	1220 K	0.577	0.096	0.476
Illinois #6	820 K	0.106	0.009	0.049
	1080 K	0.592	0.180	0.485
	1220 K	0.570	0.147	0.435
Pittsburgh #8	820 K	0.103	0.010	0.073
	1080 K	0.479	0.225	0.372
	1220 K	0.558	0.200	0.456
Pocahontas #3	820 K	0.051	0.002	0.091
	1080 K	0.271	0.096	0.224
	1220 K	0.241	0.092	0.128

As expected, the mass release increases with pyrolysis temperature for all coal. For all coals, the tar release increases with pyrolysis temperature, reaching a maximum at the 1080 K condition and decreasing slightly at the 1220 K condition. This decrease in tar yield is due to secondary reactions in which part of the released tar is broken down into smaller molecules that are able to pass through the reactor collection system as gases. Tar release is also a function of coal rank (see Figure 5.1). For each temperature condition, the tar yield increases with rank, reaching a maximum at the Pittsburgh #8 high volatile A bituminous coal and decreasing for the Pocahontas #3 low volatile bituminous coal.

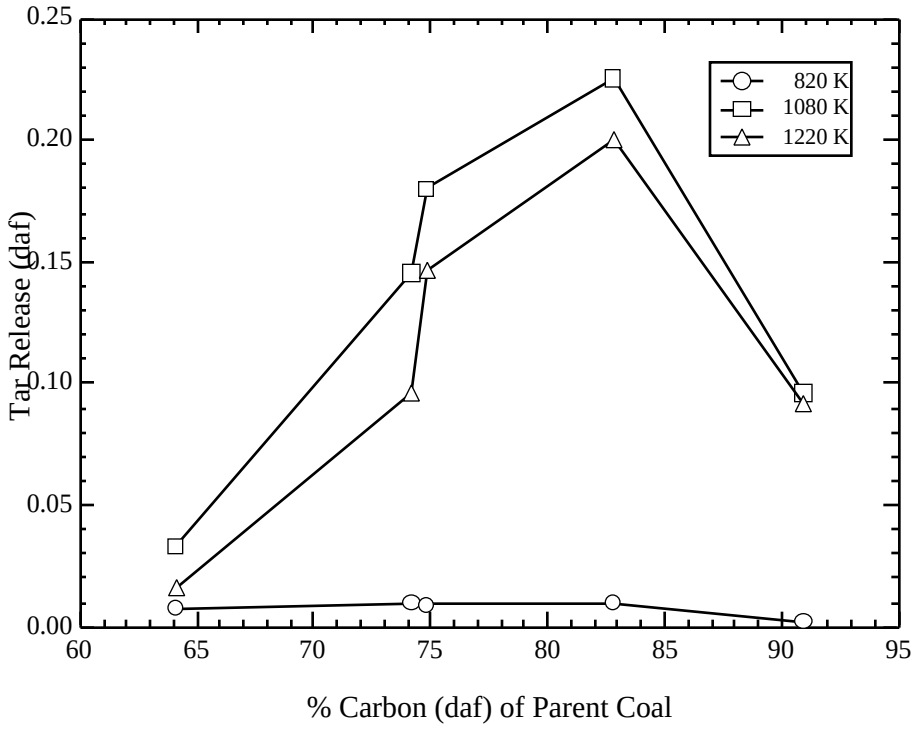

Figure 5.1. Tar Release versus Coal Rank (% Carbon (daf) used as indicator of rank).

As seen in Figure 5.2, nitrogen release lags mass release for all but one experiment. Additionally, it should be noted that as mass release increases, the difference between mass and nitrogen release also increases. Mass release and tar release versus coal rank

curves are presented in Figure 5.3 for the 1080 K pyrolysis experiments. The shape of these curves is consistent with data from other researchers[45, 61] (see Figures 2.4 and 2.5). The similarity between the results presented in Figures 5.2 and 5.3 and that of the literature[45, 61] indicates that the chars and tars produced during these Drop Tube Reactor pyrolysis experiments are similar to those produced by other researchers.

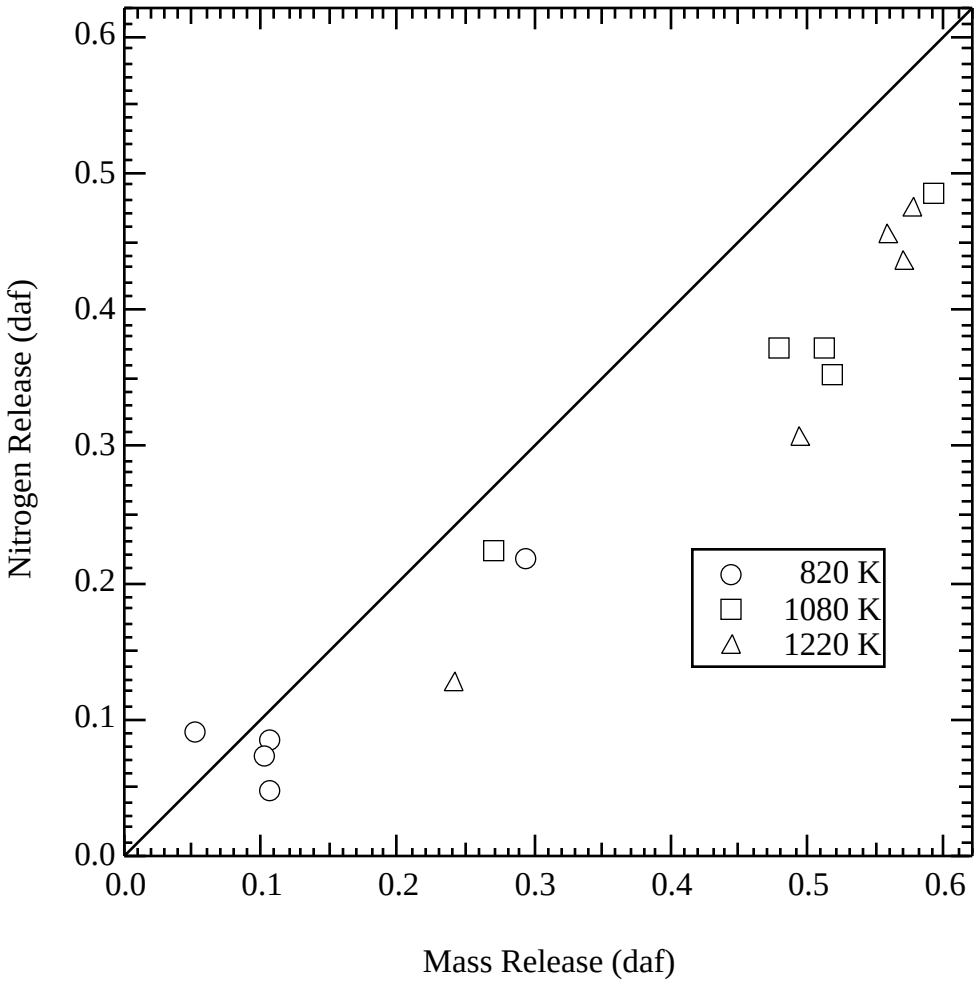

Figure 5.2. Nitrogen Release versus Mass Release for Drop Tube Reactor Pyrolysis Experiments.

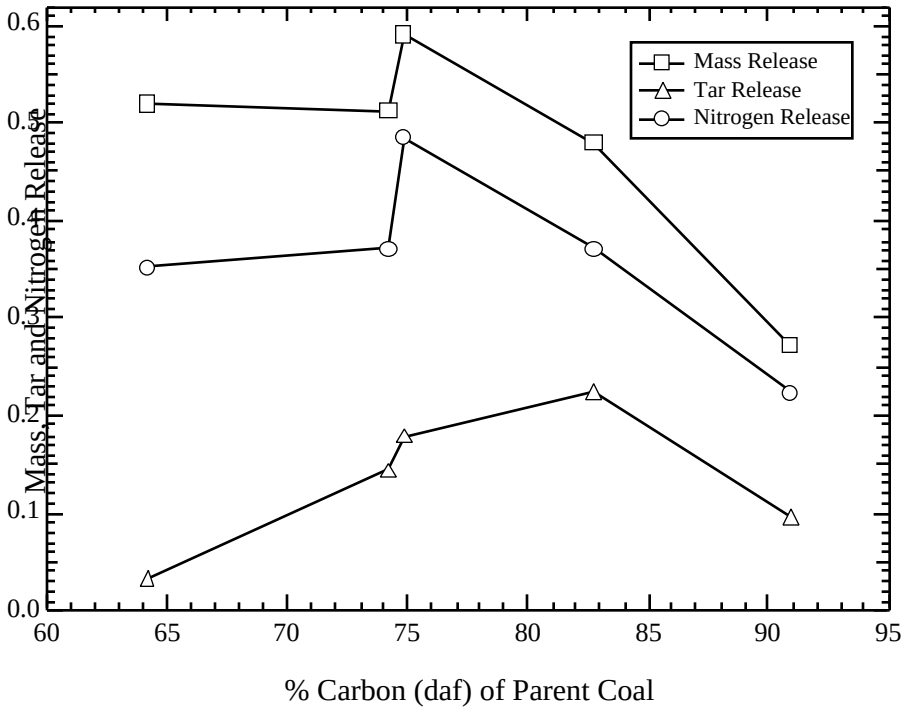

Figure 5.3. Mass, Tar and Nitrogen Release versus Coal Rank for 1080 K Condition Pyrolysis Experiments.

Flat Flame Burner Pyrolysis Experiments

Pyrolysis experiments were performed on 11 U. S. coals in the Flat Flame Burner under the conditions mentioned previously (Table 4.3). The results of these experiments are summarized in Table 5.2. Again, mass and nitrogen release are reported as a fraction of the dry, ash-free coal. These experiments were intended to do three things: (1) identify pairs of coals with similar rank and markedly different total mass release, (2) identify pairs of coals with similar total mass release and markedly different nitrogen release, and (3) determine the pyrolysis behavior of a large number of U.S. coals for which ^{13}C NMR data are available. These experiments were successful in all respects. The experiments with ~69 and ~52 percent mass release (DECS-18 and DECS-13) were identified as being similar in rank and different in total volatiles release (see Figure 5.4). Two coals (PSOC

1515 and PSOC 1520) are similar in total volatiles release (~57 % and ~56 %) and markedly different in nitrogen release (~57 % and ~45 %), as shown in Figure 5.5.

Table 5.2
Summary of Flat Flame Burner Pyrolysis Experiments

Coal	Mass Release (daf)	Nitrogen Release (daf)
DECS-1	0.627	0.569
DECS-7	0.649	0.576
DECS-11	0.576	0.513
DECS-13	0.518	0.481
DECS-18	0.688	0.674
DECS-20	0.756	0.741
DECS-21	0.363	0.364
DECS-27	0.604	0.586
PSOC-1515	0.566	0.571
PSOC-1516	0.188	0.131
PSOC-1520	0.557	0.452

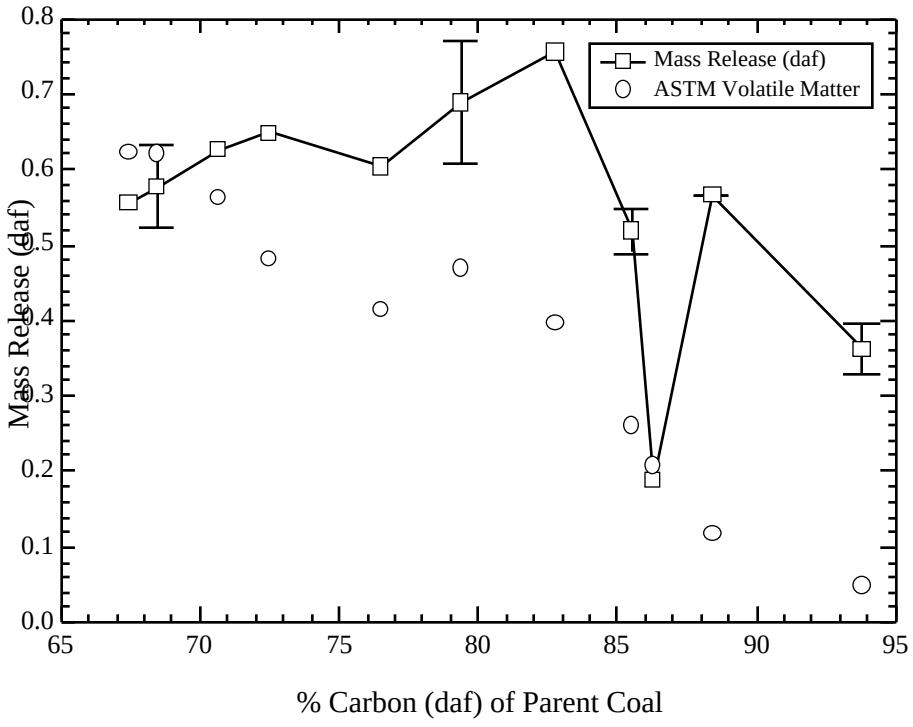

Figure 5.4. Mass Release versus Coal Rank for Flat Flame Burner Pyrolysis Experiments. The marker is the average of the data and the error bars show the maximum and minimum values.

As seen in Figure 5.4, the shape of the mass release versus coal rank curve follows the expected trend, with mass release remaining relatively constant for coals with 67 to 81 %C, then decreasing for high rank coals (%C > 83 %). Nitrogen release is equal to or less than mass release for all of the experiments performed in the Flat Flame Burner (see Figure 5.5).

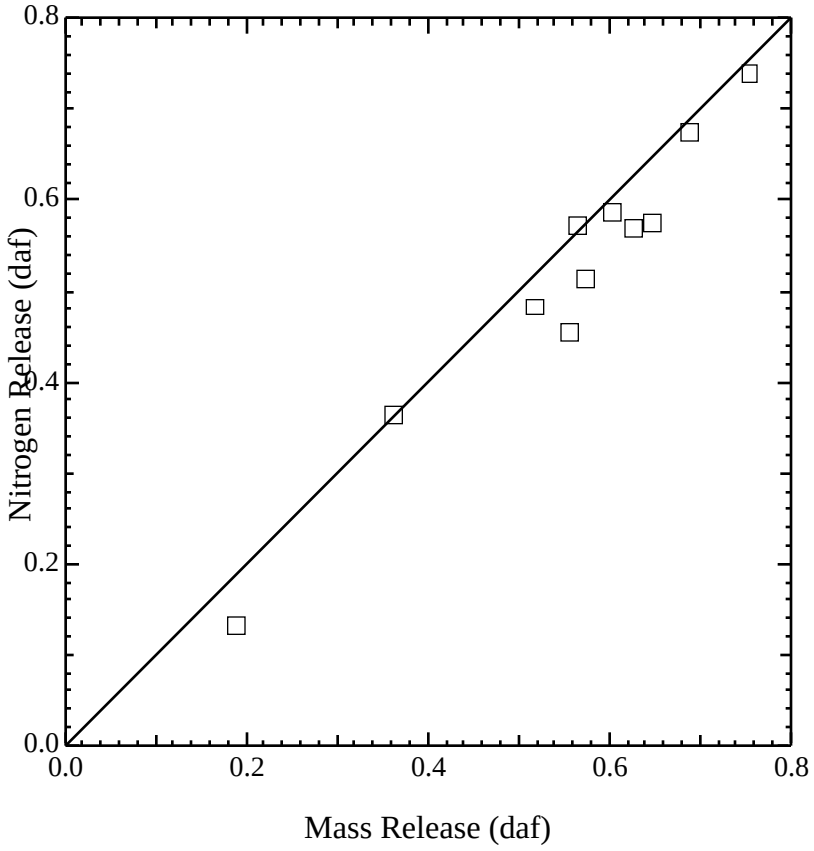

Figure 5.5. Nitrogen Release versus Mass Release for Flat Flame Burner Pyrolysis Experiments.

Ultimate and Proximate Analysis Results

The coals, chars and tars of this study were all analyzed for carbon, hydrogen nitrogen and sulfur content (oxygen content determined by difference). This elemental analysis is referred to in the coal industry as the ultimate analysis. The ultimate analyses

of the coals were given in Tables 4.2 and 4.3. Table 5.3 contains a summary of the ultimate and proximate analyses for the char samples generated in the Drop Tube Reactor.

Table 5.3
Summary of Ultimate Analysis of Chars Produced in Drop Tube Reactor Pyrolysis Experiments[a]

Coal	Condition	%C (daf)	%H (daf)	%N (daf)	%S (daf)	%O (daf) (by diff.)	%Ash (dry)
Beulah Zap	820 K	71.73	4.49	1.04	1.30	21.44	16.89
	1080 K	81.61	3.34	1.26	1.20	12.59	22.34
	1220 K	87.74	2.41	1.29	1.29	7.28	25.80
Blue #1	820 K	78.53	5.30	1.33	0.81	14.02	3.25
	1080 K	84.97	3.35	1.67	0.64	9.37	6.30
	1220 K	90.57	2.44	1.61	0.63	4.76	7.43
Illinois #6	820 K	78.36	5.10	1.57	4.42	10.56	9.84
	1080 K	86.25	3.43	1.86	3.70	4.75	16.04
	1220 K	91.85	2.57	1.94	2.62	1.02	19.18
Pittsburgh #8	820 K	84.90	5.49	1.80	1.24	6.58	4.03
	1080 K	89.83	3.60	2.10	0.84	3.63	7.36
	1220 K	93.59	2.60	2.14	0.80	0.87	8.18
Pocahontas #3	820 K	90.95	4.47	1.28	0.84	2.46	12.70
	1080 K	96.62	3.70	1.40	0.70	-2.42*	13.81
	1220 K	96.43	2.76	1.41	0.52	-1.12*	14.51

[a]Error Estimates (absolute percentage): Carbon (±1); Hydrogen (±0.05); Nitrogen (±0.1); Sulfur (±0.1). *These values are not correct, but are reported for completeness.

As seen in this table, the amount of carbon in the char increases as the total mass release increases. Additionally, the amount of hydrogen and oxygen decreases with increasing mass release. This is expected since the less stable bonds are those containing aliphatic carbons and heteroatoms and these functional group are high in hydrogen and oxygen. During pyrolysis, aliphatic compounds are released to a much greater extent than the

more stable aromatic structures. The nitrogen content of the chars increases as the mass release increases. For all coals, the increase in char nitrogen content from the 820 K to the 1080 K condition is rather large. The subsequent increase in char nitrogen content from the 1080 K to the 1220 K condition is small and may not be significant for some coals. The char generated from Blue #1 at the 1220 K condition contains slightly less nitrogen than the 1080 K condition char, although this difference is probably not significant. Generally, the sulfur content of the chars decreases with increasing mass release.

A summary of the ultimate analyses of the tars generated during these experiments is provided in Table 5.4. As with the chars, the carbon content increases and the hydrogen and oxygen contents decrease with the extent of devolatilization. This is expected, since light gas release contains high levels of CO_2, H_2O and H_2 (compounds high in H and O); the release of light gases prior to tar release results in the increase in carbon mass fraction and decreases in hydrogen and oxygen mass fractions. The nitrogen content of the tars demonstrates the same trend with mass release as that seen in the chars (nitrogen mass fraction increases with total mass release). For the three higher rank coals, the mass fraction of nitrogen in the tar is slightly lower than the mass fraction of nitrogen in the char, but these differences may not be significant.

The elemental analysis data for the tars of this study are compared to data from Freihaut, et al.,[53] Chen[72] and Watt[61] in Figures 5.6 and 5.7. Due to the presence of secondary reactions, the data from this study do not include values from the 1220 K condition. Chen used a radiant entrained flow reactor to devolatilize a number of coals at different temperatures. Freihaut and Watt devolatilized coal in entrained flow reactors at different gas temperatures and residence times. The experimental conditions used by all researchers were designed to minimize secondary reactions of the tar.

Table 5.4
Summary of Ultimate Analysis of Tars Produced in Drop Tube Reactor Pyrolysis Experiments

Coal	Condition	%C (daf)	%H (daf)	%N (daf)	%S (daf)	%O (daf) (by diff.)
Beulah Zap	820 K	71.02	8.71	0.38	1.71	18.19
	1080 K	78.71	4.90	1.30	2.38	12.71
	1220 K	85.41	4.34	1.25	2.19	6.82
Blue #1	820 K	78.39	6.59	1.20	0.52	13.30
	1080 K	83.61	4.85	1.68	0.66	9.20
	1220 K	92.05	4.41	1.72	0.70	1.12
Illinois #6	820 K	78.88	5.96	1.51	2.60	11.05
	1080 K	85.23	4.89	1.80	3.08	5.00
	1220 K	91.56	4.19	1.83	2.61	-0.19*
Pittsburgh #8	820 K	83.39	6.00	1.74	0.83	8.04
	1080 K	87.68	4.94	1.96	0.88	4.55
	1220 K	92.96	4.07	2.00	0.76	0.21
Pocahontas #3	820 K	na	na	na	na	na
	1080 K	92.13	4.86	1.34	0.93	0.73
	1220 K	95.03	4.34	1.38	0.83	-1.58*

*These values are not correct, but are reported for completeness.

Figure 5.6 shows the ratio of hydrogen to carbon (on a mass basis) in the tar as a function of parent coal rank (percent carbon is used as an indicator of coal rank). The H/C ratio appears to decrease slightly with increasing rank. The data from this study are within the bounds of the data from the literature. The mass percent of nitrogen in the tar as a function of coal rank is shown in Figure 5.7. The data appear to reach a maximum at approximately 85 % carbon in the parent coal. The data from this study follow this trend and are within the bounds of the literature data. Figure 5.8 shows the ratio of oxygen to carbon (on a mass basis) in the tar as a function of coal rank. As seen in the figure, the O/C ratio of the tars decreases steadily with rank. Although the H/C ratio of the tars

changes only slightly with rank (Figure 5.6), the O/C ratio (Figure 5.8) and the absolute percentage of carbon (Table 5.4) in the tars change significantly with rank. The fact that

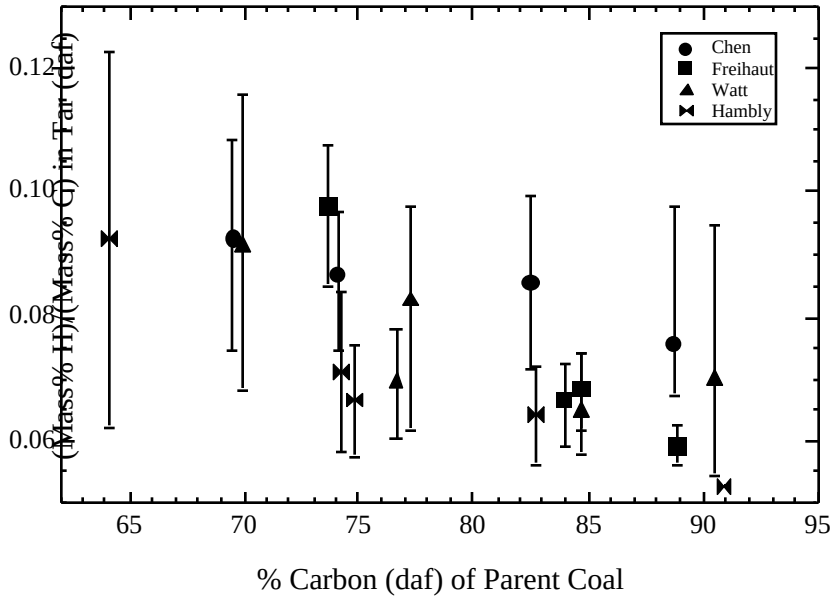

Figure 5.6. Ratio of Hydrogen to Carbon in Tar as a Function of Carbon in the Parent Coal. The marker is the average of the data and the error bars show the maximum and minimum values.

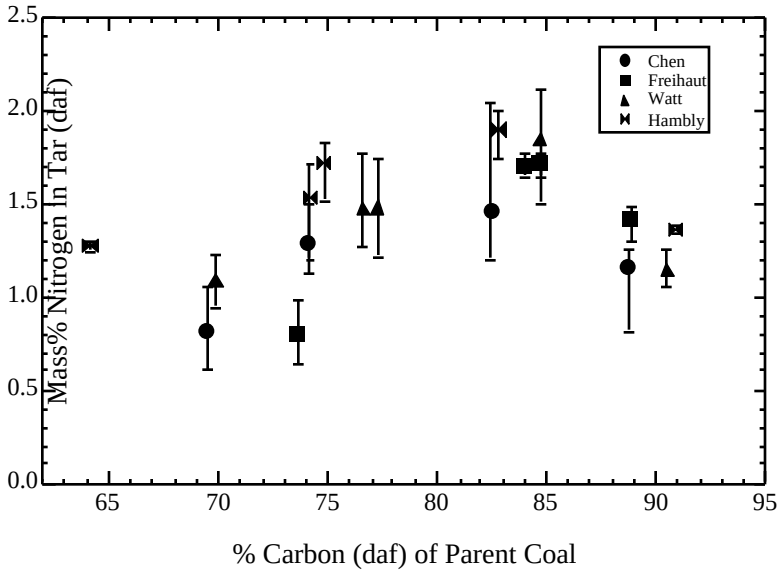

Figure 5.7. Mass of Nitrogen in Tar as a Function of Carbon in the Parent Coal. The marker is the average of the data and the error bars show the maximum and minimum values.

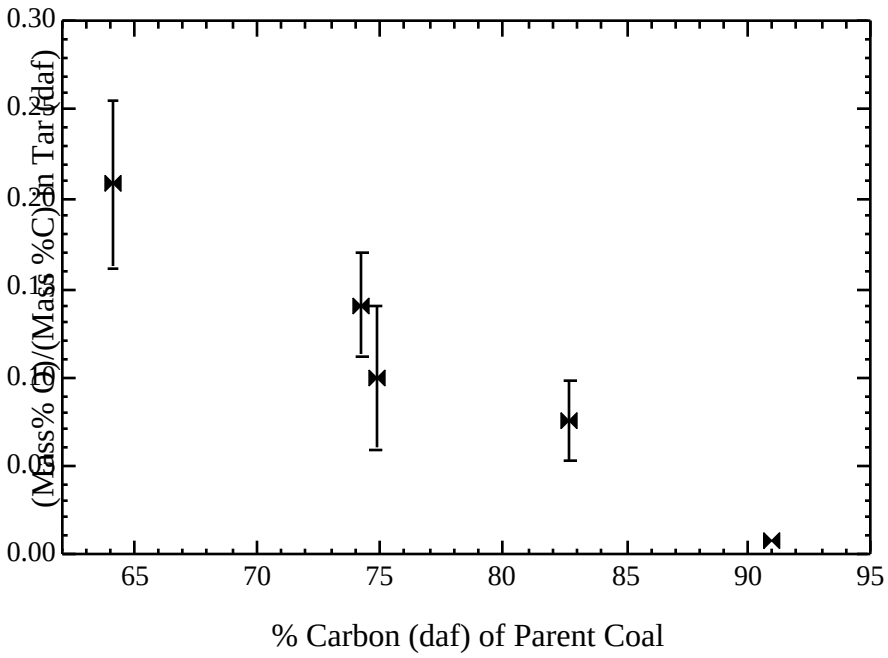

Figure 5.8. Ratio of Oxygen to Carbon in Tar as a Function of Carbon in the Parent Coal. The marker is the average of the data and the error bars show the maximum and minimum values.

the elemental compositions of the tars from this study are similar to those found in the literature provides the basis for further analyses of the tars with more advanced techniques, such as with the solid-state ^{13}C NMR technique.

A summary of the ultimate and proximate analyses of the chars generated during the Flat Flame Burner pyrolysis experiments is provided in Table 5.5. As expected, these chars exhibit the same trends as seen in the Drop Tube Reactor pyrolysis experiments. As pyrolysis proceeds, the mass fractions of carbon and nitrogen increase and the mass fractions of hydrogen and oxygen decrease.

Table 5.5
Summary of Ultimate Analysis of Chars Produced in Flat Flame Burner Pyrolysis Experiments

Coal	%C (daf)	%H (daf)	%N (daf)	%S (daf)	%O (daf) (by diff.)	%Ash (dry)
DECS-1	77.13	3.55	1.70	0.85	16.77	21.02
DECS-7	85.22	2.16	1.41	0.54	10.67	10.79
DECS-11	87.59	1.99	1.15	0.24	9.03	11.46
DECS-13	88.32	2.10	1.85	0.54	7.20	8.48
DECS-18	83.00	3.12	1.82	4.52	7.54	22.21
DECS-20	85.59	2.90	1.89	1.45	8.18	10.69
DECS-21	96.62	2.14	0.91	0.24	0.09	7.07
DECS-27	84.37	2.52	1.60	0.70	10.81	20.95
PSOC-1515	92.98	3.00	1.23	0.47	2.32	30.39
PSOC-1516	86.61	2.15	1.94	1.45	7.85	22.85
PSOC-1520	83.28	1.87	1.94	2.24	10.66	25.86

HCN Analysis Results

The hydrogen cyanide (HCN) analyzer was used for each experiment performed in the Drop Tube Reactor. The conversion of coal nitrogen to hydrogen cyanide was determined for each of these experiments. A derivation of the formula used to calculate the percent conversion of coal nitrogen to hydrogen cyanide is presented in Appendix B. Table 5.6 contains a summary of the results of this analysis, where HCN conversion is reported as the percent of coal nitrogen on a dry, ash free basis that was converted to HCN during the experiment. Figure 5.9 contains a comparison of HCN conversion versus coal type and pyrolysis temperature (note the small scale on the y-axis). Generally, the lower rank coals release more coal nitrogen as HCN. As expected, more HCN is released at the higher pyrolysis temperature as secondary reactions of the tar begin to become important. It is not clear why the Illinois #6 coal releases slightly more HCN at the 1080 K condition than at the 1220 K condition (see Figure 5.9); this may be due to instrument error.

Table 5.6
Summary of Hydrogen Cyanide (HCN) Conversion during Drop Tube Reactor Pyrolysis Experiments

Coal	Condition	Hydrogen Cyanide Conversion (% of daf Coal Nitrogen)
Beulah Zap	820 K	0.0
	1080 K	1.8
	1220 K	5.9
Blue #1	820 K	0.0
	1080 K	1.9
	1220 K	6.3
Illinois #6	820 K	0.0
	1080 K	2.5
	1220 K	1.5
Pittsburgh #8	820 K	0.0
	1080 K	1.0
	1220 K	1.5
Pocahontas #3	820 K	0.0
	1080 K	0.0
	1220 K	1.1

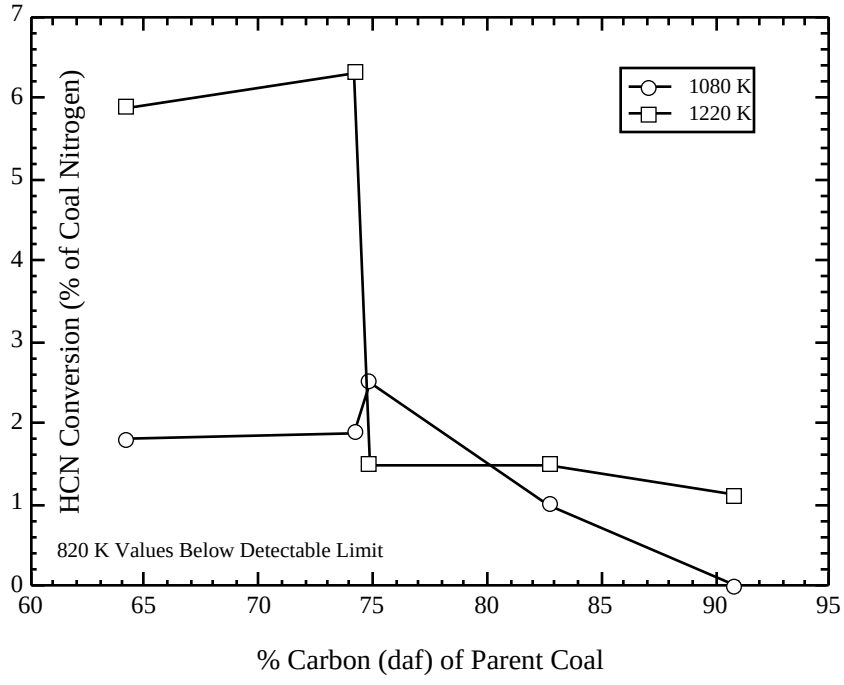

Figure 5.9. HCN Conversion during Drop Tube Reactor Pyrolysis Experiments.

^{13}C NMR Analysis Results

The char and tar samples produced in the Drop Tube Reactor at the 1080 K condition (1080 K and 285 ms) were analyzed with solid-state ^{13}C NMR. This is the first time that solid-state ^{13}C NMR has been used to examine coal tar. The results of these analyses are presented in Tables 5.7 and 5.8, along with the parent coal analyses. Table 5.7 contains the structural parameters that are directly obtained. Table 5.8 contains derived structural parameters.

Table 5.7
^{13}C NMR Analysis of Coal, Char and Tar - 1080 K Condition[a]

Coal	Sample	f_a	f_a^C	f_a'	f_a^H	f_a^N	f_a^P	f_a^S	f_a^B	f_{al}	f_{al}^H	f_{al}^*	f_{al}^O
Beulah Zap	coal	65	8	57	19	38	7	14	17	35	24	11	11
	char	91	7	84	29	55	9	23	23	9	8	1	6
	tar	88	7	81	36	45	11	22	12	12	7	5	2
Blue #1	coal	60	5	55	19	36	8	13	15	40	29	11	7
	char	94	4	90	32	58	7	19	32	6	4	2	3
	tar	88	4	84	35	49	8	18	23	12	6	6	1
Illinois #6	coal	66	3	63	21	42	7	16	19	34	24	10	8
	char	94	6	88	29	59	9	25	25	6	4	2	2
	tar	88	2	86	36	50	7	19	24	12	6	6	1
Pittsburgh #8	coal	65	3	62	23	39	5	16	18	35	24	11	7
	char	93	2	91	37	54	6	20	28	7	5	2	2
	tar	86	2	84	36	48	5	18	25	14	7	7	2
Pocahontas #3	coal	78	1	77	32	45	2	15	28	22	15	7	7
	char	92	2	90	40	50	3	17	30	8	5	3	3
	tar	89	1	88	38	50	3	18	29	11	7	4	2

[a]See footer to Table 2.1

As previously mentioned, Watt et al.[61, 64] pyrolyzed three coals of differing rank in a drop tube reactor under 100% nitrogen gas at a gas temperature of 930 K and a particle heating rate of approximately 10^4 K/s. The resulting tars were collected and analyzed with the liquid ^{13}C NMR techniques described previously (see Literature Review).

Several results of this *liquid-state* NMR analysis indicated that the chemical structure of the tar was significantly different from the original coal. Specifically, the number of aromatic carbons per cluster (C_{Cl}) in the tar was reported to be significantly lower than that of the parent coal. Additionally, the number of bridges and loops per cluster (B.L.) in the tar was reported to be much lower than that of either the coal or the matching char. These results were surprising and were subject to question based on (a) the use of solvents prior to analysis of the tar and (b) collection of tar at relatively low temperatures where devolatilization was not complete. For these and other reasons, the pyrolysis experiments and *solid-state* NMR analyses of this thesis were performed. This thesis presents *solid-state* NMR data on chars and tars produced under conditions leading to nearly complete devolatilization; these results are presented below.

Table 5.8
Derived Structural Parameters from ^{13}C NMR - 1080 K Condition[b]

Coal	Sample	χ_b	C_{Cl}	σ+1	P_0	B.L.	S.C.	MW_{Cl}	MW_δ
Beulah Zap	coal	0.246	14	5.3	0.48	2.5	2.8	440	50
	char	0.274	13	4.9	0.97	4.8	0.1	228	14
	tar	0.148	9	3.7	0.85	3.2	0.5	170	16
Blue #1	coal	0.270	13	5.0	0.48	2.4	2.6	384	45
	char	0.356	18	5.2	0.92	4.8	0.4	283	12
	tar	0.274	13	4.0	0.77	3.1	0.9	222	15
Illinois #6	coal	0.300	15	5.5	0.52	2.9	2.6	402	39
	char	0.284	14	5.4	0.94	5.1	0.3	222	9
	tar	0.279	13	3.9	0.77	3.0	0.9	213	13
Pittsburgh #8	coal	0.290	14	4.8	0.48	2.3	2.5	329	33
	char	0.308	15	4.3	0.92	4.0	0.3	220	8
	tar	0.298	14	3.8	0.70	2.7	1.1	228	14
Pocahontas #3	coal	0.364	18	4.0	0.59	2.3	1.7	316	23
	char	0.333	16.5	3.6	0.85	3.1	0.5	228	6
	tar	0.330	16	3.8	0.81	3.1	0.7	237	10

[b]See footer to Table 2.2

Comparing the solid-state NMR data for the coal, char and tar provides insight into the nature of the structural changes that occur during pyrolysis. As shown in Figure 5.10, the carbon aromaticity (f_a') of the tar is 14 to 53 percent higher than in the parent coal (on a relative basis). In general, the aromaticity of the tars seems to increase slightly with coal rank. For all coals, the aromaticity of the char is higher than the corresponding tar. With exception of the lignite, the aromaticity of the char appears to remain relatively constant with rank.

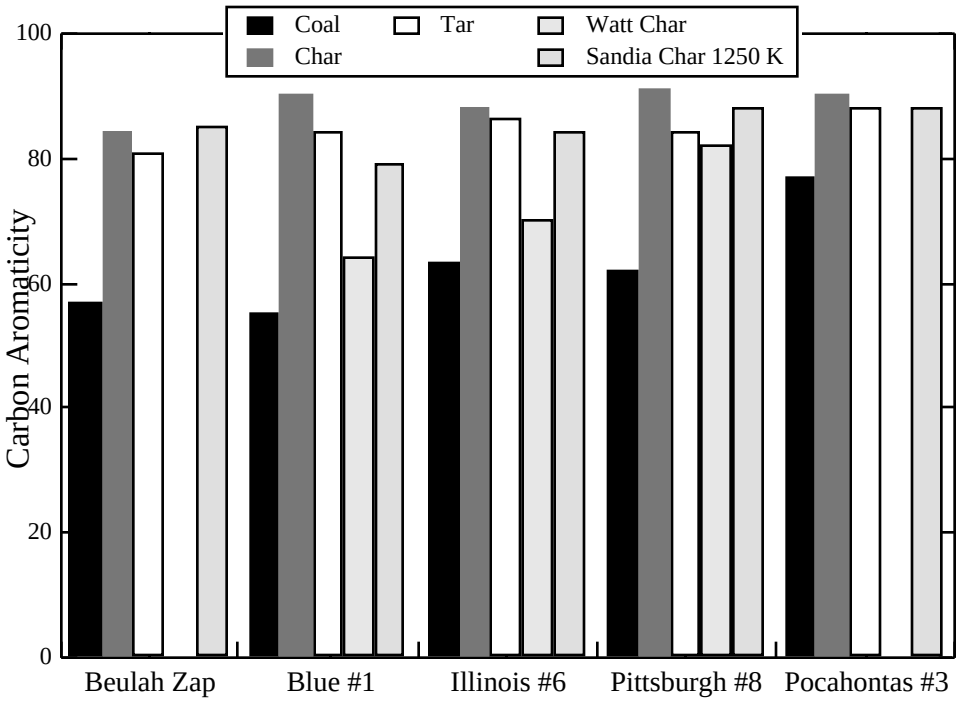

Figure 5.10. Carbon Aromaticity of Coal, Char and Tar

The aromaticity of the chars of this study are higher than the aromaticity of the chars reported in similar experiments at both lower and higher temperatures.[61, 78] It is expected that the chars of this study should have higher aromaticities than those of Watt,[61] due to the higher pyrolysis temperature (1080 vs. 930 K). Chars produced at

higher temperatures are expected to have less side chains per cluster due to the formation of light gas from the side chain material. Side chains are aliphatic in nature, so the release of side chains to the light gas will decrease the aliphatic content of the char and hence increase the aromaticity. This increase in aromaticity, due to the loss of side chain material, should lead to decreases in the ratio of hydrogen to carbon (i.e., mass% H/mass% C) since the side chains consist of aliphatic material which is known to have higher H/C ratios than the aromatic portion of the molecule. Indeed, the chars of this study have lower H/C ratios than those of Watt (13 to 35 percent lower on a relative basis). The observed decrease in the H/C ratios of the chars is consistent with the increased aromaticity. Following the same logic, the chars of this study are expected to have lower aromaticities than the chars produced at 1250 K in the Sandia CDL reactor.[78] As shown in Figure 5.10, however, the chars of this study have higher aromaticities than the Sandia 1250 K chars. Additionally, the H/C ratio of the chars of this study are higher than the Sandia chars by 7.9 to 35.9 percent on a relative basis. The higher aromaticities observed for the chars of this study should be accompanied by lower H/C ratios; that trend was not observed.

The apparent discrepancy in these two sets of char NMR data may possibly be explained by one or more of the following: (1) errors in measured gas temperatures in the Drop Tube Reactor, (2) errors in the elemental analysis of either the chars of this study or those of the Sandia experiments, (3) changes in the solid-state ^{13}C NMR techniques used to analyze the chars, and/or (4) errors in the solid-state ^{13}C NMR analysis of the chars of this study. Errors associated with measuring gas temperatures in the Drop Tube Reactor are thought to be approximately ±30 K. Even if the measured temperatures were in error by as much as 150 K, such high aromaticities would not result (based on the Sandia data). The errors associated with the elemental analysis of the char samples are also not large enough to explain the discrepancy (errors will cause H/C ratio to vary by up to 2 percent). It is not clear at this time if changes were made in the solid-state ^{13}C NMR

techniques used to analyze the chars or if errors occurred during the NMR analysis of the chars of this study.

Cluster Properties

The values of C_{Cl} in the coal range from 13 to 18, which corresponds to structures with 3 to 5 aromatic rings. These values are in agreement with previous data[78] that showed values of C_{Cl} ranging from 10 to 18 for coals with rank ranging from lignite to low volatile bituminous. The values of C_{Cl} in the tar range from 9 to 16 (see Figure 5.11). With the exception of the lignite, the value of C_{Cl} in the tar is similar to that of the corresponding parent coal (within 13 % on a relative basis). These new solid-state NMR data on tar help to confirm the assumption that the values of C_{Cl} in the tar are comparable to those in the parent coals, an assumption that is used extensively in the network coal pyrolysis models.[4]

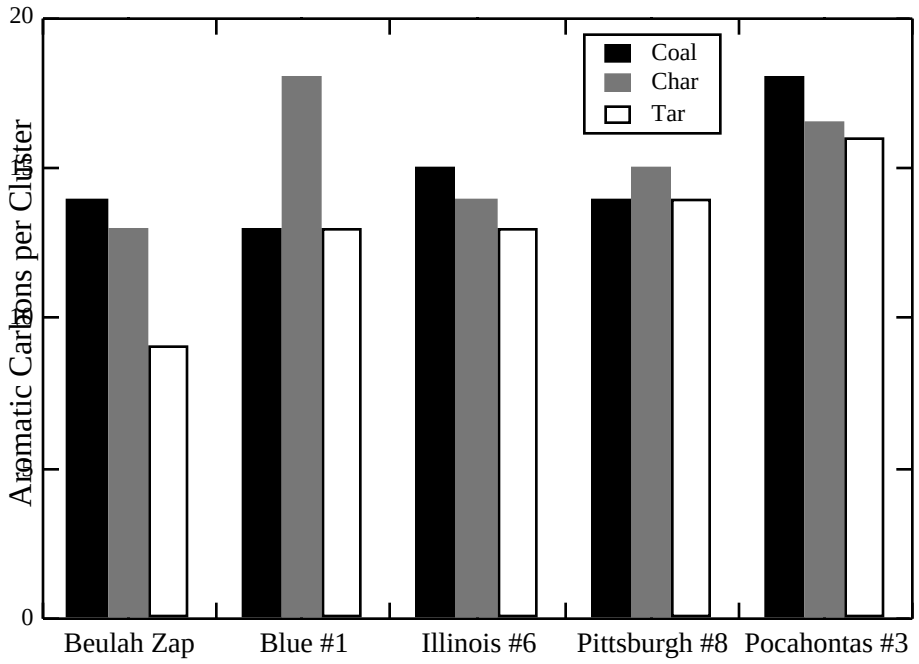

Figure 5.11. Aromatic Carbons per Cluster in Coal, Char and Tar. Results of solid-state ^{13}C NMR analysis of char and tar produced at 1080 K condition in the Drop Tube Reactor.

The values of C_{Cl} in the char range from 13 to 18. With the exception of the char produced from the subbituminous coal, Blue #1, the value of C_{Cl} in the char is similar to that of the corresponding parent coal. These char data are consistent with those of Watt[61, 64]. However, these char data differ slightly from other previous work[58, 59, 62, 78] that indicated that the number of aromatic carbons per cluster in the char does not increase substantially during pyrolysis. The previous data showed values of C_{Cl} generally staying in the range of 12 to 16, whereas the current data show slight increases in range (13 to 18), but these data are within experimental error. For all coals, the values of C_{Cl} in the char are larger than the corresponding tar. This is the first set of data in which matched sets of char and tar have been analyzed with *solid-state* ^{13}C NMR techniques, so comparisons with previous data are not available. The fact that the char contains more aromatic carbons per cluster than the tar is consistent with general theories of coal pyrolysis.

The average cluster molecular weight (MW_{Cl}) in the coal, char and tar are shown in Figure 5.12. This cluster molecular weight contains the weight of the aromatic rings, side chains and half of the bridges of a cluster. For all coals, the average cluster molecular weight in the char and tar are lower than in the parent coal. The values of MW_{Cl} in the coals decrease from 440 to 316 with increasing rank; this trend is not seen in the chars or the tars due to the loss side chain material. Except for the Beulah Zap lignite, MW_{Cl} in the tars is relatively constant with rank. In the chars, MW_{Cl} is relatively constant with rank, except for the Blue #1 char. As seen in the figure, for the bituminous coals (Illinois #6, Pittsburgh #8 and Pocahontas #3), the values of MW_{Cl} in the chars are very similar to that of the tars.

Several sets of data indicate that tar molecular weight distributions peak in the range of 250 to 400 daltons.[43, 53, 65] The tars in this study have molecular weights per cluster in the range of 170 to 240 daltons. These results seem to indicate the presence of

species in the tars that contain more than one cluster per molecule (i.e., dimers and trimers rather than monomers).

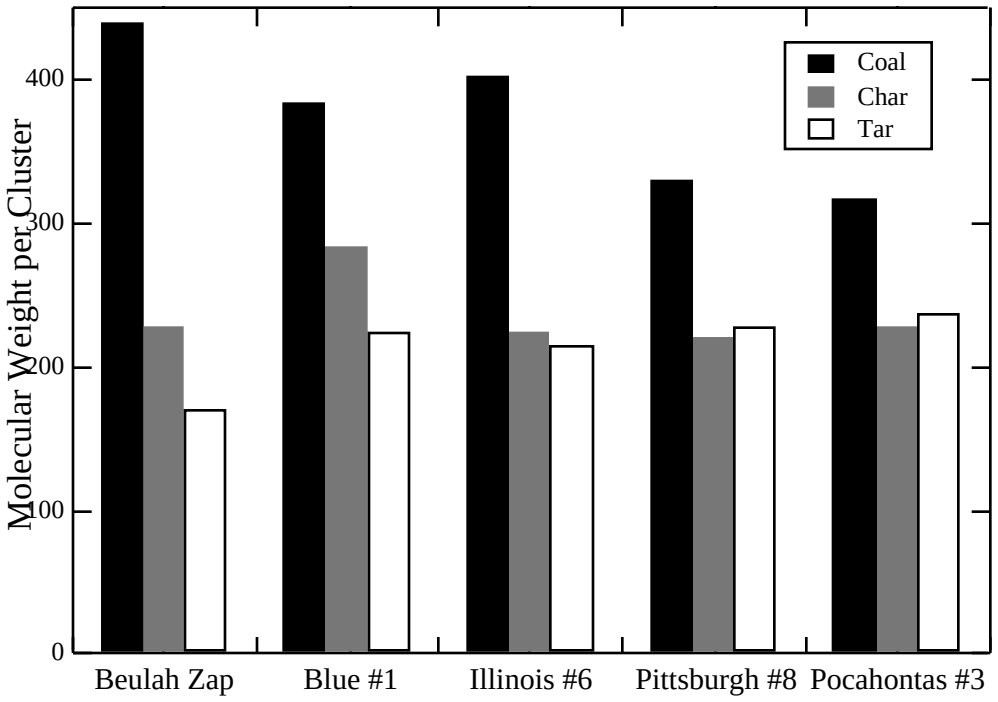

Figure 5.12. Molecular Weight per Cluster in Coal, Char and Tar. Results of solid-state ^{13}C NMR analysis of char and tar produced at 1080 K condition in the Drop Tube Reactor.

The average molecular weight per cluster in the chars of this study (220 to 283) are much smaller than those reported by Watt[61] (315 to 402). These experiments were performed at temperatures approximately 180 K higher than those of Watt, leading to much more completely devolatilized chars. Since the number of aromatic carbons per cluster in the chars of both sets of experiments are similar, this observed decrease in cluster molecular weight is mainly due to decreases in the number and size of cluster attachments (bridges and loops and side chains). A decrease in the number and size of side chains should lead to decreases in the H/C ratio (mass basis) since the side chains

consist of aliphatic material which is known to have higher H/C ratios than the aromatic portion of the molecule. The chars of this study have lower H/C ratios than those of Watt (13 to 35 percent lower on a relative basis). It is thought that these changes are due to the increased pyrolysis temperature.

Cluster Attachments

Several of the derived ^{13}C NMR structural parameters provide information about the number (σ+1, B.L., S.C.) and size (MW_{δ}) of attachments to clusters. Additional insight into the pyrolysis process is gained by observing the changes in these parameters in the pyrolysis products. As seen in Figure 5.13, the number of side chains per cluster (S.C.) in the chars and tars are much lower than in the corresponding coals.

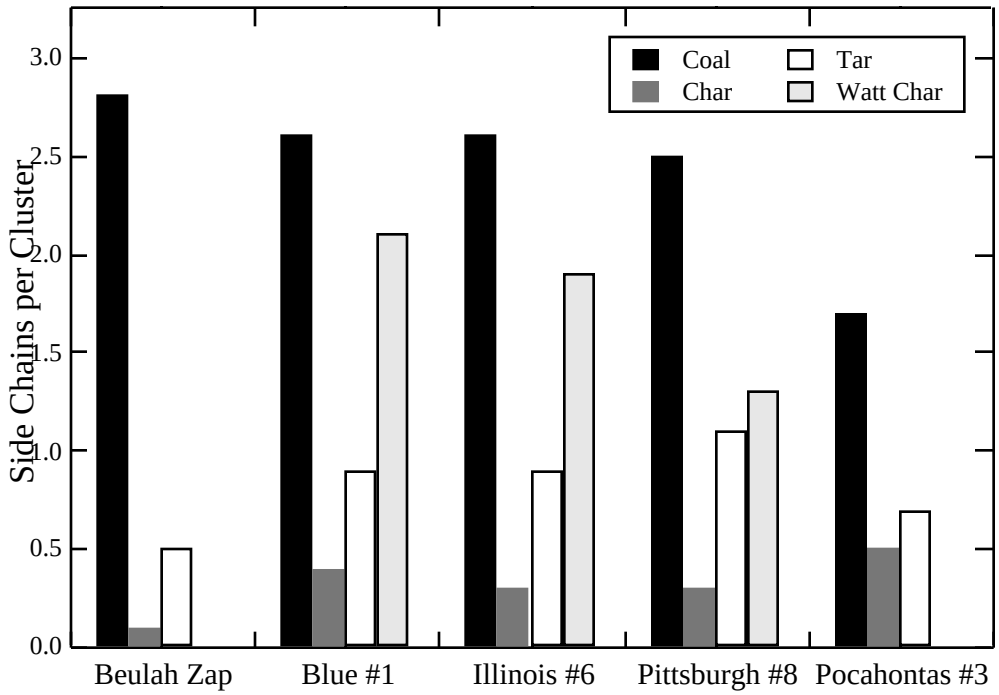

Figure 5.13. Side Chains per Cluster in Coal, Char and Tar. Results of solid-state ^{13}C NMR analysis of char and tar produced at 1080 K condition in the Drop Tube Reactor.

In the parent coals, the values of S.C. decrease with rank, while this trend is not seen in the resulting chars and tars. This change in trend was first reported by Fletcher et al.[58] For all coals, the number of side chains per cluster observed in the char is smaller than in the corresponding tar. The fact that the number of aromatic carbons per cluster are similar for coal, char and tar, and that the number of side chains per cluster are greatly lower in the char and tar, is consistent with the increased aromaticity in the chars and tars as compared to the parent coals.

The total number of attachments per cluster (σ+1) in the coal, char and tar are shown in Figure 5.14. As seen in the figure, σ+1 varies with coal type in the coals and chars. For all coals, σ+1 in the char is similar to the parent coal. Watt[61] reported values of σ+1 in the chars that were slightly higher than in the parent coals. The number of attachments per cluster in the tar is less than in the parent coal. Interestingly, while σ+1 varies with coal type in the parent coals, σ+1 in the tars is nearly constant with coal type.

The number of bridges and loops per cluster (B.L.) in the char are generally much higher than in the parent coals, as shown in Figure 5.15. Values of B.L. in the tars are only moderately higher than in the corresponding coals, except for the Illinois #6 coal, where the values of B.L. in the tar and coal are similar. The marked increase in B.L. in the chars is consistent with previously reported data.[58, 62, 78]

The slight increase in the number of bridges and loops per cluster (B.L.) in the tar may indicate that some form of polymerization may have occurred in the tars. This result would be consistent with the presence of dimers in the tar, and helps rationalize the difference between the measured value of MW_{Cl} and the reported values of the average tar molecular weight.[43, 53, 65]

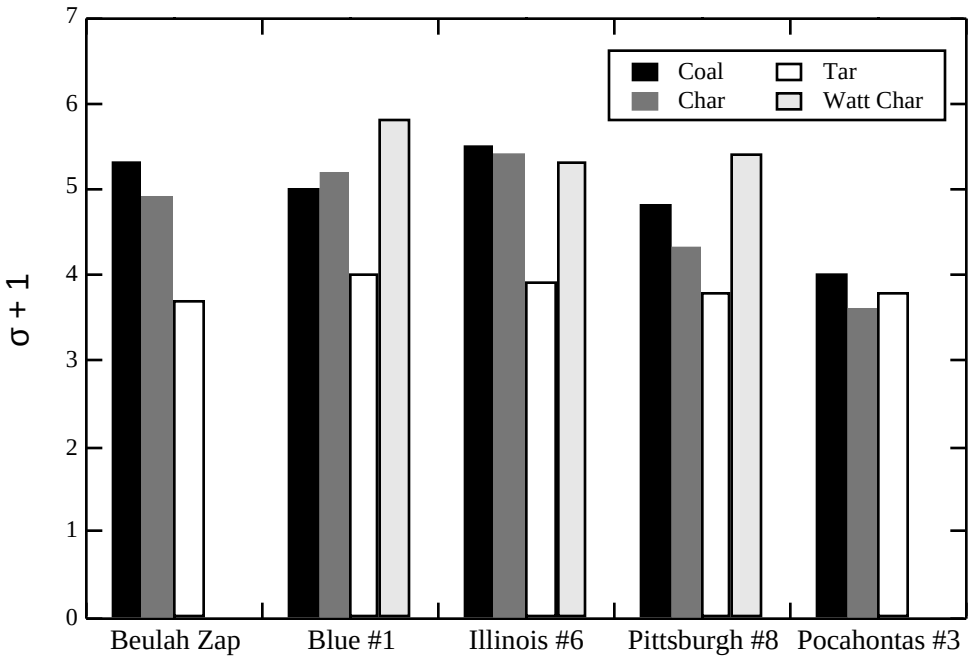

Figure 5.14. Attachments per Cluster in Coal, Char and Tar. Results of solid-state ^{13}C NMR analysis of char and tar produced at 1080 K condition in the Drop Tube Reactor.

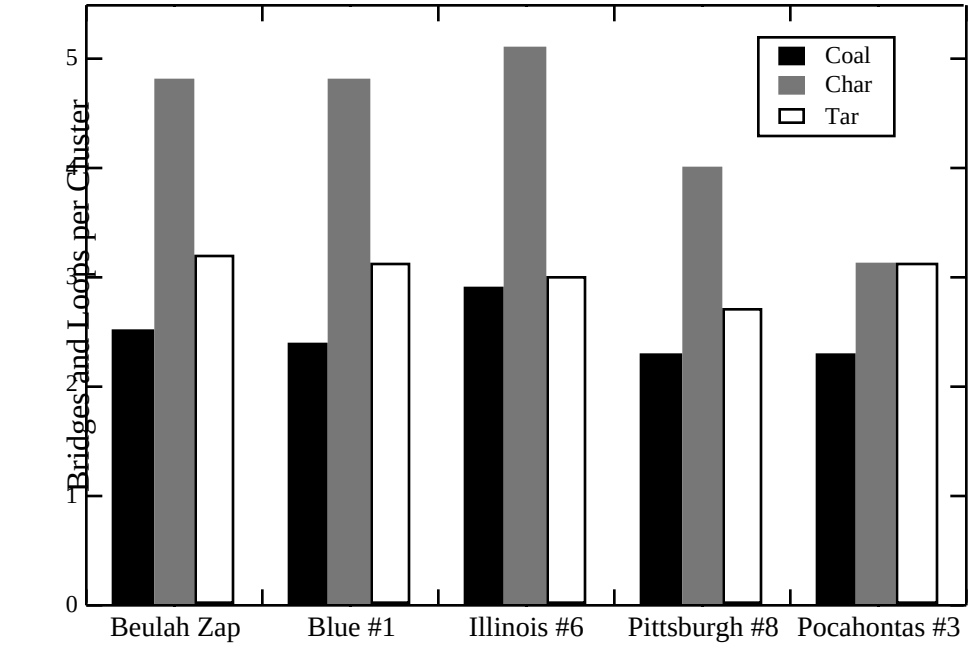

Figure 5.15. Bridges and Loops per Cluster in Coal, Char and Tar. Results of solid-state ^{13}C NMR analysis of char and tar produced at 1080 K condition in the Drop Tube Reactor.

The average molecular weight of attachments (MW_δ) in the tar and char are much lower than that found in the parent coals (see Figure 5.16). While MW_δ decreases steadily with rank in the coals, the values of MW_δ in the tars change only slightly with rank, with no distinguishable trend. In the chars, a slight decrease in MW_δ may be seen with rank, which is similar to the trend reported by Fletcher et al.[58]

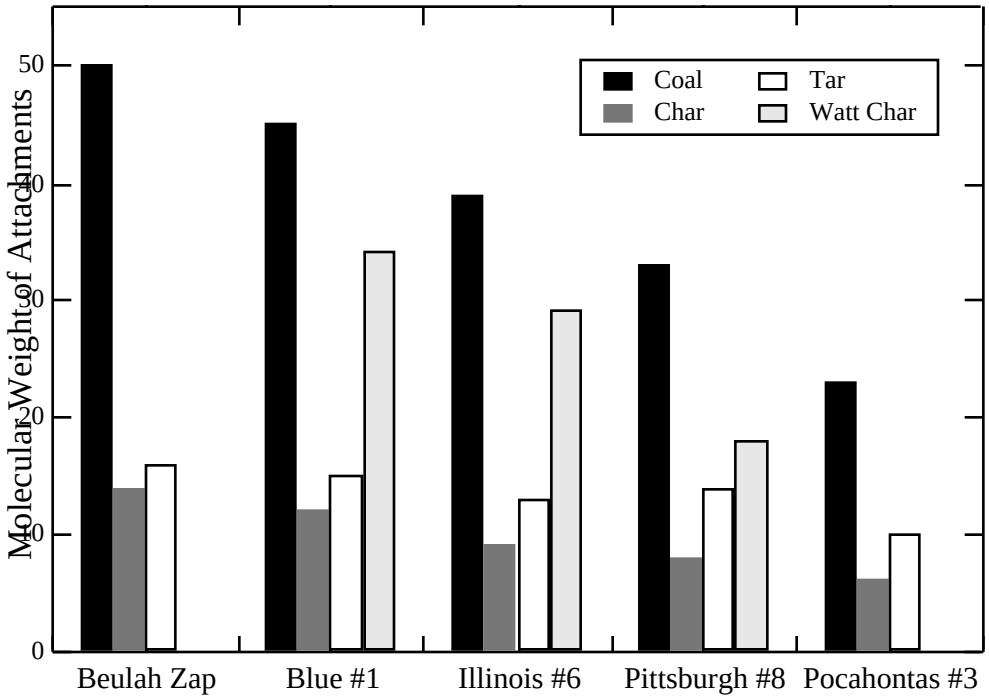

Figure 5.16. Molecular Weight of Attachments in Coal, Char and Tar. Results of solid-state ^{13}C NMR analysis of char and tar produced at 1080 K condition in the Drop Tube Reactor.

^{13}C NMR Results Summary

The chemical structure of the tars from the 1080 K experiments, as determined from solid-state ^{13}C NMR spectroscopy, do not vary greatly with coal rank. The greatest differences seem to be in the tar from the lignite. However, large differences in tar yield are seen as a function of coal rank, as expected. The similarity in chemical structure

of the coal tars is somewhat surprising since large differences are seen in both the elemental composition of these tars and the chemical structural features of the parent coals.

Nitrogen-specific Gas Chromatography/Mass Spectroscopy Analysis of Coal Tar

A preliminary analysis of coal tar was performed using nitrogen-specific chromatography. This initial investigation was limited in scope in this thesis project and was directed at developing the techniques required to apply nitrogen-specific gas chromatography/mass spectrometry to coal tars. The methods and results of this analysis are presented in Appendix C. Preliminary analysis of the nitrogen-containing fractions in the tar by gas chromatography with a nitrogen-selective detector (NPD) and GC/MS showed that there were extremely complex mixtures of nitrogen-containing compounds in the tars. Despite the lack of good resolution in the total ion chromatograms, more than 30 nitrogen-containing polycyclic aromatic compounds were tentatively identified. These compounds were mainly pyridinic and pyrrolic, with numbers of fused aromatic rings ranging from 2 to 5. These results are in agreement with previous investigations of coal tar.[79]

^{15}N NMR Analysis Results

Solid-state ^{15}N NMR techniques (CP/MAS) were used to examine the chemical structure of the chars and tars from the 1080 K Drop Tube Reactor pyrolysis experiments of Pittsburgh #8 and Pocahontas #3 coals. The ^{15}N NMR spectra of Pocahontas and Pittsburgh coals and their matched char-tar pairs are shown in Figures 5.17 and 5.18 (see Pugmire, et al.[32]). As can be seen in these figures, the signal to noise observed in the tar and char samples is not very high, due to the low natural abundance of

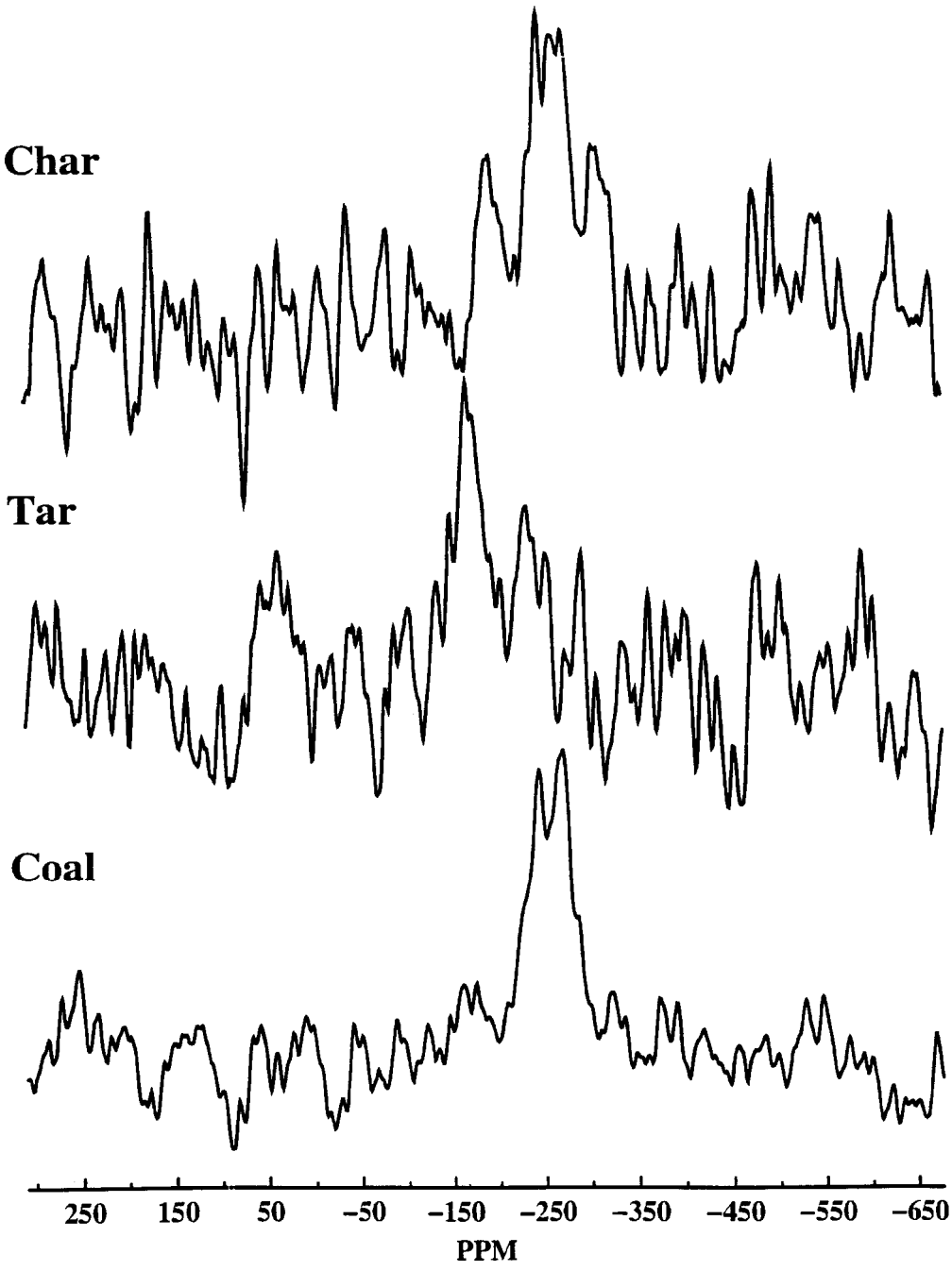

Figure 5.17. ^{15}N CP/MAS spectra of Pocahontas #3 coal and its matched char-tar pair.

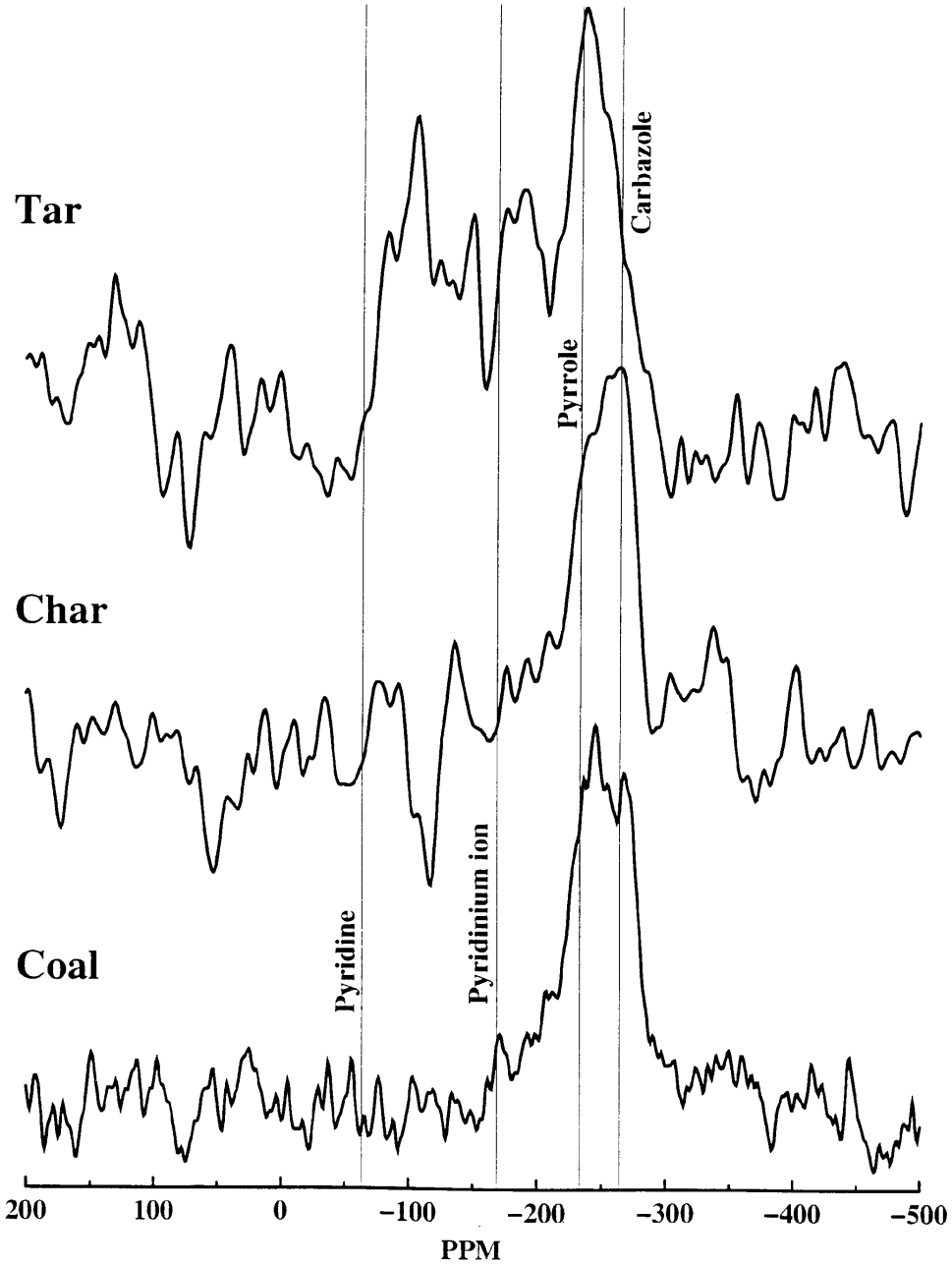

Figure 5.18. ^{15}N CP/MAS spectra of Pittsburgh #8 coal and its matched char-tar pair.

nitrogen in coal. However, it is clear that differences exist in the types of nitrogen species present in the coal/tar/char samples, despite the poor signal to noise ratio. For example, a peak centered at approximately -150 ppm is observed in the tar samples but not in the parent coals. At this point, the lack of signal quality prevents a further interpretation of the results of ^{15}N NMR analyses on a quantitative basis, but qualitative trends are observable. It is anticipated that improvements in NMR techniques, such as Dynamic Nuclear Polarization (DNP) can reduce the amount of noise in this type of analysis and therefore permit more detailed analyses.

6. Discussion

The findings of this thesis will be discussed as they pertain to (a) coal devolatilization modeling, (b) the chemical structure of pyrolysis products, and (c) the chemistry of nitrogen-containing species during pyrolysis. An analysis of the validity of several assumptions that are commonly made in current coal devolatilization models will be presented. Next, an analysis of the changes that occur to the aromatic clusters of char and tar during pyrolysis will be presented. Lastly, the nitrogen chemistry during pyrolysis will be discussed.

Analysis of Coal Devolatilization Model Assumptions

Coal devolatilization models have advanced to the state that total volatiles and tar release during pyrolysis can be related to the macromolecular chemical structure of the parent coal. The most advanced coal devolatilization models are the CPD, FG-DVC and the FLASHCHAIN models.[10, 45, 80] These models all use a statistical network approach to describe the parent coal structure and its devolatilization behavior. Coal is modeled as a matrix of aromatic clusters connected by bridges. Kinetic expressions are used to predict the rate of bridge scission, and then statistical methods are used to predict the number of clusters that are liberated from the coal matrix based on the number of bridges remaining in the char. These models all attempt to relate chemical structural features of the coal (average cluster size, number of bridges and side chains and average size of bridges and side chains) to its pyrolysis behavior. Several reviews of these devolatilization models have been published.[1, 4]

Several attempts have recently been made to model the release of nitrogen during devolatilization with these models.[61, 81] The following assumptions are commonly made in these devolatilization models:

1. The number of aromatic carbons per cluster (C_{Cl}) in the tar is equal to the number of aromatic carbons per cluster in the coal.
2. The carbon aromaticity (f_a') of the tar is equal to the carbon aromaticity of the coal.
3. The mass of nitrogen per cluster (M_{Cl}^{N}) in the tar is equal to the mass of nitrogen per cluster in the char at any time during the pyrolysis process.

This thesis presents data on the chemical structural features and elemental compositions of chars and tar produced during the devolatilization of five coals of different rank. These results allow validity of the devolatilization model assumption to be analyzed.

Aromatic Carbons per Cluster

Recently, Watt et al.[64] published data that indicated that the number of aromatic carbons per cluster in the tar is *not* equal to that of the coal. These data were based on the *liquid-state* ^{13}C NMR analysis of tars produced at 930 K. These data indicated that assumption 1 above was not valid and that changes were necessary in the current devolatilization models. The new *solid-state* ^{13}C NMR data presented here, on tars generated during nearly complete devolatilization, indicate that this assumption (i.e., that $C_{Cl,tar}$ $C_{Cl,coal}$) may be reasonable for all but the lignite (see Figure 5.11).

Carbon Aromaticity

The aromaticity of coal, char and tar were presented in Figure 5.10. As seen in the figure, the aromaticity of both the char and tar are significantly higher than that of the parent coal. These data indicate that assumption (2), that the carbon aromaticity of the tar is equal to the carbon aromaticity of the coal, is *not* accurate for nearly complete devolatilization. Since the number of aromatic carbons per cluster in the tar and coal are similar (see Figure 5.11), the increased aromaticity of the tars is due mainly to a decrease

in the number (S.C.) and size (MW_δ) of side chains. These results are consistent with light gas release prior to and during tar release, which is known to occur.

Mass of Nitrogen per Cluster

It has been shown previously[61, 64] that the mass of nitrogen per aromatic cluster (M_{Cl}^{N}) in coal, char or tar may be calculated as follows:

$$M_{Cl}^{N} = MW_{Cl}\, x_N \qquad (6.1)$$

The number of moles of nitrogen per cluster (N_{Cl}) may be obtained by dividing M_{Cl}^{N} by the molecular weight of nitrogen (MW_N). The number of moles of nitrogen per cluster was determined for the coals, chars and tars of this study and the results are presented in Figure 6.1. For all coals, the moles of nitrogen per cluster in the char and tar are lower than in the parent coal. Additionally, the values of N_{Cl} in the char are larger than in the tar for the low rank coals (Beulah Zap and Blue #1). For the three higher rank coals (Illinois #6, Pittsburgh #8 and Pocahontas #3) the values of N_{Cl} in the char and tar are very similar (most likely within the combined experimental error of the analysis techniques). These data indicate that for the higher rank coals, assumption 3 above may be reasonable; namely that the mass of nitrogen per cluster in the *tar* is equal to the mass of nitrogen per cluster in the *char* at any time during the pyrolysis process. This assumption does not seem to hold true for the two low rank coals.

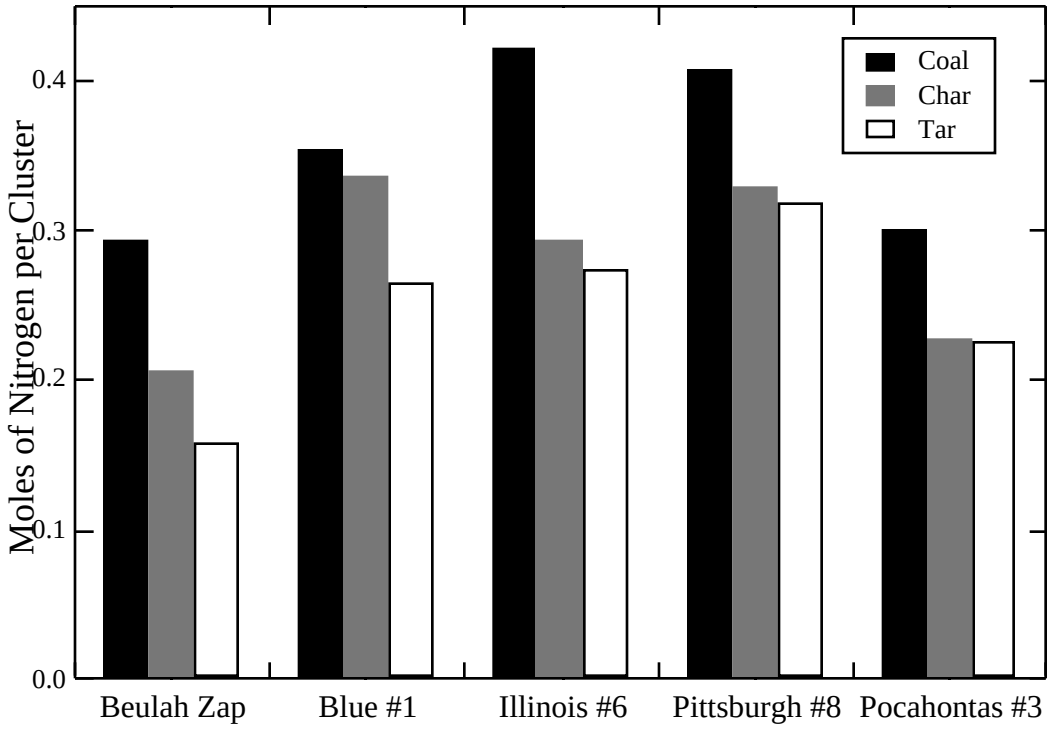

Figure 6.1. Moles of Nitrogen per Cluster in Coal, Char and Tar

Aromatic Clusters

The ^{13}C NMR data reported in this thesis make possible an analysis of the changes that occur to the aromatic clusters of char and tar during the pyrolysis process. Of particular interest is the question of whether aromatic ring opening and/or ring condensation reactions occur in the char and/or tar during pyrolysis. To answer this question, the number of clusters in the coal, char and tar are analyzed to see if clusters are destroyed or created. Watt[61] showed that the number of moles of clusters per kilogram of coal (n_{Cl}) may be calculated as:

$$n_{Cl}^{i} = \frac{m_i}{MW_{Cl,i}} \qquad (6.2)$$

where m_i is the mass (per kilogram of unreacted daf coal), i represents the coal, char or tar and $MW_{Cl,i}$ is the average molecular weight per cluster. If no ring opening and/or ring condensation reactions occur and no aromatic clusters are released as light gases, then the number of moles of clusters in the coal should equal the number of moles of clusters in the char plus tar. Figure 6.2 presents the ratio of the moles of clusters in the char plus tar divided by the moles of clusters in the coal. The combined error in the analysis techniques is estimated to be approximately ± 0.1. As seen in the figure, for four coals, the maximum difference between the number of clusters in the coal and in the pyrolysis products is 10%. This is within the experimental error and therefore signifies that there is no significant change in the number of clusters for these four coals. It is possible that the Pocahontas #3 coal demonstrates a small amount of condensation reactions, although errors in the amount of tar produced may account for this value.

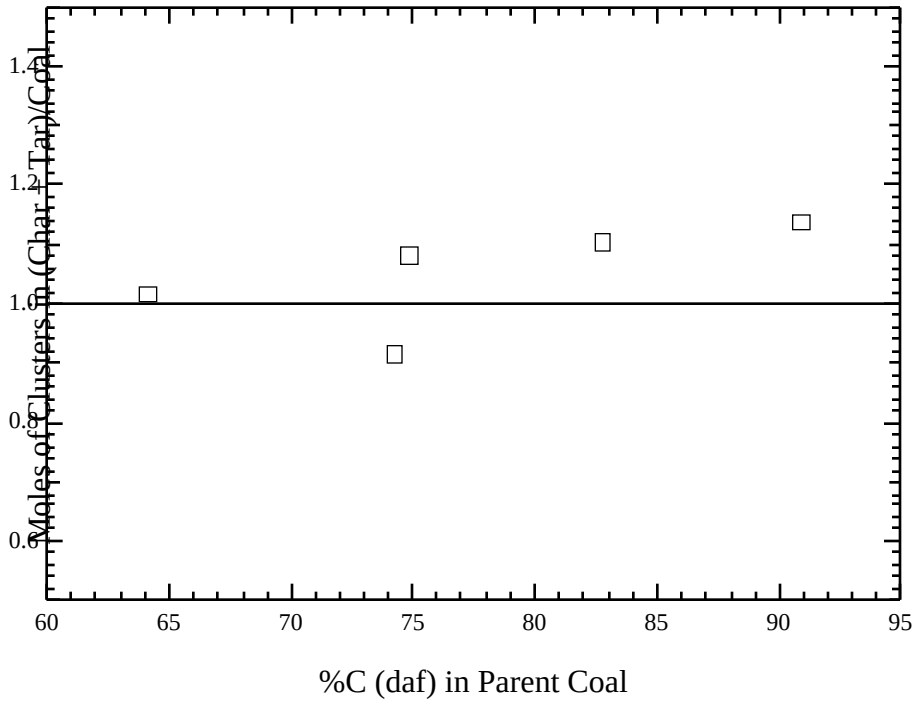

Figure 6.2. Moles of Clusters in Coal, Char and Tar

Nitrogen Balance

As previously mentioned, for all coals, the number of moles of nitrogen per cluster in the coal is higher than that seen in either the char or the tar (at the 1080 K condition). As described above, there is no significant loss or creation of clusters. These trends, taken together, indicate that a fraction of the nitrogen in the coal is released to the gas phase during pyrolysis. An increased knowledge of the extent and chemical form of this nitrogen release is made possible by the results of this thesis. The distribution of coal nitrogen to the pyrolysis products (char, tar, and HCN) has been calculated for each of the Drop Tube Reactor pyrolysis experiments of this thesis. The results of these calculations are presented in Table 6.1 as the percentage of daf coal nitrogen released to char, tar, and HCN.

Table 6.1
Distribution of Nitrogen in Pyrolysis Products

Coal	Condition	N_{Char} (%)	N_{Tar} (%)	N_{HCN} (%)	Δ (%)
Beulah Zap	820 K	78.3	0.3	0.0	21.4
	1080 K	64.8	4.6	1.8	28.8
	1220 K	69.4	2.2	5.9	22.5
Blue #1	820 K	91.5	0.9	0.0	7.6
	1080 K	62.8	18.7	1.9	16.6
	1220 K	52.4	12.8	6.3	28.5
Illinois #6	820 K	95.1	1.0	0.0	3.9
	1080 K	51.5	21.9	2.5	24.1
	1220 K	56.5	18.3	1.5	23.7
Pittsburgh #8	820 K	92.7	1.0	0.0	6.3
	1080 K	62.8	25.3	1.0	10.8
	1220 K	54.4	23.0	1.5	21.1
Pocahontas #3	820 K	90.9	0.0	0.0	9.1
	1080 K	77.6	9.6	0.0	12.7
	1220 K	87.2	9.5	1.1	2.2

*Mass unaccounted for in mass balance

The percentage of coal nitrogen unaccounted for is determined by difference (100 - N_{Char} - N_{Tar} - N_{HCN}). It is possible that the lack of mass balance could be attributed to another nitrogen-containing light gas species, such as NH_3 or HNCO. The nitrogen mass balance is generally within 25%, with some trends versus coal rank and temperature.

Several interesting trends are seen in these nitrogen release data. At the 820 K condition, very little nitrogen is released with the tar and none is released as HCN; most nitrogen at this temperature shows up as a difference in the mass balance. The lignite (Beulah Zap) shows the largest discrepancy in the mass balance; this coal is thought to release some NH_3 as a pyrolysis product.[82] At the 1080 K condition, more nitrogen is released to the tar as tar production begins to increase. At this condition, a small amount of nitrogen is released as HCN. At the 1220 K condition, the largest release of nitrogen as HCN is observed, as expected. For three of the coals, the mass balance decreases with increasing temperature, suggesting that secondary reactions of tar and char, leading to non-HCN species, may be occurring. It is not clear from the NMR data obtained for the 1080 K samples why some coals release more total nitrogen and more HCN than others.

It is recommended that ^{13}C NMR analysis of the chars and tars from the 820 K and 1220 K conditions be performed. These data would allow the number of moles of nitrogen per cluster to be followed as the pyrolysis process proceeds. Also, ^{15}N NMR data on pyrolysis chars and tars may indicate the changing nature of the chemical forms of nitrogen in the coal during the pyrolysis process. This information may help indicate why some coals release a larger fraction of nitrogen as HCN than others. Such data would significantly increase the understanding of the nitrogen chemistry during pyrolysis.

7. Conclusions and Recommendations

In this study, pyrolysis experiments were performed on sixteen well characterized research coals in an electrically heated drop tube furnace and a methane air flat-flame burner (FFB). The coals and the resulting chars and tars were analyzed with some of the most advanced analysis techniques currently available. In particular, coal, char and tar samples from the Drop Tube Reactor pyrolysis experiments were analyzed with solid-state ^{13}C NMR. This work represents the first time that matching sets of coal, char and tar samples from high temperature pyrolysis experiments have been analyzed with solid-state ^{13}C NMR.

It was found that the number of aromatic carbons per cluster in the tars are similar to that of the parent coals. Previous NMR data, obtained for coal tar after using a solvent, indicated that the number of aromatic carbons per cluster in the tars were *not* similar to that of the parent coals. These liquid-state NMR data were suspect for several reasons; these new solid-state NMR data confirm that the liquid-state data are not correct. These new solid-state NMR data also help to confirm an assumption that is used extensively in the network coal pyrolysis models. Several sets of data indicate that tar molecular weight distributions peak in the range of 250 to 400 daltons. The tars in this study have molecular weights per cluster in the range of 170 to 240 daltons. These results seem to indicate the presence of species in the tars that contain more than one cluster per molecule (i.e., dimers and trimers rather than monomers).

The char and tar NMR data of this study demonstrated that the number of bridges and loops per cluster (B.L.) in the char and tar are higher than in the corresponding coal. This increase in B.L. in the chars is consistent with previous work in the literature. The average molecular weight of attachments (MW_δ) in the coal, char and tar were determined. It was shown that the values of MW_δ in the tar and char are much lower than that found

in the parent coals. Additionally, it was shown that while MW_{δ} changes with rank in the coals, MW_{δ} is relatively constant with coal type in the chars and tars.

The first ^{15}N NMR (CP/MAS) spectra of matching sets of coal, char and tar were obtained. These spectra demonstrate that differences exist in the types of nitrogen species present in the coal/char/tar samples. However, due to the low abundance of nitrogen in coal, the ^{15}N NMR spectra have too much noise to provide detailed characteristics.

Several attempts have recently been made to model the release of nitrogen during devolatilization with network coal devolatilization models. The following assumptions are commonly made in these devolatilization models: (1) the number of aromatic carbons per cluster (C_{Cl}) in the tar is equal to the number of aromatic carbons per cluster in the coal; (2) the carbon aromaticity (f_a') of the tar is equal to the carbon aromaticity of the coal; and (3) the mass of nitrogen per cluster (M_{Cl}^{N}) in the tar is equal to the mass of nitrogen per cluster in the char at any time during the pyrolysis process. The data obtained from this thesis were used to demonstrate that assumptions 1 and 3 are most likely reasonable for most coals and that assumption 2 is *not* reasonable for the samples obtained at 1080 K.

The distribution of coal nitrogen to the pyrolysis products (char, tar, and HCN) was calculated for each of the Drop Tube Reactor pyrolysis experiments of this thesis. These data provide additional insight into the fate of coal nitrogen during the pyrolysis process. These data also indicate the inadequacy of ^{13}C NMR, taken alone, in the study of coal nitrogen chemistry during pyrolysis. It is not clear from these ^{13}C NMR data why a coal releases a larger fraction of its nitrogen during pyrolysis or why some coals release a larger fraction of nitrogen as HCN than others. It is recommended that ^{15}N NMR (DNP) data on chars and tars be obtained as a function of the extent of devolatilization. These data, in combination with ^{13}C NMR analyses, would significantly increase the understanding of the nitrogen chemistry during pyrolysis.

References

1. Solomon, P. R. and T. H. Fletcher, *25th Symposium (Int.) on Combustion*; The Combustion Institute, Pittsburgh, PA, pp 463 (1994).

2. Blair, D. W., J. O. L. Wendt and W. Bartok, *16th Symposium (Int.) on Combustion*; The Combustion Institute, Pittsburgh, PA, pp 475 (1977).

3. Chen, S. L., M. P. Heap, D. W. Pershing and G. B. Martin, *19th Symposium (Int.) on Combustion*; The Combustion Institute, Pittsburgh, PA, pp 1271 (1982).

4. Smith, K. L., L. D. Smoot, T. H. Fletcher and R. J. Pugmire, *The Structure and Reaction Processes of Coal*, Plenum, New York, (1994).

5. Spiro, C. L. and P. G. Kosky, *Fuel,* **61**, 1080-1084 (1982).

6. Solomon, P. R., *Coal Structure and Thermal Decomposition,* In New Approaches in Coal Chemistry, B. D. Blaustein, B. C. Bockrath and S. Friedman, Ed., American Chemical Society, Washington, D.C., Vol. 169, pp 61-71 (1981).

7. Krevelen, D. W. v., *Coal: Typology, Chemistry, Physics, and Constitution*, Elsevier, New York, (1981).

8. Brendenberg, J. B., M. Huuska and A. Vuori, *Latest Advances in Thermal and Catalytic Reactions of the Ether Bond in Coal and Related Model Compounds,* In Coal Science and Chemistry, A. Volborth, Ed., Amsterdam, Vol. Elsevier, pp 1-30 (1987).

9. Solomon, P. R. and M. A. Serio, *Evaluation of Coal Pyrolysis Kinetics,* In Fundamentals of the Physical-Chemistry of Pulverized Coal Combustion, J. Lahaye and G. Prado, Ed., Martinus Nijhoff, Dordrecht, Netherlands, pp 126-151 (1987).

10. Solomon, P. R., D. G. Hamblen, R. M. Carangelo, M. A. Serio and G. V. Deshpande, *Energy and Fuels,* **2**, 405-422 (1988).

11. Marzec, A. and H.-R. Schulten, *Preprint, American Chemical Society, Division of Fuel Chemistry,* **34**, 668-675 (1989).

12. Given, P. H., A. Marzec, W. A. Barton, L. J. Lynch and B. C. Gerstein, *Fuel,* **65**, 155-163 (1986).

13. Meuzelaar, H. L. C., A. M. Harper, G. R. Hill and P. H. Given, *Fuel,* **63**, 640-652 (1984).

14. Meuzelaar, H. L. C., W. Windig, A. M. Harper, S. M. Huff, W. H. McClennen and J. M. Richards, *Science,* **226**, 268-274 (1984).

15. Harper, A. M., H. L. C. Meuzelaar and P. H. Given, *Fuel,* **63**, 793-802 (1984).

16. Chang, H.-C. K., Ph. D. Dissertation, Chemistry Department, Brigham Young University (1989).

17. Chang, H.-C. K., K. D. Bartle, K. E. Markides and M. L. Lee, *Structural Comparison of Low-Molecular-Weight Extractable Compounds in Different Rank Coals Using Capillary Column Chromatography,* In Advances in Coal Spectroscopy, H. L. C. Meuzelaar, Ed., Plenum, New York, pp 141-164 (1992).

18. Solomon, P. R., M. A. Serio, R. M. Carangelo and R. Bassilakis, *Energy & Fuels,* **4**, 319-333 (1990).

19. Orendt, A. M., M. S. Solum, N. K. Sethi, R. J. Pugmire and D. M. Grant, *^{13}C NMR Techniques for Structural Studies of Coals and Coal Chars,* In Advances in Coal Spectroscopy, H. L. C. Meuzelaar, Ed., Plenum Press, New York, pp 215-254 (1992).

20. Fletcher, T. H., S. Bai, R. J. Pugmire, M. S. Solum, S. Wood and D. M. Grant, *Energy and Fuels,* **7**, 734-742 (1993).

21. Bai, S., R. J. Pugmire, C. L. Mayne and D. M. Grant, *Analytical Chemistry,* **67**, 3433-3440 (1995).

22. Solum, M. S., R. J. Pugmire and D. M. Grant, *Energy and Fuels,* **3**, 187 (1989).

23. Boudou, J.-P., A. Mariotti and J.-L. Oudin, *Fuel,* **63**, 1508 (1984).

24. Burchill, P. and L. S. Welch, *Fuel,* **68**, 100 (1989).

25. Bartle, K. D., D. L. Perry and S. Wallace, *Fuel Processing Technology,* **15**, 351 (1987).

26. Wojtowicz, M. A., J. R. Pels and J. A. Moulijn, *Fuel,* **74**, 507-515 (1995).

27. Kelemen, S. R., M. L. Gorbaty, S. N. Vaughn and P. J. Kwiatek, *ACS Division of Fuel Chemistry Preprints,* **38**, 384 (1993).

28. Kelemen, S. R., M. L. Gorbaty and P. J. Kwiatek, *Energy & Fuels,* **8**, 896 (1994).

29. Kambara, S., T. Takarada, Y. Yamamoto and K. Kato, *Energy & Fuels,* **7**, 1013 (1993).

30. Kelemen, S. R., M. L. Gorbaty, P. J. Kwiatek, T. H. Fletcher, M. Watt, M. S. Solum and R. J. Pugmire, *Energy & Fuels,* **12**, 159-173 (1998).

31. Mullins, O. C., S. Mitra-Kirtley, J. V. Elp and S. P. Cramer, *Applied Spectroscopy*, **47**, 1268 (1993).

32. Pugmire, R. J., M. S. Solum, D. M. Grant, T. H. Fletcher and R. A. Wind, "^{15}N NMR Spectroscopy of Coals and Pyrolysis Products," *International Conference on Coal Science*, Essen, Germany, 417-420 (1997).

33. Solum, M. S., D. M. Grant, R. J. Pugmire, S. R. Kelemen, M. L. Gorbaty and R. A. Wind, *Energy and Fuels,* **11**, 491 (1997).

34. Solum, M. S., K. A. Anderson-Altman, M. Strohmeyer, D. Burges, Y. Zhang, J. C. Facelli, R. J. Pugmire and D. M. Grant, *J. Am. Chem. Soc.*, **119**, 9804-9809 (1997).

35. Hu, J. Z., J. Zhou, B. Yang, L. Li, J. Qiu, C. Ye, M. S. Solum, R. A. Wind, R. J. Pugmire and D. M. Grant, *Solid State Nucl. Magn. Reson.*, **8**, 129-137 (1997).

36. Anthony, D. B., J. B. Howard, H. C. Hottel and H. P. Meissner, *15th Symposium (Int.) on Combustion*; The Combustion Institute, Pittsburgh, PA, pp 1303-1317 (1974).

37. Suuberg, E. M., W. A. Peters and J. B. Howard, *17th Symposium (Int.) on Combustion*; The Combustion Institute, Pittsburgh, PA, pp 117-130 (1978).

38. Gibbins, J. and R. Kandiyoti, *Energy & Fuels*, **3**, 670-677 (1989).

39. Solomon, P. R., T. H. Fletcher and R. J. Pugmire, *Fuel*, **72**, 587-597 (1993).

40. Chen, J. C. and S. Niksa, *Energy & Fuels*, **6**, 254-264 (1992).

41. Chen, J. C. and S. Niksa, *24th Symposium (Int.) on Combustion*; The Combustion Institute, Pittsburgh, PA, pp 1269 (1992).

42. Ibarra, J. V., R. Moliner and M. P. Gavilan, *Fuel*, **70**, (1991).

43. Solomon, P. R., M. A. Serio, G. V. Despande and E. Kroo, *Energy and Fuels*, **4**, 42-54 (1990).

44. Freihaut, J. D., W. M. Proscia and J. C. Mackie, *Combustion Science and Technology*, **93**, 323 (1993).

45. Fletcher, T. H., A. R. Kerstein, R. J. Pugmire and D. M. Grant, *Energy and Fuels*, **6**, 414 (1992).

46. Hodek, W., M. Kraemer and H. Juntgen, *Fuel*, **70**, 424-428 (1990).

47. Winans, R. E., R. L. McBeth, P. E. Melnikov and R. E. Botto, "Variations in Organic Oxygen Structures in the Argonne Premium Coals as a Function of Rank," *7th International Conference on Coal Science*, Banff, Alberta, Canada, 515-518 (1993).

48. Cody, G. D., P. Thiyagarajan and R. E. Winans, *Energy and Fuels*, **8**, 1370-1378 (1994).

49. Pohl, J. H. and A. F. Sarofim, *16th Symposium (Int.) on Combustion*; The Combustion Institute, Pittsburgh, PA, pp 491 (1977).

50. Wendt, J. O. L. and D. W. Pershing, *Combustion Science and Technology*, **16**, 111 (1977).

51. Solomon, P. R. and M. B. Colket, *Fuel*, **57**, 749 (1978).

52. Mitchell, R. E., R. H. Hurt, L. L. Baxter and D. R. Hardesty, *Milestone Report, Sandia Report SAND92-8208*, (1992).

53. Freihaut, J. D., W. M. Proscia and D. J. Seery, *Energy and Fuels,* **3**, 692-703 (1989).

54. Freihaut, J. D. and W. M. Proscia, *Energy & Fuels*, **3**, 625 (1989).

55. Bassilakis, R., Y. Zhao, P. R. Solomon and M. A. Serio, *Energy & Fuels,* **7**, 710-720 (1993).

56. Nelson, P. F., M. D. Kelly and M. J. Wornat, *Fuel,* **70**, 403 (1991).

57. Nelson, P. F., A. N. Buckley and M. D. Kelly, *24th Symposium (International) on Combustion,* **24**, 1259 (1992).

58. Fletcher, T. H., M. S. Solum, D. M. Grant and R. J. Pugmire, *Energy and Fuels,* **6**, 643-650 (1992).

59. Pugmire, R. J., M. S. Solum, D. M. Grant, S. Critchfield and T. H. Fletcher, *Fuel,* **70**, 414 (1991).

60. Pugmire, R. J. and M. S. Solum, *ACERC Annual Report,* **2**, 28 (1992).

61. Watt, M., M. S. Thesis, Chemical Engineering Department, Brigham Young University (1996).

62. Fletcher, T. H., M. S. Solum, D. M. Grant, S. Critchfield and R. J. Pugmire, *23rd Symposium (Int.) on Combustion*; The Combustion Institute, Pittsburgh, PA, pp 1231 (1990).

63. Yun, Y., H. L. C. Meuzelaar and N. Simmleit, *Energy & Fuels,* **5**, 22-29 (1991).

64. Watt, M., T. H. Fletcher, S. Bai, M. S. Solum and R. J. Pugmire, *26th Symposium (Int.) on Combustion*; Pittsburgh, PA, The Combustion Institute, pp 3153 (1996).

65. Simmleit, N., Y. Yun, H. L. C. Meuzelaar and H.-R. Schulten, *Thermochemical Analysis of U.S. Argonne Premium Coal Samples by Time-resolved Pyrolysis Field Ionization Mass Spectrometry,* In Advances in Coal Spectroscopy, Plenum, New York (1992).

66. Monson, C. R., Ph. D Dissertation, Mechanical Engineering, Brigham Young University (1987).

67. Monson, C. R. and G. K. Germane, *Energy and Fuels,* **7**, 928-936 (1993).

68. Bateman, K. J., M. S. Thesis, Mechanical Engineering, Brigham Young University (1991).

69. Gale, T. K., T. H. Fletcher and C. H. Bartholomew, *Energy & Fuels,* **9**, 513-524 (1995).

70. Gale, T. K., M. S. Thesis, Mechanical Engineering, Brigham Young University (1993).

71. Daines, R. L., M. S. Thesis, Mechanical Engineering, Brigham Young University (1990).

72. Chen, J. C. “Effect of Secondary Reactions on Product Distribution and Nitrogen Evolution from Rapid Coal Pyrolysis,” Stanford University, HTGL Report No. T-280 (1991).

73. Ma, J., T. H. Fletcher and B. W. Webb, "Effect of Flame Environment on Soot Formation in Coal Combustion," *8th International Conference on Coal Science*, Oviedo, Spain, (1995).

74. Ma, J., Ph. D. Dissertation, Chemical Engineering Department, Brigham Young University (1996).

75. McLean, W. M., D. R. Hardesty and J. H. Pohl, *18th Symposium (Int.) on Combustion*; The Combustion Institute, Pittsburgh, PA, pp (1980).

76. Pace, R. S., M. S. Thesis, Chemical Engineering Department, Brigham Young University (1982).

77. Baxter, L. L. “The Release of Inorganic Material During Coal Combustion,” Sandia National Labs, SAND95-8252 (1995).

78. Fletcher, T. H. and D. R. Hardesty “Milestone Report for DOE's Pittsburgh Energy Technology Center,” contract FWP 0709, Sandia Report No. SAND92-8209, available NTIS (1992).

79. Nelson, P. F. and R. J. Tyler, *25th Symposium (Int.) on Combustion*; Pittsburgh, PA, The Combustion Institute, pp 427 (1986).

80. Niksa, S., *Energy and Fuels*, **5**, 673-683 (1991).

81. Niksa, S., *Energy and Fuels*, **9**, 467-478 (1995).

82. Freihaut, J. D., W. Proscia, N. Knight, A. Vranos, H. Kollick and K. Wicks “Combustion Properties of Micronized Coal for High Intensity Combustion Applications,” Final Report for DOE/PETC Contract DE-AC22-85PC80263 (1989).

83. Wan, J. Y. and M. L. Lee, Preliminary Results of Analysis for Nitrogen-containing Polycyclic Aromatic Compounds in Pyrolysis Tars, 1996.

84. Later, D. W., Ph. D. Dissertation, Chemistry Department, Brigham Young University (1982).

Appendix A

The reactor, preheater and flow rate setting used in the Drop Tube Pyrolysis experiments are provided in Table A.1. The settings are listed by pyrolysis conditions as described in Table 4.4.

Table A.1
Summary of Apparatus Settings used in Drop Tube Reactor Pyrolysis Experiments

Condition	Secondary N_2 Flow Rate (slpm)	Primary N_2 Flow Rate (cc/min)	Quench N_2 Flow Rate (slpm)	Reactor Temp (°C)	Preheater Temp (°C)	Distance (mm)
820 K	30	345	25	1000	1000	118
1080 K	20	100	15	1100	1050	171
1220 K	15	100	10	1150	1050	211

Appendix B

A derivation of the formula that was used to calculate the percent conversion of coal nitrogen to hydrogen cyanide is provided below. The assumptions that were made in this derivation are also detailed.

The fraction of dry, ash free coal nitrogen that is converted to hydrogen cyanide (X_N^{HCN}) is defined as:

$$X_N^{HCN} = \frac{\text{mass of coal N as HCN}}{\text{mass of coal N}} \qquad \text{(B.1)}$$

dividing top and bottom by the molecular weight of nitrogen:

$$X_N^{HCN} = \frac{\dot{n}\ \text{coal N as HCN}}{\dot{n}_{\text{coal N}}} \qquad \text{(B.2)}$$

where $\dot{n}$ is the molar flow rate. Since one mole of HCN is formed from one mole of coal nitrogen:

$$X_N^{HCN} = \frac{\dot{n}_{HCN}}{\dot{n}_{\text{coal N}}} \qquad \text{(B.3)}$$

and since $\dot{n}_{HCN} = \left(\dot{n}_T\right)\left(y_{HCN}\right)$:

$$X_N^{HCN} = \frac{\left(\dot{n}_T\right)\left(y_{HCN}\right)}{\dot{n}_{\text{coal N}}} \qquad \text{(B.4)}$$

where $\dot{n}_T$ is the total molar flow rate and y_{HCN} is the mole fraction of HCN. Since the mole fraction is equal to the volume fraction (Q = volumetric flow rate), the mole fraction of HCN can be expressed as:

$$y_{HCN} = \frac{Q_{HCN}}{Q_T} \qquad \text{(B.5)}$$

The HCN analyzer determines the concentration of HCN in ppb. The relationship between the concentration in ppb and the volumetric flow rate is as follows:

$$ppb = \frac{Q_{HCN}}{Q_T} 10^9 \qquad \text{(B.6)}$$

The mole fraction of HCN can therefore be expressed in the following way:

$$y_{HCN} = \frac{ppb}{10^9} \qquad \text{(B.7)}$$

Substituting this into equation B.4 yields:

$$X_N^{HCN} = \frac{\left(\dot{n}_T\right)\left(\frac{ppb}{10^9}\right)}{\dot{n}_{coal\,N}} \qquad \text{(B.8)}$$

The molar flow of coal nitrogen may be replaced with the mass flow ($\dot{m}_{coal\,N}$) divided by the molecular weight of nitrogen (MW_N):

$$X_N^{HCN} = \frac{\left(\dot{n}_T\right)\left(\frac{ppb}{10^9}\right)\left(MW_N\right)}{\dot{m}_{coal\,N}} \qquad \text{(B.9)}$$

The mass flow of coal nitrogen ($\dot{m}_{coal\,N}$) is replaced with the mass flow of coal ($\dot{m}_{coal}$) multiplied by the mass fraction of nitrogen in the coal (x_N^{coal}). Additionally, an assumption is made that the total molar flow rate ($\dot{n}_T$) is approximately equal to the molar flow rate of nitrogen gas through the reactor ($\dot{n}_{N_2}$). This assumption is discussed below. These steps yield the following result:

$$X_N^{HCN} = \frac{\left(\dot{n}_{N_2}\right)\left(\frac{ppb}{10^9}\right)\left(MW_N\right)}{\left(\dot{m}_{coal}\right)\left(x_N^{coal}\right)} \qquad \text{(B.10)}$$

From this expression, the percent conversion of dry, ash free coal nitrogen to hydrogen cyanide is obtained by multiplying by 100 percent.

The assumption that the total molar flow rate is approximately equal to the molar flow rate of nitrogen gas through the reactor was analyzed. The total molar flow is due to the flow of nitrogen gas plus any gas produced during the pyrolysis of coal (light gas and tar). This assumption will be least accurate at the high temperature condition because the nitrogen gas flow rate is the lowest and the pyrolysis gas flow rate the highest at this condition. The combined flow of nitrogen gas at the high temperature condition is approximately 35.1 slpm (~1.43 mole/min at these conditions). The coal feed rate is approximately 0.02 gram/min (daf). Assuming the highest possible volatiles formation during pyrolysis to be approximately 60%, the largest possible volatiles flow rate is approximately 0.012 gram/min. In the worst case, 10 percent of these volatiles are tar. Assuming the average molecular weight of the light gases to be approximately 30 gram/mole and the average molecular weight of the tar to be approximately 350 gram/mole, the total molar flow rate of pyrolysis products may be calculated. For the scenario described above, the molar flow rate of pyrolysis products is approximately 3.6×10^{-4} mole/min. This was determined to be negligible compared to the total molar flow rate of nitrogen gas (~1.43 mole/min).

Appendix C

A preliminary nitrogen-specific chromatography analysis of coal tars was performed as part of this thesis. This initial investigation was limited in scope and was directed at developing the techniques required to apply nitrogen-specific gas chromatography/mass spectrometry to coal tars. Watt pyrolyzed Illinois #6 coal at three conditions in the HPCP.[61] These conditions are listed in Table C.1. The resulting tars were analyzed with nitrogen-specific gas chromatography/mass spectrometry under the direction of Dr. Milt Lee at Brigham Young University. The experimental procedure for this analysis is described below, followed by a presentation and discussion of the results.

Experimental Procedure of Nitrogen-specific GC/MS Analysis of Coal Tar

The experimental procedure used in the nitrogen-specific gas chromatography/mass spectroscopy analysis of coal tar was detailed by Wan et al.[83] and is provided here.

The coal tar samples were stored in a freezer (-20 °C) under an argon atmosphere until analyzed. The tar samples were grayish tan residues adsorbed on filter paper. It was discovered that the solubilities of the tars in methylene chloride and tetrahydrofuran were quite low. Therefore, the tars could not be analyzed directly, and pre-fractionation was necessary.

The tar samples were scraped carefully off the filter paper with a spatula and transferred to pre-weighed and clean 3 ml vials, and then weighed. A portion (0.5 ml) of methylene chloride (HPLC pure) was added to each vial, and the mixture was stirred well, followed by addition of 0.2 g of neutral aluminum oxide (Aldrich). The solvent was allowed to evaporate under a stream of nitrogen after mixing. This mixture was introduced onto the top of a 2-ml disposable pipette containing 1.2 g of aluminum oxide

supported on a silica wool plug. A portion (10 ml) of methylene chloride was added to the column to elute the tar compounds of relatively low molecular weight until clear eluent indicated completeness of the elution.

The solvent in the eluted yellow solutions was allowed to evaporate using a rotatory evaporator, and a dark semisolid resulted. This was transferred to another pre-weighed vial, dried under vacuum and weighed.

The fractionation procedure was similar to the cleaning procedure described above, except for the elution solvents used. Hexane (10 ml), benzene (10 ml), chloroform (20 ml) and tetrahydrofuran (10 ml) were used to elute the aliphatic, aromatic, nitrogen polycyclic aromatic, and phenolic compounds, respectively. All of the solvents were carefully removed, and each fraction was collected in a vial, dried and weighed.

The fractions were analyzed using a Hewlett-Packard (HP) 5890 gas chromatograph equipped with a nitrogen phosphorus detector. GC/MS analysis was performed using a JEOL JMS-SX102A mass spectrometer coupled to an HP 5890 gas chromatograph. A fused silica capillary column (30 m x 0.25 mm i.d.) coated with 0.25 μm SE-54 was used.

Results of Nitrogen-specific GC/MS Analysis of Coal Tar

The results of the fractionation procedure are presented in Table C.2. As shown in the table, only approximately 25% of the tar could be eluted with methylene chloride during the first fractionation step. The nitrogen-containing polycyclic aromatic compounds account for approximately 5-6% of the original tar.

Preliminary analysis of the separated fractions by gas chromatography with a nitrogen-selective detector (NPD) and GC/MS showed that there were extremely complex mixtures of nitrogen-containing compounds in the tars (see Figures C.1 and C.2). Despite the lack of good resolution in the total ion chromatograms, more than 30 nitrogen-

containing polycyclic aromatic compounds were tentatively identified. These compounds are provided in Table C.3. These compounds were mainly pyridinic and pyrrolic, with numbers of fused aromatic rings ranging from 2 to 5. These results are in agreement with previous investigations of coal tar.[79]

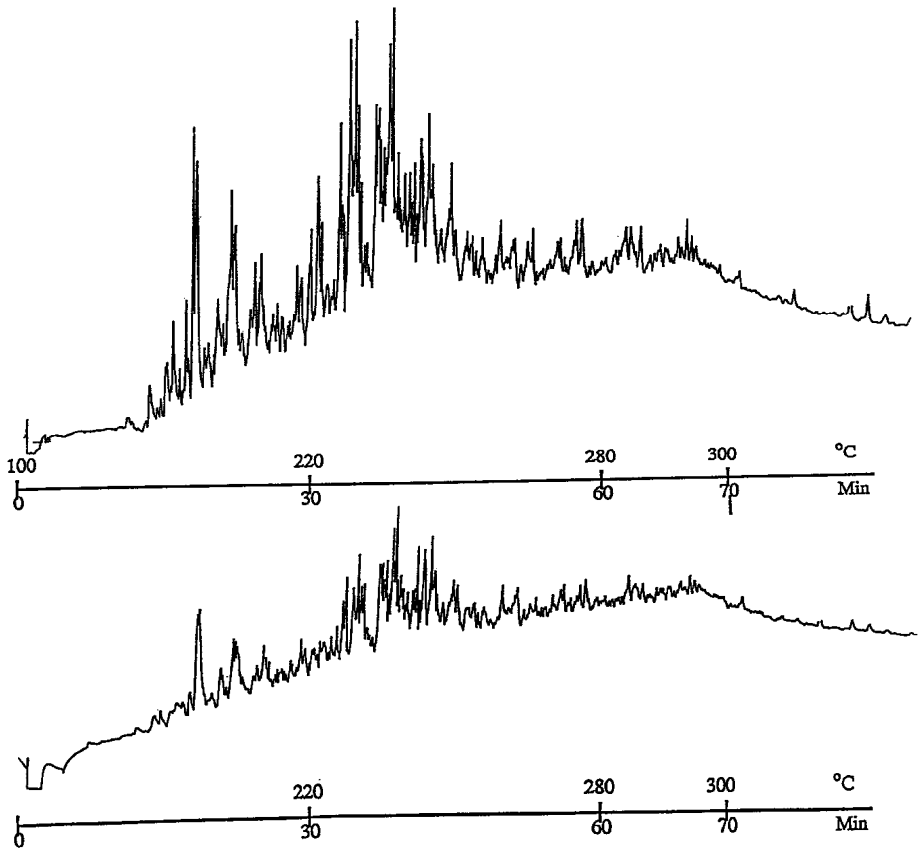

Figure C.1. Capillary Gas Chromatograms (NPD) of the First Portion of the Nitrogen-Containing Polycyclic Aromatic Fraction of Samples 2 (top) and 3 (bottom). Conditions: 30 m x 0.25 mm i.d. column coated with SE-54 stationary phase, programmed from 373 K to 493 K at 4 K/min, then to 573 K at 2 K/min.

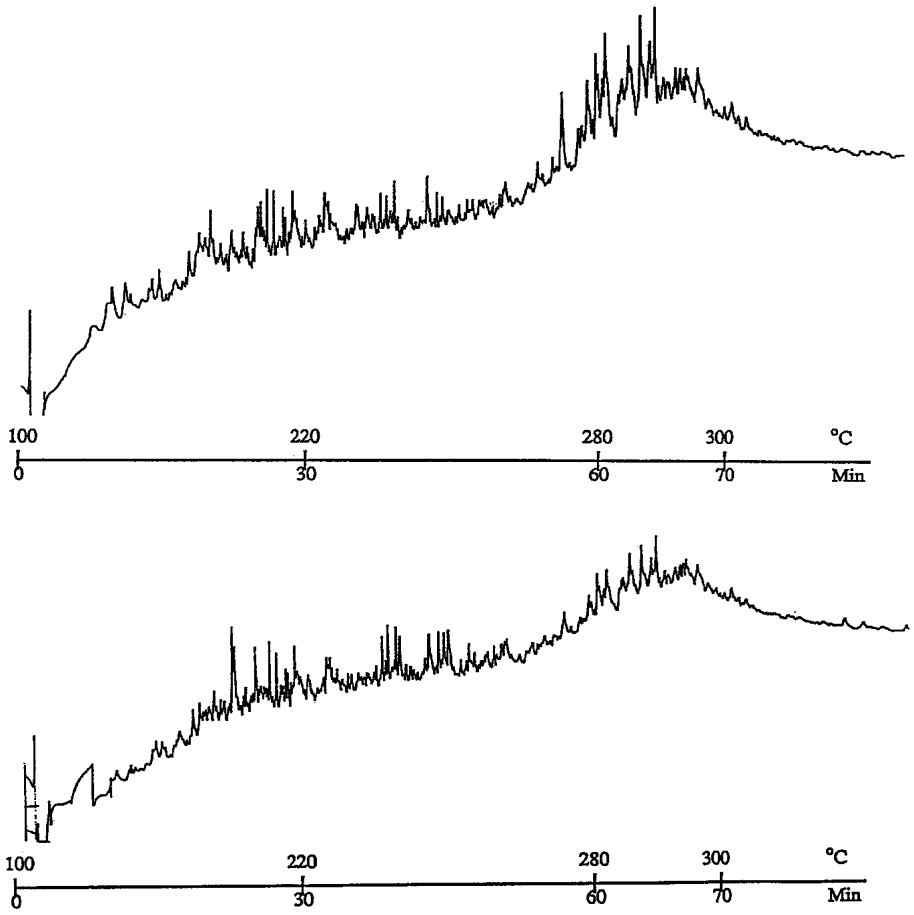

Figure C.2. Capillary Gas Chromatograms (NPD) of the Second Portion of the Nitrogen-Containing Polycyclic Aromatic Fraction of Samples 2 (top) and 3 (bottom). Conditions: same as Figure C.1.

The majority of the compounds making up the coal tars of this study are high molecular weight compounds that are well beyond the volatility range of gas chromatography. For this reason, GC analysis can be used to analyze only a small fraction of the nitrogen-containing compounds in the tars. Several problems were seen to exist in the fractionation method mentioned above. The alumina column fractionation method was originally developed for the group separation of low molecular weight coal products such as solvent refined coal.[84] The results of this study indicate that this

method is not completely effective for the group separation of pyrolysis coal tars due to the presence of high molecular weight component in the tar. Additionally, the tar samples were seen to be an extremely complex mixture of compounds. These problems lead to a lack of clean cut-off points between the fractions.

Due to the large number of potential isomers and the extreme complexity of the mixture of nitrogen compounds in the tars, it is difficult to identify and quantify each individual nitrogen compound. In future experiments it may be more practical to separate the nitrogen-containing compounds into basic and acidic groups before GC/MS analysis. It is expected that this type of separation would yield fractions of pyridinic and pyrrolic compounds, respectively.

Table C.1
Pyrolysis Conditions for Illinois #6 Coals used in Nitrogen-specific GC/MS Experiments

Sample	Maximum Gas Temperature (K)	Residence Time (ms)
1	880	190
2	920	228
3	920	416

Table C.2
Fractionation Yields of Three Pyrolysis Coal Tar Samples

	Sample 1	Sample 2	Sample 3
Sample mass (mg)	32	40	40
Tar mass eluted with CH_2Cl_2 (mg)	7.0	8.9	10.0
Percentage eluted (%)	22	21	25
Aliphatic Fraction (mg)	1.1	1.5	0.5
Aromatic Fraction (mg)	1.8	2.5	1.9
Nitrogen Polycyclic Aromatic Fraction (mg)	2.0	2.5	2.0
Phenolic Fraction (mg)	na	na	na

Table C.3
Nitrogen-containing Compounds Tentatively Identified in GC/MS Experiments

Compound	Molecular Weight	Molecular Formula
Thiazolidine	89	C_3SNH_7
Quinoline	129	C_9H_7N
C_1-Quinoline	143	$C_{10}H_9N$
C_2-Quinoline	157	$C_{11}H_{11}N$
Carbazole	167	$C_{12}H_9N$
C_3-Quinoline	171	$C_{12}H_{13}N$
C_1-Carbazole	181	$C_{13}H_{11}N$
C_4-Quinoline	185	$C_{13}H_{15}N$
C_1-Acridine	193	$C_{14}H_{11}N$
C_2-Carbazole	195	$C_{14}H_{13}N$
Phenylisoquinoline	205	$C_{15}H_{11}N$
C_2-Acridine	207	$C_{15}H_{13}N$
C_3-Carbazole	209	$C_{15}H_{15}N$
C_2-Tetrahydroacridine	211	$C_{15}H_{17}N$
Benzocarbazole	217	$C_{16}H_{11}N$
C_3-Acridine	221	$C_{16}H_{15}N$
C_3-Dihydroacridine	223	$C_{16}H_{17}N$
C_1-Benzocarbazole	231	$C_{17}H_{13}N$
C_4-Acridine	235	$C_{17}H_{17}N$
C_1-Dibenzoquinoline	243	$C_{18}H_{13}N$
C_2-Benzocarbazole	245	$C_{18}H_{15}N$
C_2-Benzacridine	257	$C_{19}H_{17}N$
C_3-Benzocarbazole	259	$C_{19}H_{17}N$
C_3-Benzacridine	271	$C_{20}H_{19}N$
C_4-Benzocarbazole	273	$C_{20}H_{19}N$
Dibenzacridine	279	$C_{21}H_{13}N$
C_4-Benzacridine	285	$C_{21}H_{21}N$
C_1-Dibenzacridine	293	$C_{22}H_{15}N$
C_2-Dibenzacridine	307	$C_{23}H_{17}N$
C_3-Dibenzacridine	321	$C_{24}H_{19}N$

The Chemical Structure of Coal Tar and Char During Devolatilization

Eric M. Hambly
Department of Chemical Engineering
M.S. Degree, August 1998

ABSTRACT

The power generation industry in the United States is being driven by environmental legislation to reduce emission levels of nitrogen oxide (NO_X) pollution. Low-NO_X burners provide the least expensive emission control strategy currently available and are therefore the preferred method to limit the amount of NO_X formed during combustion. Low-NO_X burners are designed on the basis that volatile nitrogen may be converted to N_2 rather than NO_X under locally fuel-rich conditions with sufficient residence time at appropriate temperatures. The amount and chemical form of nitrogen released during devolatilization greatly influences the amount of NO_X reduction achieved using this strategy. Due to the importance of devolatilization in the coal combustion process, increases in the understanding of the devolatilization process and the release of nitrogen-containing species during this process are necessary so that better low-NO_X burners may be designed.

This thesis seeks to provide additional insight into the coal devolatilization process by examining the structure of the devolatilization products char and tar. Coal pyrolysis experiments were performed on sixteen well characterized research coals in an electrically heated drop tube furnace and a methane air flat-flame burner (FFB). Coal, char and tar samples from the drop tube furnace pyrolysis experiments were analyzed with solid-state ^{13}C NMR. This work represents the first time that matching sets of coal, char and tar samples from high temperature pyrolysis experiments have been analyzed with solid-state ^{13}C NMR.

It was found that the number of aromatic carbons per cluster in the tars are similar to that of the parent coals. These data also indicate that previous NMR data, obtained for tar after using a solvent, may be in error. The chemical structural features of matching sets of coal char and tar were compared. The data obtained from this thesis were used to demonstrate that two assumptions that are commonly made in coal nitrogen devolatilization models ($C_{Cl,tar} = C_{Cl,coal}$ and $M^N_{Cl,tar} = M^N_{Cl,char}$) may be reasonable for primary pyrolysis.

COMMITTE APPROVAL:

_____
Thomas H. Fletcher, Advisor

_____
Ronald J. Pugmire, Advisory Committee

_____
Paul O. Hedman, Advisory Committee

_____
Merrill W. Beckstead, Acting Department Chair